



**National and Kapodistrian University**

**Comparative study and performance evaluation of MC-CDMA  
and OFDM over AWGN and fading channels environment**

A PhD Dissertation submitted to the  
Division of Graduate Studies and Research  
of the University of Physics  
in partial fulfillment of the  
requirements for the degree of

**DOCTOR OF PHILOSOPHY**

in the  
Department of Electronics, Computers, Telecommunications  
& Control  
of the College of Physics

By

**Akil Mansour**

**Dissertation Advisor and Committee Chair: Professor G.S. Tombras  
Professor I. Tigelis  
Researcher F. Lazarakis**

**Athens, 2010**

## **ACKNOWLEDGEMENT**

I would like to give my thanks to my advisor, Prof. G.S. Tombras, without his guidance and support I would have never involved in and completed this interesting work in my PhD. His valuable thoughts and recommendations are critical throughout all the stages of this work. I also would like to thank Dr. I. Tigelis, Dr. F. Lazarakis for taking the time and effort to serve on my dissertation committee and give me useful suggestions.

Thanks to the State Scholarships Foundation. I.K.Y. who supported me for a long time in a really difficult financial period and to the National Demokritos Research Institute (Dr. K. Dangaki and Dr. A. Alexandridi) as I did research and study, and certainly this experience was critical for first step of my study. I would like to thank my colleagues and friends Dr.K. Peppas, Dr.Salih Salih,and Dr.Omar Sabah for help me not only enjoy my life, but also enjoy some of the hardness of this research.

In particular, I would like to thank my father, my mother, my wife Loula Mandoginakou and her family, my daughters and son. Without their love and support, I would never have the courage to finish this work.

## Ευχαριστίες

Στο σημείο αυτό θα ήθελα να ευχαριστήσω τους εξαιρετικούς καθηγητές μου κ.κ. Γ. Τόμπρα, Ι. Τίγκελη και Φ. Λαζαράκη για την πολύτιμη βοήθεια, τη συνεχή καθοδήγηση και την ηθική υποστήριξη που μου παρείχαν σε όλη τη διάρκεια της προσπάθειάς μου. Ειδικά ο κος Γ. Τόμπρας ήταν πάντα δίπλα μου όταν τον είχα ανάγκη, ο οποίος με ξεχωριστές γνώσεις, με ήθος και συνέπεια με οδήγησε κάθε φορά προς την σωστή κατεύθυνση προκειμένου να διεκπεραιώσω τη διδακτορική μου διατριβή.

Επίσης να ευχαριστήσω το Ίδρυμα Κρατ. Υποτρ. ΙΚΥ που με στήριξε για αρκετό διάστημα σε μία πραγματικά δύσκολη οικονομική περίοδο και το Εθν. Ίδρυμα Ερευνών Δημόκριτος(κ.κ. Κ. Δαγκάκη και Α. Αλεξανδρίδη), όπου έκανα έρευνα και μελέτη και σίγουρα η εμπειρία αυτή ήταν καθοριστικής σημασίας για μένα. Ενώ δε μπορώ να παραλείψω τους αγαπητούς φίλους κ.κ. Kostas Peppas, Salih Salih και Omar Sabah για την όμορφη και αποδοτική συνεργασία που είχαν μαζί μου.

Τέλος να ευχαριστήσω τους γονείς μου, τη σύζυγό μου Λούλα Μαντογιαννάκου και την οικογένειά της όπως επίσης και τα τρία μου παιδιά, για την αμέριστη συμπαράσταση, αγάπη και αγωνία που είχαν μαζί μου όλ' αυτά τα χρόνια.

# Contents

<b>Preface</b>	<b>vii</b>
List of Abbreviations	<b>xi</b>
List of Symbols	<b>xii</b>
Chapter One	
1.1 Abstract	<b>1</b>
1.2 Literature Survey	2
1.3 Aim of the Work	6
1.4 Mobile radio channels	7
1.4.1 Attenuation	7
1.4.2 Delay Spread	8
1.4.3 Doppler Shift	9
1.4.4 Multipath Effects	10
1.5 Channel Models	14
1.5.1 The Scattering Function and Related Channel Parameters	14
1.5.2 Frequency-Nonselective Channel	15
1.5.3 Frequency-Selective Channel	16
Chapter two	18
2.1 Code-Division Multiple Access (CDMA)	18
2.2 Orthogonal Frequency Division Multiplexing (OFDM)	20
2.3 The Importance of Orthogonality	22
2.3.1 Create the OFDM symbol	25
2.4 Basic OFDM Transmitter Analysis	27
2.5 Basic OFDM Receiver Analysis	28
2.6 OFDM System Difficulties	30
2.6.1 Peak-to-Mean Power Ratio	30
2.6.2 Synchronization	
31	
2.7 OFDM System Model	31

2.7.1	Guard Interval	32
2.7.2	Cyclic Prefix	34
2.7.3	Zero Padding	35
2.8	Inter-carrier Interference	35
2.9	Combining OFDM and CDMA	36
2.10	Multi-Carrier Code Division Multiple Access	27
2.10.1	Spreading Sequences	40
2.10.1.1	Walsh-Hadamard Code	41
2.10.1.2	Gold Sequences	42
2.10.1.3	Maximal Length Sequences (m-Sequences)	43
2.10.2	MC-DS-CDMA	43
2.10.3	Multi-Tone Code Division Multiple Access (MT-CDMA)	45
Chapter Three		
3	OFDM System Model Based Wavelet Transform	46
3.1	Wavelet Transform	47
3.1.1	Haar Wavelet Transform	50
3.1.2	The Ordered Fast Haar Wavelet Transform	52
3.1.3	The Wavelet Packet Transform (WPT)	54
3.2	A proposed Model ‘1’ of OFDM based In-Place Wavelet Transform	57
3.2.1	In-Place Fast Haar Wavelet Transform	58
3.2.2	The In-Place Fast Haar Wavelet Transform Analysis	60
3.2.3	The In-Place Fast Inverse Haar Wavelet Transform Analysis	61
3.2.4	Simulation Results	62
3.2.5	Performance of the Proposed System in AWGN Channel	62
3.2.6	Performance of the Proposed System in Flat Fading Channel	63
3.2.7	Performance of the Proposed System in Selective Fading Channel	65
3.2.8	A Demonstrated Graphical Example for Model ‘1’	66
3.2.9	Conclusions	67
3.3	A proposed Model ‘2’ based In-Place Wavelet Transform Algorithm and Phase Matrix	68

3.3.1	Phase Matrix Performance Analysis	70
3.3.2	Properties and Advantages of Phase Matrix	72
3.3.3	The Mean Value of the Transmitted Symbols	73
3.3.4	Performance Analysis of Model ‘2’	74
3.3.5	Demonstration of Graphical Example	78
3.3.6	Simulation Results	80
3.3.7	Performance of the Proposed System in AWGN Channel	80
3.3.8	Performance of the Proposed System in Selective Fading Channel	81
3.3.9	A Demonstration Numerical Example for Model ‘2’	85
3.3.10	Conclusion	90
3.4	Multiwavelet Theory	91
3.4.1	A proposed Model ‘3’ of MC-CDMA Based on Multi-wavelet Transform	92
3.4.2	Proposed System For MC-CDMA BASED on DMWT	94
3.4.3	Choice of Multi-filter	97
3.4.4	Preprocessing	101
3.4.5	The Results Of The Proposed System	102
3.4.6	Performance of the Proposed Systems in AWGN Channel	103
3.4.7	Performance of the Proposed System in Flat Fading Channel	103
3.4.8	Performance of the Proposed Systems in Selective Fading Channel	104
3.4.9	Conclusions	108
Chapter Four		
4.1	Conclusions	109
4.2	Suggestions for Future Work	111
4.3	Last Work	112
References		113

## PREFACE

Wireless communication has become increasingly important not only for professional applications but also for many fields in our daily routine and in consumer electronics. In 1990, a mobile telephone was still quite expensive, whereas today most teenagers have one, and they use it not only for calls but also for data transmission. More and more computers use wireless local area networks (WLANs), and audio and television broadcasting has become digital.

For systems beyond 3G, there may be a requirement for a new wireless access technology for the terrestrial components [1]. It's envisaged that these potential new radio interfaces will support up to approximately 100 Mbps for high mobility and up to 1 Gbps for the low mobility, such as nomadic, leads to the 4G system.

Many of the above-mentioned communication systems make use of one of two sophisticated techniques that are known as orthogonal frequency division multiplexing (OFDM) and code division multiple access (CDMA).

The first, OFDM, is a digital multicarrier transmission technique that distributes the digitally encoded symbols over several subcarrier frequencies in order to reduce the symbol clock rate to achieve robustness against long echoes in a multipath radio channel, even though the spectra of the individual subcarriers overlap, the information can be completely recovered without any interference from other subcarriers. This may be surprising, but from a mathematical point of view, this is a consequence of the orthogonality of the base functions of the Fourier series.

The second, CDMA, is a multiple access scheme where several users share the same physical medium, that is, the same frequency band at the same time. In an ideal case, the signals of the individual users are *orthogonal* and the information can be recovered without interference from other users.

The concept of orthogonality is quite important to understand why CDMA works. It is due to the fact that pseudorandom sequences are approximately orthogonal to each other or, in other words, they show good correlation properties. CDMA is based on spread spectrum, that is, the spectral band is spread by multiplying the signal with

such a pseudorandom sequence. One advantage of the enhancement of the bandwidth is that the receiver can take benefit from the multipath properties of the mobile radio channel.

OFDM transmission is used in several digital audio and video broadcasting systems. The pioneer was the European DAB (Digital Audio Broadcasting) system [2]. At the time when the project started in 1987, hardly any communication engineers had heard about OFDM, one author (Henrik Schulze) remembers well that many practical engineers were very suspicious of these rather abstract and theoretical underlying ideas of OFDM. However, only a few years later, the DAB system became the leading example for the development of the digital terrestrial video broadcasting system, DVB-T. Here, in contrast to DAB, coherent higher-level modulation schemes together with a sophisticated and powerful channel estimation technique are utilized in a multipath-fading channel. High-speed WLAN systems like IEEE 802.11a and IEEE 802.11g use OFDM together with very similar channel coding and modulation. The European standard HIPERLAN/2 (High Performance Local Area Network, Type 2) has the same OFDM parameters as these IEEE systems and differs only in a few options concerning channel coding and modulation. Recently, a broadcasting system called DRM (Digital Radio Mondiale) has been developed to replace the antiquated analog AM radio transmission in the frequency bands below 30 MHz. DRM uses OFDM together with a sophisticated multilevel coding technique.

The idea of spread spectrum systems goes back to military applications, which arose during World War II, and were the main field for spread spectrum techniques in the following decades. Within these applications, the main benefits of spreading are to hide a signal, to protect it against eavesdropping and to achieve a high robustness against intended interference, that is, to be able to separate the useful signal from the strong interfering one. Furthermore, correlating to a spreading sequence may be used within radar systems to obtain reliable and precise values of propagation delay for deriving the position of an object.

A system where different (nearly orthogonal) spreading sequences are used to separate the signals transmitted from different sources is the Global Positioning System (GPS) developed in about 1970. Hence, GPS is the first important system where code division multiple access (CDMA) is applied. Within the last 10 years, CDMA has emerged as the most important multiple access technique for mobile communications. The first concept for a CDMA mobile communication system was

developed by Qualcomm Incorporated in approx 1988. This system proposal was subsequently refined and released as the so-called IS-95 standard in North America. In the meantime, the system has been rebranded as cdmaOne, and there are more than 100 millions of cdmaOne subscribers in more than 40 countries. Furthermore, cdmaOne has been the starting point for cdma2000, a third-generation mobile communication system offering data rates of up to some Mbit/s. Another very important third-generation system using CDMA is the Universal Mobile Telecommunications System (UMTS), UMTS is based on system proposals developed within a number of European research projects. Hence, CDMA is the dominating multiple access technique for third generation mobile communication systems.

In 1993, a novel transmission technique employing a combination of Orthogonal Frequency Division Multiplexing (OFDM) and Code Division Multiple Access was proposed [11]. This combination is called MC-CDMA or OFDM-CDMA. In radio link, multi-path fading distorts the transmitted signal. To overcome the multi-path fading, mitigates the Inter-Symbol Interference (ISI) and achieve a good performance, we may use an OFDM transmission scheme. OFDM is based on a parallel data transmission scheme that reduces the effects of multi-path fading and makes complex equalizers unnecessary. The OFDM system transforms a wide-band signal into an array of parallel narrow band signals that are more insusceptible to multi-path fading. CDMA based digital wireless communication systems are of increasing significance today both in science and practice.

Multicarrier techniques can combat hostile frequency selective fading countered in mobile communications. The robustness against frequency selective fading is very attractive, especially for high-speed data transmission [3].

MC-CDMA signaling have gained much attention, because the signals can be easily generated and demodulated using Fast Fourier Transforms (FFTs) without increasing the transmitter or receiver complexity and because the technique is potentially robust to channel frequency-selective fading with good spectral efficiency. We denote these systems by OFDM-CDMA. In 1997s, Prasad and Hara compared various methods of combining OFDM and CDMA techniques, identifying three different structures, namely multi-carrier CDMA (MC-CDMA), multi-carrier direct sequence CDMA (MC-DS-CDMA) and multi-tone CDMA (MT-CDMA). The MC-CDMA suffers only slightly in presence of interference as opposed to Direct

Sequence-CDMA (DS-CDMA) whose performance decreases significantly in the presence of interference [4].

The transmitter structure of OFDM is similar to that of MC-CDMA scheme. The main difference is that OFDM transmits different symbols on each sub-carrier, whereas MC-CDMA transmits the same symbol in parallel through many sub-carriers.

Last decade, the availability of FFT algorithms was critical for their success in signal processing. Fourier analysis has a serious drawback. When a signal is transformed into the frequency domain, time information is lost.

After that, The Short-Time Fourier Transform (STFT) was developed, The Short-Time Fourier Transform (STFT) maps a signal into a 2-D function of time and frequency. However, the time and frequency information can only be obtained with limited precision.

The precision is determined by the size of the window used to analyze the signal.

Recently, Wavelet analysis is a windowing technique, similar to the STFT, with variable-sized windows. It allows the use of long time intervals, when more low frequency information is sought, and shorter regions, when more high frequency information is what you are after. Wavelet analysis is capable of revealing aspects of data that other signal analysis techniques miss, including aspects such as trends, breakdown points, discontinuities, and self- similarity. It is also often used to compress or denoise a signal without any appreciable degradation.

Last years, it was found that based on Haar-wavelets, discrete wavelet based OFDM (DWT-OFDM) is capable of reducing the inter symbol interference (ISI) and ICI, which are caused by the loss in orthogonality between the carriers. WT-OFDM can also support much higher spectrum efficiency than discrete Fourier-based OFDM (DFT-OFDM). The interest in wavelets has grown substantially in the past 10 years ago because wavelets solve basic problems in signal processing such as data approximation (smoothing), noise reduction, data compression, time-frequency analysis and image analysis.

## List of Abbreviations

AWGN	Additive White Gaussian Noise
BER	Bit Error Rate
CDMA	Code Division Multiple Access
CP	Cyclic Prefix
CSDMWT	Critically Sampling Discrete Multiwavelet Transform
DS-CDMA	Direct Sequence Code Division Multiple Access
DMWT	Discrete Multiwavelet Transform
DWPT	Discrete Wavelet Packet Transform
DWT	Discrete Wavelet Transform
DWT-OFDM	Discrete Wavelet Transform-Orthogonal Frequency Division Multiplexing
DFT-OFDM	Discrete Fourier Transform-Orthogonal Frequency Division Multiplexing
DIT	Decimation In-Time
DIF	Decimation In-Frequency
DSP	Digital Signal Processor
DSL	Digital Subscriber Line
DAB	Digital Audio Broadcasting
DVB	Digital Video Broadcasting
DFT	Discrete Fourier Transform
FFT	Fast Fourier Transform
FRAT	Finite Radon Transform
HIPERLAN	High Performance Local Area Network
IFFT	Inverse Fast Fourier Transform
ISI	Inter-Symbol Interference
IPM	Inverse of Phase Matrix
IS-95	Interim Standard-95
ICI	Inter-Carrier Interference
IDWPT	Inverse Discrete Wavelet Packet Transform
IP-WT	In-Place Wavelet Transform
IP-IWT	In-Place Inverse Wavelet Transform
IMT-2000	International Mobile Telecommunications-2000
LAN	Local Area Network

LFSR	Linear Feedback Shift Register
MC-CDMA	Multicarrier Code Division Multiple Access
MC-DS-CDMA	Multi-Carrier-Direct Sequence Code Division Multiple Access
MT-CDMA	Multi-Tone Code Division Multiple Access
MAI	Multiple Access Interference
O-QAM	Orthogonal-Quadrature Amplitude Modulation
OFDM	Orthogonal Frequency Division Multiplexing
OOB	Out Of Band
PAN	Personal Area Network
PM	Phase Matrix
PN	Pseudo-Noise
PSK	Phase Shift Keying
QAM	Quadrature Amplitude Modulation
QPSK	Quadrature Phase Shift Keying
QMF	Quadrature Mirror Filter
SNR	Signal-to- Noise Ratio
SIS	Successive Interference Cancellation
STBC	Space Time Block Code
TDMA	Time Division Multiple Access
WT	Wavelet Transform
WLAN	Wireless Local Area Network
WPT	Wavelet Packet Transform
ZP	Zero Padding

## List of Symbols

$F_d$		Doppler frequency
$B_d$		Doppler spread
$B_{coh}$		Channel coherence bandwidth
$G_0, G_1$		Filtering-down sampling process coefficients of the Wavelet Packet Transform
$g_0, g_1$		Quadrature Mirror Filter coefficients of Wavelet Packet Transform
$\oplus$		Module-2 addition (XOR)
$L$		Number of resolvable multipath
$l$		Sweep number in the Wavelet Transform
$m$		Degree of the generator polynomial
$N$		Fast Fourier Transform size
$N$		Number of subcarriers
$N_s$		Subset carrier number of total subcarriers
$N_T$		Total number of subcarriers
$n$		Iteration of the Wavelet Transform
$P$		The number of stages for radix-2 N-point DFT
	$Q$	Gold sequence length
$\tau$		Time delay
$t$		Time domain
$T$		Time of OFDM symbol
	$T_b$	Bit duration
	$T_c$	Chip duration
$T_g$		Guard period interval time
$T_u$		Pulse duration

$T_m$	Multipath spread
$T_{coh}$	Channel coherence time
$\nu$	Cyclic prefix length
$a_k, c_k$	Wavelet coefficients
$E_{Tm}$	The transmitted energy per sub-carrier
$C(t)$	Spreading code
$c(t, \tau)$	Time response of the channel
$C(t, f)$	Frequency response of the channel
$G(x)$	Generator polynomial
$N(t)$	Additive noise
$R(t)$	Low pass received signal
$S(\tau, \lambda)$	The scattering function
$S_c(\tau)$	Delay power spectrum
$X(k)$	Discrete spectral sample
$X(n)$	Input signal to the FFT
$X(t)$	Transmitted signal through the channel
$x_k(n)$	Discrete transmitted signal
$h_k(n)$	Frequency response of the channel
$\eta_k(n)$	Complex Gaussian random variable
$\tilde{f}$	Approximating function of the Haar Wavelet transform
$\psi_{[u, w]}$	Basic Wavelet in the interval $u, w$
$\phi_{[u, w]}$	Wider step in the interval $u, w$
$\tilde{f}^{(n)}$	Sampled step function
$\varphi_n(x)$	Wavelet Packet
$X(f)$	Frequency content of the transmitted signal
$\theta$	Phase shift

## 1.1 Abstract

The demand for high data rate wireless multi-media applications has increased significantly in the past few years. The wireless user's pressure towards faster communications, no matter whether mobile, nomadic, or fixed positioned, without extra cost is nowadays a reality. To fulfill these demands, a new scheme which combines wireless digital modulation and multiple accesses was proposed in the recent years, namely, Multicarrier-Code Division Multiple Access (MC-CDMA).

The Fourier based OFDM uses the complex exponential bases functions and it is replaced by wavelets in order to reduce the level of interference. It is found that the Haar-based wavelets are capable of reducing the ISI and ICI, which are caused by the loss in orthogonality between the carriers. Further performance gains can be made by looking at alternative orthogonal basis functions and finding a better transform rather than Fourier and wavelet transform.

In this thesis, there are three proposed models [Model '1' (OFDM based on In-Place Wavelet Transform, Model '2' (MC-CDMA based on IP-WT and Phase Matrix) and Model '3' (MC-CDMA based on Multiwavelet Transform)] were created and then comparison their performances with the traditional models for single user system were compared under different channel characteristics (AWGN channel, flat fading and selective fading).

The conclusion of my study as follows, the models (1) was achieved much lower bit error rates than traditional models based FFT. Therefore these models can be considered as an alternative to the conventional MC-CDMA based FFT. The main advantage of using In-Place wavelet transform in the proposed models that it does not require an additional array at each sweep such as in ordered Fast Haar wavelet transform, which makes it simpler for implementation than FFT. The model (2) gave a new algorithm based on In-Place wavelet transform with first level processing multiple by PM was proposed. The model (3) gave much lower bit error than other two models in additional to traditional models.

## 1.2 Literature Survey

The first scheme for OFDM was proposed by Chang in 1966 [5, 6] for dispersive fading channels. OFDM was standardized as the European Digital Audio Broadcasting (DAB) as well as Digital Video Broadcasting (DVB) scheme [7]. The OFDM was used in recent third-generation mobile radio standard competition in Europe; also OFDM was recently selected as the High Performance Local Area Network (HIPERLAN) transmission technique as well as becoming part of IEEE 802.11 WLAN standard [6].

In the OFDM system the bandwidth is divided into high narrow sub-bands in which the mobile channel can be considered no dispersive. When the OFDM was developed, it was no channel equalizer is required and instead of implementing a bank of sub-channel modems, they can be conveniently implemented with the aid of a single Fast Fourier Transform (FFT) [6].

The employment of the Discrete Fourier Transform (DFT) to replace the banks of sinusoidal generators and the demodulators that had suggested by Weinstein and Ebert [8] in 1971, which significantly reduces the implementation complexity of OFDM modems, also they conceived the guard interval to avoid the Inter-Symbol Interference (ISI) and the Inter-Carrier Interference (ICI). This proposal opened a new era for OFDM.

In 1980, Hirosaki [9] had suggested an equalization algorithm in order to suppress both intersymbol and intercarrier interference caused by the channel impulse response or timing and frequency errors. Then he had analyzed the Orthogonal-Quadrature Amplitude Modulation (O-QAM) system in 1981 [10]. It has been shown that the validity of the digital signal processing where 16-point FFT is used, and the proposed method using  $N/2$  point DFT is more economical than the digitally implemented conventional single-channel data environment system.

The combination of multicarrier OFDM system with CDMA system was first introduced by Yee, et.al. [11], and then by Chouly, et.al. [12], and after that by Fettweis et.al. [13].

Fazel and Papke [14] had investigated convolution coding in conjunction with OFDM/CDMA. Parasad and Hara [15] compared various methods of combining the two techniques, identifying three different structures, namely MC-CDMA, Multi-

Carrier Direct Sequence CDMA (MC-DS-CDMA) and Multi-Tone CDMA (MT-CDMA).

The first wavelet systems were introduced by Alfred Haar [16,17]. Wavelet systems of the Haar type have been generalized to higher dimensions and high rank (multiplier  $>2$ ). The higher rank generalization leads naturally to the notion of the Haar wavelet matrices and their classifications.

Schott L. Miller [18] had investigated the Minimum Mean Square Error (MMSE) detection of MC-CDMA; he compared two different strategies for MMSE detection techniques, in the first one the MMSE filters are designed separately for each carrier, while in the other case the optimization of the filters is done jointly.

Shinsuke Hara and Ramjee Prasad [19] presented the advantages and disadvantages of MC-CDMA system. The transmitter/receiver structure and the bandwidth of transmitted signal spectrum are compared with those of a conventional DS-CDMA system, and a MC-CDMA design method, how to determine the number of subcarriers and the length of guard interval was discussed. The Bit Error Rate (BER) lower bounds for DS-CDMA and MC-CDMA systems are derived and their equivalence is theoretically demonstrated. The BER performance in downlink and uplink channels with frequency-selective Rayleigh fading was showed by computer simulation.

In 2000, [20] Mottier, and Castelain proposed and investigated a novel spreading sequence allocation procedure for MC-CDMA systems. This new technique, which relies on an analytical evaluation of the Multiple Access Interference (MAI), mitigates the interference between different users by optimizing the spreading sequence selection within a given spreading sequence family.

Eric Phillip [21] had investigated methods for maximizing the spectral efficiency of OFDM systems. As part of this, an investigation of detrimental effects on OFDM was presented; showing the effect of band pass filtering, the use of a raised cosine guard period, clipping distortion, time synchronization error, and frequency offset errors. Adaptive modulation independently optimizes the modulation scheme applied to each subcarrier so that the spectral efficiency is maximized, while maintaining a target Bit Error Rate (BER). The Signal-to-Noise Ratio (SNR) required maintaining a given BER, as compared with fixed modulation. Adaptive user allocation exploits the difference in frequency selective fading between users to optimize user subcarrier allocation.

Ramasamy (2003), [22] had investigated the multi-antenna receivers for OFDM and MC-CDMA systems, especially he investigated adaptive antenna algorithms for MC-CDMA for every different channel condition, frequency domain beamforming was studied in this research predominantly through simulation, and an alternative time domain beamforming was also studied.

Hongbing Zhang (2004), [23] developed and evaluated a wavelet packet based MC-CDMA wireless communication system. In this system design a set of wavelet packets are used as the modulation waveforms in a MC-CDMA system. The need for cyclic prefix is eliminated in the system design due to the good orthogonality and time-frequency localization properties of the wavelet packets. New detection algorithms are developed to work in either time domain or wavelet packet domain to combat multiuser and inter symbol interferences. He explored a new method of channel modeling by using wavelet packets as basis functions.

A high capacity, low complexity, and robust system design for a Successive Interference Cancellation (SIC) system was developed and analyzed in 2004 by Jeffrey G. and Teresa H. [24]. In addition, an optimal power control algorithm for MC-CDMA with SIC is derived, allowing analytical BER expressions to be found for an uncoded system. Low-rate forward error correcting codes are added to the system to achieve robustness. They have found that the capacity of the coded system approaches the additive white Gaussian noise capacity for SIC, even in a fading multipath channel with channel estimation error. This indicates that MC-CDMA is very attractive for systems employing SIC.

The implementation of OFDM transceiver on TMS320C6711 was done by Mustafa (2004), [25], where the soft radios is the proposed solution for implementing a robust and flexible Cyclic Prefix (CP) and Zero Padding-OFDM (CP-OFDM, ZP-OFDM) modulation on a digital signal processing, where Texas TMS320C6711 floating point processor was used. Great effort has been put to minimize loop size in OFDM structure to achieve efficient implementation.

The description of MC-CDMA system design process for indoor propagation scenarios was introduced by Sebastien [26]. The system specifications and simulations are firstly given, and then implementation aspects on a mixed, multi-DSP and Field Programmable Gate Array (FPGA) architecture are presented. In order to reduce development cycle, he proposed the use of efficient design to improve development steps such as complexity evaluation, system distribution according to the

architecture, and hardware-software code generation. Implementation results of the considered MC-CDMA system are given.

In 2004 Zhang, et. al. [27] carried out research on DFT-OFDM and Discrete Wavelet Transform-OFDM (DWT-OFDM) on different transmission scenarios. To combat ISI, and ICI, cyclic prefix is inserted between DFT-OFDM symbols, and this will take up nearly 25 percent of bandwidth. To improve the bandwidth efficiency and ISI, ICI, DWT-OFDM was proposed. The performance comparison of DFT-OFDM and DWT-OFDM on three different channel models was given in this paper. Simulation results show that DFT-OFDM and DWT-OFDM perform different when the transmission scenarios are different.

Acharya, et. al. stated in 2005, [28] that any system supporting broadband mobile services over wireless channels suffer from dispersion along time and frequency, and the transmission by spreading information along both these dimensions leads to diversity gain in each dimension. Hence, generalized two dimensional spreading schemes, in which symbol is transmitted across several subcarriers with a total power constraint and along each subcarrier it is spread with CDMA codeword.

In the same year [29] Kasliwal, et al, discussed the use of wavelets in OFDM. Normally OFDM is implemented using FFT and IFFT's. The FFT uses a rectangular window. A rectangular window produces high side lobes. This causes interference when the impairments are not compensated. However, they look at the replacement of Fourier transform by wavelet transform and the restrictions imposed by this and the condition on the wavelet construction.

A new modulation technique in the realization of OFDM, as well as the MC-DS-CDMA transceivers named as Finite Radon Transform (FRAT) was introduced by Omar Mowaffac [30]. The Radon transform is chosen in the OFDM structure to serve as a data mapper instead of the conventional data mapping techniques like Phase Sift Keying (PSK) and QAM schemes, in a way that ensures increasing the orthogonality of the system. He showed that the new application increases the orthogonality significantly in this case due to the use of IFFT twice, namely, in the data mapping and in the sub-carrier modulation.

The replacement of FFT with the multiwavelet transform for OFDM was introduced by Saad Nihad [31]. He introduced a new structure for OFDM based on multiwavelet transform. The performance was improved for such system under

different channel models, namely AWGN, flat fading and frequency selective fading. Then he examined the multiwavelet transform in MC-CDMA structure with a performance comparison for MC-CDMA based FFT or based on wavelet transform. In his simulation results the Multiwavelet transform outperforms the other two structures under different models of channels.

A Space Time Block Code-OFDM (STBC-OFDM) block has been studied extensively by Laith Ali [32], and a new structure for STBC-OFDM is proposed based on Multiwavelet transform. The proposed STBC-OFDM systems have been examined with different channel models AWGN, flat fading, and selective fading and he found that STBC-OFDM are able to improve the performance of the conventional OFDM system. This modification gave a significant improvement in the BER performance in comparison with the conventional OFDM and conventional FRAT.

Osama Q. J. [33] used in his research, a FRAT and Critically Sampling Discrete Multiwavelet Transform (CSDMWT) as a new mapper (instead of QPSK and QAM in conventional system), and modulator techniques (instead of IFFT in conventional system) respectively in the realization of OFDM, as well as being tested for the MC-CDMA transceivers. He found that the use of the two new schemes with each other is able to improve significantly the performance of the two proposed systems against the use of one of them alone. The existence of IFFT in the FRAT scheme makes it a good orthogonal mapper, which can strongly return the data after mapping, and the perfect properties that the Discrete Multiwavelet Transform (DMWT) has such as orthogonality, symmetry, and linearity, makes it a better modulation technique which can also demodulate the modulated data after denoising it with smallest error.

### **1.3 Aim of the Work**

In this thesis, a suggestion of four improvement models was discussed and simulated by Matlab version 7

1. Model '1' (OFDM based on In-Place Wavelet Transform)
2. Model '2' (MC-CDMA based on IP-WT and Phase Matrix)
3. Model '3' (MC-CDMA based on Multiwavelet Transform)
4. Model '4' (Dual-hop transmissions with fixed-gain relays over Generalized -Gamma fading channels)

## **1.4 Mobile radio channels**

The channels define as the electromagnetic media between the transmitter and the receiver. The most common channel model is the Gaussian channel, which is generally called the additive white Gaussian noise (AWGN) channel. The AWGN channel is simple and usually it is considered as the starting point to develop the basic system performance results. Under certain conditions, the channel cannot be classified as an AWGN channel but classified as a multipath fading channel.

In an ideal radio channel, the received signal would consist of only a single direct path signal, which is a perfect reconstruction of the transmitted signal. However, in a real channel, the signal is modified during transmission. The received signal consists of a combination of attenuated, reflected, refracted, diffracted replicas of the transmitted signal, and the delays associated with different signal paths in a multipath fading channel change in an unpredictable manner and can only be characterized statistically. However for all described before, the channel adds noise to the signal and can cause a shift in the carrier frequency if the transmitter, or receiver is moving (Doppler Effect). Understanding of these effects on the signal is important because the performance of a radio system is dependent on the radio channel characteristics.

### **1.4.1 Attenuation**

Attenuation is the drop in the signal power when transmitting from one point to another. It can be caused by the transmission path length, obstructions in the signal path, and multipath effects. Figure (1.1) shows some of the radio propagation effects that cause attenuation. Any objects which obstruct the line of sight (LOS) signal from the transmitter to the receiver can cause attenuation [37, 39].

The statistics describing the fading signal amplitude are frequently characterized as either Rayleigh or Ricean. Rayleigh fading occurs when there is no line of sight (LOS) component present in the received signal. If there is a LOS component present, the fading follows a Ricean distribution. There is frequently no direct LOS path to a mobile, because the very nature of mobile communications means that mobiles can be in a building or behind one or other obstructions. This leads to Rayleigh fading but also results in a shadow loss. These conditions, along

with the inherent variation in signal strength caused by changes in the distance between a mobile and cell site.

Shadowing of the signal can occur whenever there is an obstruction between the transmitter and receiver. It is generally caused by buildings and hills, and is the most important environmental attenuation factor. Shadowing is most severe in heavily built up areas, due to the shadowing from buildings. However, hills can cause a large problem due to the large shadow they produce. Radio signals diffract off the boundaries of obstructions, thus preventing total shadowing of the signals behind hills and buildings. To overcome the problem of shadowing, transmitters are usually elevated as high as possible to minimize the number of obstructions.

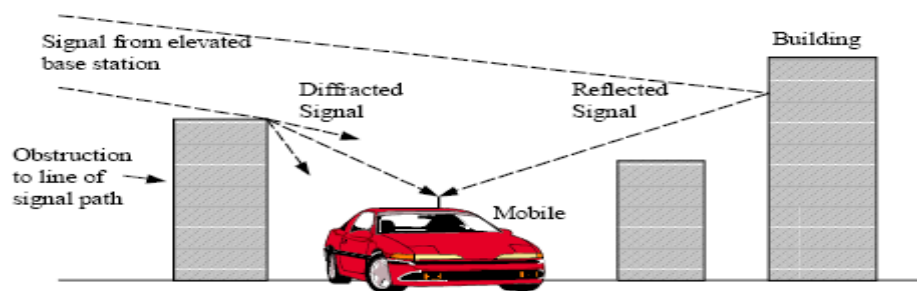


Figure 1.1 Radio Propagation Effects

### 1.4.2 Delay Spread

The received radio signal from a transmitter consists of typically a direct signal, plus reflections of object such as buildings, mountings, and other structures. In a digital system, the delay spread can lead to ISI. This is due to the delayed multipath signal overlapping with the following symbols. This can cause significant errors in high bit rate systems [37].

### 1.4.3 Doppler Shift

When a wave source and a receiver are moving relative to one another the frequency of the received signal will not be the same as the source. When they are moving toward each other the frequency of the received signal is higher than the source, and when they are approaching away each other the frequency decreases.

Doppler has the effect of shifting, or spreading, the frequency components of a signal. The coherence time of the channel is the inverse of the Doppler spread and is a measure of the speed at which the channel characteristics change. This in effect determines the rate at which fading occurs. When the rate of change of the channel is higher than the modulated symbol rate, fast fading occurs. Slow fading, on the other hand, occurs when the channel changes are slower than the symbol rate.

This is called the Doppler Effect. An example of this is the change of pitch in a car's horn as it approaches then passes by. This effect becomes important when developing mobile radio systems. The amount the frequency changes due to the Doppler Effect depends on the relative motion between the source and receiver and on the speed of propagation of the wave. The Doppler shift in frequency can be written:

$$f_d = f_c \times \frac{v}{c} \quad (1.1)$$

Where  $f_c$  is the carrier frequency,  $v$  is the speed of the source, and  $c$  is the speed of light [37].

#### 1.4.4 Multipath Effects

Multipath is a phenomenon that occurs as a transmitted signal is reflected by objects in the environment between the base station and a user. These objects can be buildings, trees, hills, or even trucks and cars. The reflected signals arrive at the receiver with random phase offsets, because each reflection generally follows a different path to reach the user's receiver. The result is random signal fades as the reflections destructively (and constructively) superimpose on one another, which effectively cancels part of the signal energy for brief periods of time. The degree of cancellation, or fading, will depend on the delay spread of the reflected signals, as embodied by their relative phases, and their relative power. Figure (1.2) shows the arrival of a signal and two multipath components.

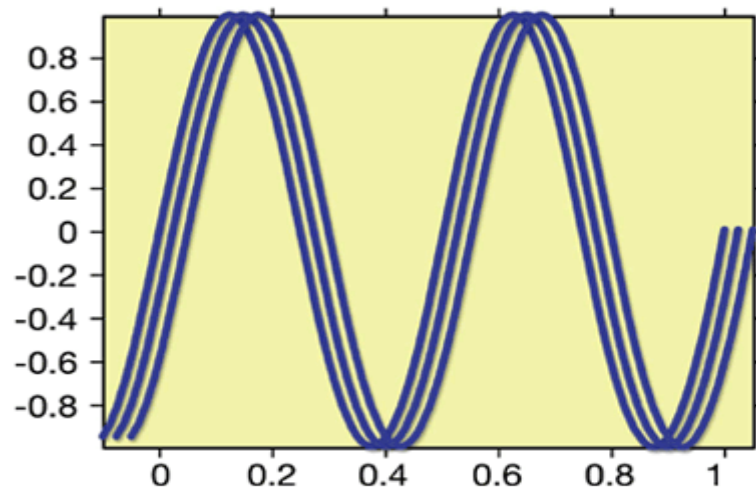


Figure 1.2 Examples of Time-Delayed Multipath Signals

The relative phase of multiple reflected signals can cause constructive or destructive interference at the receiver [37, 40].

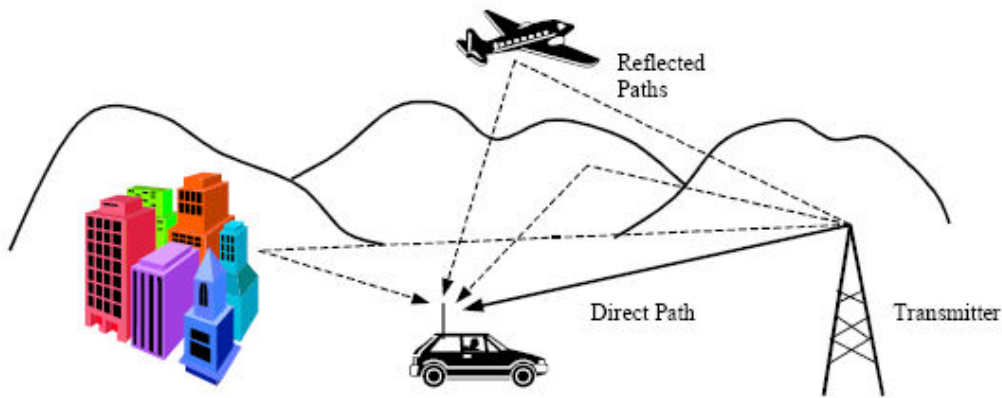


Figure 1.3 Multipath Signals

In many instances, the fading due to multipath will be frequency selective, randomly affecting only a portion of the overall channel bandwidth at any given time. Frequency selective fading occurs when the channel introduces time dispersion and when the delay spread exceeds the symbol period. When there is no dispersion and the delay spread is less than the symbol period, the fading will be flat, thereby affecting all frequencies in the signal equally.

The impulse response of a multi-path channel generally exhibits a delay spread. The actual multi-path intensity profile for a certain channel needs to be estimated to have the characteristics of the channel. For a single transmitted impulse, the time between the first and the last received components is called the maximum excess delay  $\tau_{max}$ . Beyond  $\tau_{max}$  the power will fall below certain threshold level and can be discarded without causing any significant error.

If the maximum excess delay  $\tau_{max}$  lasts longer than the signal symbol time interval  $T_s$ , it will generate the ISI distortion and the channel is said to be frequency selective fading. Otherwise if  $\tau_{max} < T_s$ , all the received multi-path components arrive within a symbol time interval. In this case there is no channel induced ISI distortion and the channel is said to be frequency nonselective or flat fading.

The multi-path phenomenon can also be specified in frequency domain. Another useful parameter of the multi-path fading channel is the reciprocal of the time spread, called the coherent bandwidth  $B_c$ . If frequency components within this bandwidth receive approximately the same attenuation and group delay, the channel is

said to be frequency nonselective. If the frequency components within the bandwidth often experience dramatically different attenuation and phase shift, the channel is frequency selective.

The coherent bandwidth  $B_c$  and maximum excess delay  $\tau_{max}$  are reciprocally related and can be calculated approximately with the knowledge of the other. The characteristics of a flat fading multi-path channel are shown in Figure (1.4). It can be seen that the coherence bandwidth is wider than the signal bandwidth, therefore all the signal frequency components are affected the same. In this situation the channel effect can be compensated easily [36].

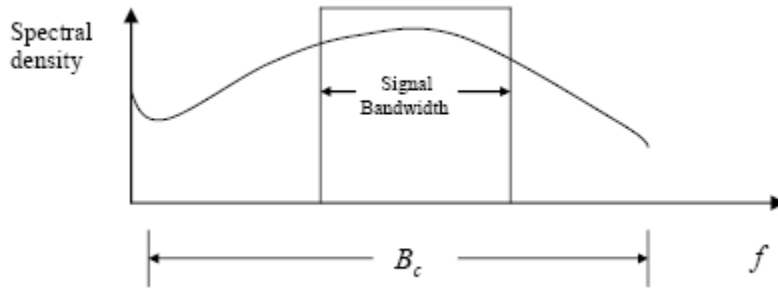


Figure 1.4 Flat fading multi-path channel

As the signal is assumed to be band-limited, the time delay line model can describe this multi-path phenomenon with time varying coefficients and a fixed tap spacing. If assumed that there are infinite scatters, then the channel impulse response can be considered to be complex Gaussian process. If there are multiple reflective paths and if there is no single dominant path, then the process is of zero mean and the envelope of such a received signal is statistically described by a Rayleigh probability density function and the channel is said to be Rayleigh fading.

If there is a single dominant path, then the process is of nonzero mean and the fading envelope is described by a Rician probability density function. In this case the channel is considered to be Rician fading. In practice, there are many channel models for wireless communication environments. In the present work, the wireless channel is assumed to be the Rayleigh fading channel as this channel model is simple and very common. The multi-path power profile is assumed to be exponential decaying.

The maximum channel delay spread lasts  $u$  samples, the coefficients of  $a_0, a_1, \dots, a_u$  are the attenuations of the different paths. These coefficients are Rayleigh distributed random variables. The delay  $T_s$  denotes the unit sample delay. The output of the multi-path channel can be expressed as follows:

$$y(n) = \sum_{i=0}^u a_i x(n-i) \quad (1.2)$$

Taking the AWGN noise  $z(n)$  into account, the received signal can be written as:

$$y(n) = \sum_{i=0}^u a_i x(n-i) + z(n) \quad (1.3)$$

It can be seen from the above equation that the multi-path fading affects  $u$  samples. This will introduce ISI/ICI if no anti-measure is employed at the receiver [36].

The delay spread can cause ISI, when adjacent data symbols overlap and interfere with each other due to different delays on different propagation paths. The number of interfering symbols in a single carrier modulated system is given by

$$N_{ISI, \text{single carrier}} = \frac{\tau_{\max}}{T_s} \quad (1.4)$$

For high data rate applications with very short symbol duration  $T_s < \tau_{\max}$ , the effect of ISI can increase significantly. If the duration of the transmitted symbol is significantly larger than the maximum delay  $T_s \gg \tau_{\max}$ , the channel produces a negligible amount of ISI. This effect is exploited with multi-carrier transmission where the duration of the transmitted symbol increases with the number of sub-carrier  $N$  and, hence, the amount of ISI decreases. The number of the interfering symbols in a multicarrier modulated system is given by

$$N_{ISI, \text{multi carrier}} = \frac{\tau_{\max}}{N T_s} \quad (1.5)$$

There are various discrete multi-path channel models for indoor and outdoor cellular systems with different cell sizes have been specified. These channel models define the statistics of the discrete propagation paths.

## 1.5 Channel Models

A brief description of the statistical models of fading multipath channels are described now, these are frequently used in the analysis and design of communication systems [64].

### 1.5.1 The Scattering Function and Related Channel Parameters

A fading multipath channel is generally characterized as a linear, time-varying system having an impulse response  $c(t, \tau)$  or a time-varying frequency response  $c(t, f)$ . Time variations in the channel impulse response or frequency response result in frequency spreading, generally called Doppler spreading, of the signal transmitted through the channel. Multipath propagation results in spreading the transmitted signal in time. Consequently, a fading multipath channel may be generally characterized as a doubly spread channel in time and frequency.

By assuming that the multipath signals propagating through the channel at different delays are uncorrelated, a doubly spread channel may be characterized by the scattering function  $S(\tau, \lambda)$ , which is a measure of the power spectrum of the channel at delay and frequency offset (relative to the carrier frequency). From the scattering function, one can obtain the delay power spectrum of the channel by simply averaging  $S(\tau, \lambda)$  over  $\lambda$ , i.e.

$$S_c(\tau) = \int_{-\infty}^{\infty} S(\tau; \lambda) d\lambda \quad (1.6)$$

Similarly, the Doppler power spectrum is

$$S_c(\lambda) = \int_0^{\infty} S(\tau; \lambda) d\tau \quad (1.7)$$

The range of values over which the delay power spectrum  $S_c(\tau)$  is nonzero is defined as the multipath spread  $T_m$  of the channel. Similarly, the range of values over which the Doppler power spectrum  $S_c(\lambda)$  is nonzero is defined as the Doppler spread  $B_d$  of the channel. The value of the Doppler spread  $B_d$  provides a measure of how rapidly the channel impulse response varies in time. The larger the value of  $B_d$ , the more rapidly the channel impulse response is changing with time. This leads us to define another channel parameter, called the channel coherence time  $T_{coh}$  as

$$T_{coh} = \frac{1}{B_d} \quad (1.8)$$

Thus a slowly fading channel has a large coherence time and a fast fading channel has a small coherence time [65].

In a similar manner, the channel coherence bandwidth  $B_{coh}$  can be defined as the reciprocal of the multipath spread, i.e.

$$B_{coh} = \frac{1}{T_m} \quad (1.8)$$

$B_{coh}$  Provides us with a measure of the width of the band of frequencies which are similarly affected by the channel response, i.e., the width of the frequency band over which the fading is highly correlated.

The product  $T_m B_d$  is called the spread factor of the channel. If  $T_m B_d < 1$ , the channel is said to be underspread; otherwise, it is overspread. Generally, if the spread factor  $T_m B_d \ll 1$ , the channel impulse response can be easily measured and that measurement can be used at the receiver in the demodulation of the received signal and at the transmitter to optimize the transmitted signal. Measurement of the channel impulse response is extremely difficult and unreliable, if not impossible, when the spread factor  $T_m B_d > 1$  [64].

### 1.5.2 Frequency-Nonselective Channel: Multiplicative Channel Model

Let us now consider the effect of the transmitted signal characteristics on the selection of the channel model that is appropriate for the specified signal. Let  $x(t)$  be the equivalent low pass signal transmitted over the channel and let  $X(f)$  denote its frequency content. Then, the equivalent low pass received signal, exclusive of additive noise is:

$$r(t) = \int_{-\infty}^{\infty} c(t; \tau) x(t - \tau) d\tau = \int_{-\infty}^{\infty} C(t; f) X(f) e^{j2\pi ft} df \quad (1.9)$$

Now, suppose that the bandwidth  $W$  of  $X(f)$  is much smaller than the coherence bandwidth of the channel.  $W \ll B_{coh}$ , then all the frequency components of  $X(f)$  undergo the same attenuation and phase shift in transmission through the channel. But this implies that, within the bandwidth  $W$  occupied by  $X(f)$ , the time-variant

transfer function  $C(t,f)$  of the channel is constant in the frequency variable. Such a channel is called frequency-nonselctive or *flat fading*.

For the frequency-nonselctive channel, (1.9) simplifies to

$$r(t) = C(t;0) \int_{-\infty}^{\infty} X(f) c^{j2\pi ft} df = C(t)x(t) = \alpha(t) c^{j\theta(t)} x(t) \quad (1.10)$$

Where, by definition,  $C(t;0) = \alpha(t)e^{j\theta(t)}$ ,  $\alpha(t)$  represents the envelope and  $\theta(t)$  represents the phase of the equivalent lowpass channel response.

Thus the frequency-nonselctive fading channel has a time-varying multiplicative effect on the transmitted signal. In this case, the multipath components of the channel are not resolvable because the signal bandwidth  $W \ll B_{coh} = 1/T_m$ . equivalently,  $T_m \ll 1/W$ . Fig. (1.5) illustrates the multiplicative channel model.

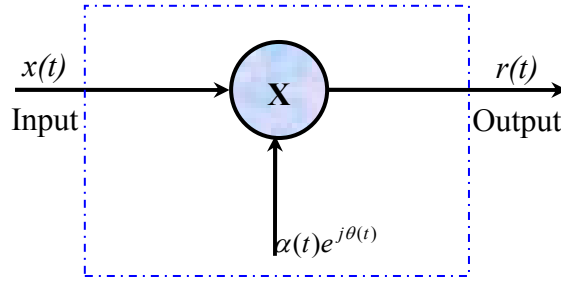


Figure 1.5 the Multiplicative Channel Model

A frequency-nonselctive channel is said to be slowly fading if the time duration of a transmitted symbol, defined as  $T_s$ , is much smaller than the coherence time of the channel,  $T_s \ll T_{coh}$ . Equivalently,  $T_s \ll 1/B_d$  or  $B_d \ll 1/T_s$ . since in general, the signal bandwidth  $W \geq 1/T_s$ , it follows that a slowly fading frequency-nonselctive channel is underspread. It may also define a rapidly fading channel as one which satisfies the relation  $T_s \geq T_{coh}$ .

### 1.5.3 Frequency-Selective Channel: The Tapped Delay Line Channel Model

When the transmitted signal  $X(f)$  has a bandwidth  $W$  greater than the coherence bandwidth  $B_{coh}$  of the channel, the frequency components of  $X(f)$  with frequency separation exceeding  $B_{coh}$  are subjected to different gains and phase shifts. In such case, the channel is said to be frequency selective. Additional distortion is caused by the time variations in  $C(t,f)$ , which is the fading effect that is evidenced as a time variation in the received signal strength of the frequency components in  $X(f)$ .

When  $W \gg B_{\text{coh}}$ , the multipath components in the channel response that are separated in delay by at least  $1/W$  are resolvable. In this case the representation of the time-varying channel impulse response is [64, 65]

$$C(t; \tau) = \sum_{n=1}^L c_n(t) \delta(\tau - n/W) \quad (1.11)$$

and the corresponding time-variant transfer function as

$$C(t; f) = \sum_{n=1}^L c_n(t) e^{j2\pi f n/W} \quad (1.12)$$

where  $C_n(t)$  is the complex valued channel gain of the  $n$ th multipath component and  $L$  is the number of resolvable multipath components. Since the multipath spread is  $T_m$  and the time resolution of the multipath is  $1/W$ , it follows that

$$L = \lceil T_m W \rceil + 1. \quad (1.13)$$

A channel having the impulse response given by (1.12) may be represented by a tapped-delay line with  $L$  taps and complex-valued, time varying tap coefficients  $C_n(t)$ . The randomly time varying tap gains  $C_n(t)$  may also be represented by:

$$c_n(t) = \alpha_n(t) e^{j\theta_n(t)} \quad (1.14)$$

Where  $\alpha_n(t)$  represents the amplitude and  $\theta_n(t)$  represents the corresponding phase.

Fig. (1.6) illustrates the tapped-delay-line channel model that is appropriate for the frequency selective channel.

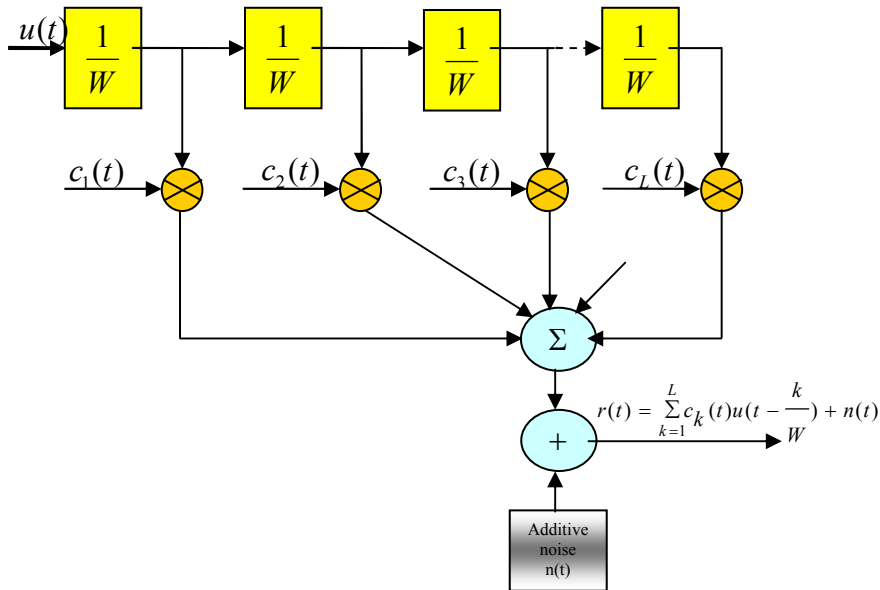


Figure 1.6 Tapped-Delay-Line channel model

## **2 Chapter two**

In order to provide a high data rate and high quality digital communication system is required in a restricted bandwidth. A major limiting factor is, however, the multipath propagation phenomenon. It causes frequency-selective fading due to different echoes of transmitted symbols overlapping at the receiving end, which can lead to the bit-error-rate (BER) degradation. One way to effectively combat the multipath channel impairments and still provide high-data rates in a limited bandwidth is use of an (OFDM) system.

### **2.1 Code-Division Multiple Access (CDMA)**

CDMA has been a strong candidate to support multimedia mobile services because it has the ability to cope with the asynchronous nature of the multimedia traffic and can provide higher capacity as opposed to the conventional access schemes such as TDMA or FDMA. By employing Rake receivers CDMA systems can coherently combine the multipath components due to the hostile frequency selective channel. The processing gain due to spreading provides robustness to the multi-user interference. The use of conventional CDMA does not seem to be realistic when the data rates go up to a hundred megabits per second due to severe ISI and the difficulty in synchronizing a fast sequence. Techniques for reducing the symbol and chip rate are essential in this case.

The CDMA allows the transmission of different users in parallel by allocating to each one a distinct spreading sequence, which is uncorrelated with the sequences of other users. CDMA has emerged as the most important multiple access technology for second- and third-generation (2-3G) wireless systems exemplified by its popularity in several major mobile cellular standards. Technical requirements in future gigabit wireless systems will be very different from 2-3G mobile cellular systems, which were developed basically for low-speed continuous traffic, although recently some more emphasis has been given to data applications such as stationary image transmissions and low-rate video streaming.

The appreciation of CDMA technologies in the 2-3G systems is partly due to the fact that they provide on average higher bandwidth efficiency than do any other multiple access techniques, so that one of the most important characteristics of CDMA is that it allows users in a cell to send their information at the same frequency and time simultaneously by using different codes as shown in Figure (2.1). Therefore, orthogonality among CDMA codes or sequences plays a critical role.

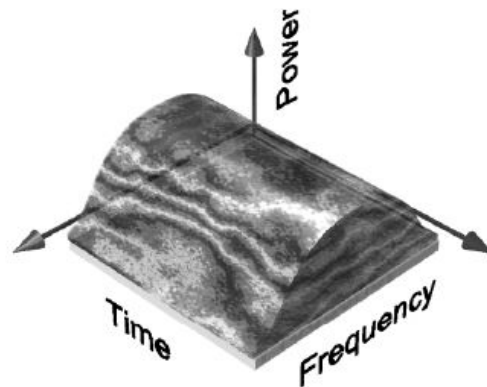


Figure 2.1 Code division multiple access (CDMA)

Figure (2.1) shows the general use of the spectrum using CDMA, and the process of a CDMA transmission is shown in Figure (2.2) where the data to be transmitted (a) is spread before transmission by modulating the data using a pseudo noise sequence (PN sequence) (PN code). This broadens the spectrum as shown in (b). Part (c) shows the received signal. This consists of the required signal, plus background noise, and any interference from other CDMA users or radio sources. The received signal is recovered by multiplying the signal by the original spreading code. This process causes the wanted received signal to be de-spread back to the original transmitted data. However, all other signals which are uncorrelated to the PN spreading code used become more spread. The wanted signal in (d) is then filtered removing the wide spread interference and noise signals.

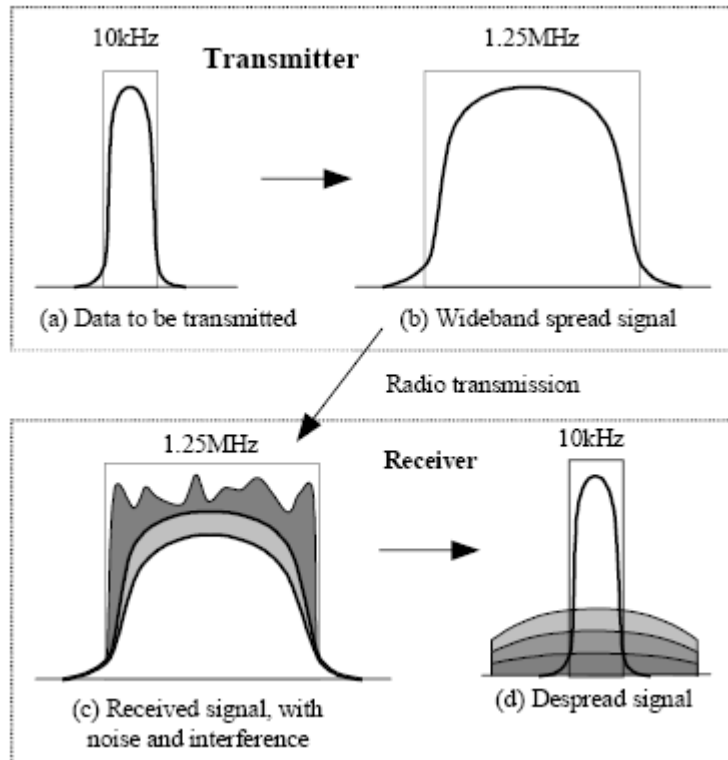


Figure 2.2 Basic CDMA transmissions

## 2.2 Orthogonal Frequency Division Multiplexing (OFDM)

Orthogonal Frequency Division Multiplexing (OFDM) is special form of multi-carrier modulation, patented in 1970. It is particularly suited for transmission over a dispersive channel.

OFDM is a combination of modulation and multiplexing:

Modulation – a mapping of the information on changes in the carrier phase, frequency or amplitude or combination.

Multiplexing – method of sharing a bandwidth with other independent data channels (multiplexing is applied to independent signals but these signals are a sub-set of the main signal). In OFDM the signal itself is first split into independent channels, modulated by data and then re-multiplexed to create the OFDM carrier.

OFDM is a special case of Frequency Division Multiplex (FDM). A (FDM) is like water flow out of a faucet, in contrast the OFDM signal is like a shower. In a faucet all water comes in one big stream and cannot be sub-divided. OFDM shower is made up of a lot of little streams.

Think about what the advantage might be of one over the other? One obvious one is that if I put my thumb over the faucet hole, I can stop the water flow but I cannot do the same for the shower.



Fig. 2.3(a) A regular FDM single carrier

(b) OFDM same amount of water coming from a lot of small streams.

In a multipath channel, most conventional modulation techniques are sensitive to intersymbol interference unless the channel symbol rate is small compared to the delay spread of the channel. OFDM is significantly less sensitive to intersymbol interference, because a special set of signals is used to build the composite transmitted signal. The basic idea is that each bit occupies a frequency-time window which ensures little or no distortion of the waveform. In practice, it means that bits are transmitted in parallel over a number of frequency-nonselective channels. OFDM has recently been applied widely in wireless communication systems due to its high data rate transmission capability with high bandwidth efficiency, it requires a relatively simple equalizer at the receiver can reduce or eliminate (ISI, ICI) and it is particularly suitable for transmission over multipath fading channels.

The main idea of using OFDM is to avoid problems caused by multipath reflections by sending the message bits slowly enough so that any delayed copies (reflections) are late by only a small fraction of a bit time. To maintain a high bit rate, multiple carriers are used to send many low speed messages at the same time which can be combined at the receiver to make up one high speed message. In this way, the

distortion caused by reflections can be avoided. If single carrier communication systems (SCCM) is used instead of OFDM, then the delayed copies of bits will be mixed together by the multipath, and the multipath distortion must be cancelled out using a so-called equalizer, i.e. the idea behind it is to divide the frequency selective channel into a number of parallel, frequency flat sub-channels.

An introduction to OFDM is given in [34], and [35], which presents the basic concepts of OFDM and its applications. Multicarrier techniques can provide high data rate at reasonable receiver complexities and increasingly becoming popular in audio/video broadcasting, mobile local area networks and future generation wideband cellular systems.

OFDM is a spectrum efficient kind of multicarrier transmission technique based on the discrete Fourier transform. By using a DFT, the whole bandwidth will be split into  $N$  sub-channels. As a result, a high data stream will be transformed into  $N$  low rate streams, which are transmitted over different sub-channels. OFDM symbols, which contain several modulation symbols, are formed as linear combinations of mutually orthogonal complex exponentials of finite duration [36].

### **2.3 The Importance of Orthogonality**

The “Orthogonal” part of the OFDM name indicates that there is a precise mathematical relationship between the frequencies of the carriers in the system. In a normal FDM system, the many carriers are spaced apart in such way that the signals can be received using conventional filters and demodulators. In such receivers, guard bands have to be introduced between the different carriers as shown in Figure (2.5), and the introduction of these guard bands in the frequency domain results in lowering the spectrum efficiency. It is possible, however, to arrange the carriers in an OFDM signal so that the sidebands of the individual carriers overlap and the signals can still be received without adjacent carrier interference. In order to do this the carriers must be mathematically orthogonal.

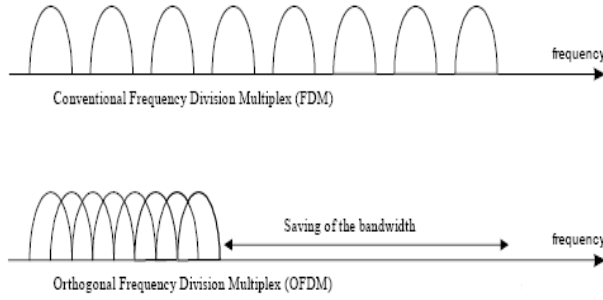


Figure (2.5) Comparison of the bandwidth utilization for FDM and OFDM

The main concept in OFDM is orthogonality of the sub-carriers. Since the carriers are all sine/cosine wave, we know that area under one period of a sine or a cosine wave is zero. In OFDM we have  $N$  carriers,  $N$  can be anywhere from 16 to 1024 in present technology and depends on the environment in which the system will be used.

Mathematically, suppose that  $F$  represents a set of signals, where  $F_p$  is the  $p$ -th element in the set. The signals are orthogonal if

$$\int_a^b F_p(t)F_q^*(t)dt = \begin{cases} K & \text{for } p=q \\ 0 & \text{for } p \neq q \end{cases} \quad (2.1)$$

where the (\*) indicates the complex conjugate and interval  $[a,b]$  is a symbol period. A fairly simple mathematical proof exists, that the series  $\sin(mx)$  for  $m=1,2,\dots$  is orthogonal over the interval  $(-\pi$  to  $-\pi)$ .

Mathematically, each carrier can be described as a complex wave:

$$S_c(t) = A_c(t)e^{j[\omega_c t + \phi_c(t)]} \quad (2.2)$$

The real signal is the real part of  $S_c(t)$ . Both  $A_c(t)$  and  $\phi_c(t)$ , the amplitude and phase of the carrier respectively, can vary on a symbol by symbol basis. The values of the parameters are constant over the symbol duration period  $T_s$ . OFDM consists of many carriers. Thus the complex signals  $S_s(t)$  is represented by equation (2.3), and shown in Figure (2.6):

$$S_s(t) = \frac{1}{N} \sum_{n=0}^{N-1} A_N(t)e^{j[\omega_n t + \phi_n(t)]} \quad (2.3)$$

where

$$\omega_n = \omega_0 + n\Delta\omega \quad (2.4)$$

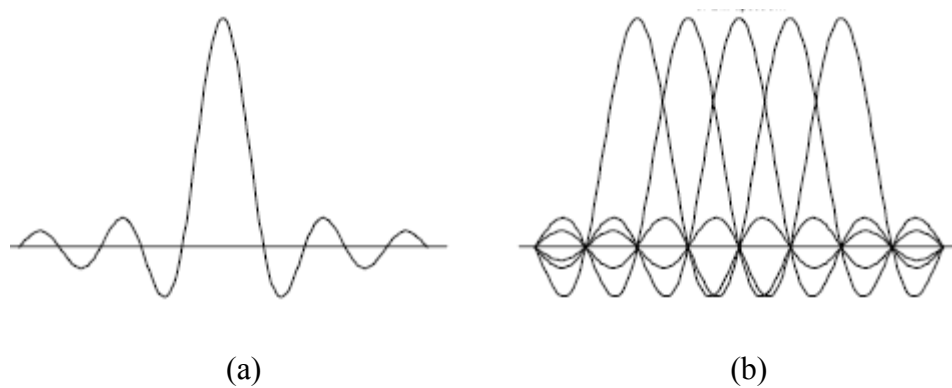


Figure (2.6) Examples of OFDM spectrum (a) a single sub-channel, (b) 5 carriers, so that at the central frequency of each sub-channel, there is no crosstalk from other sub-channels.

This is of course a continuous signal. If the waveforms of each component of the signal is considered over one symbol period, then the variables  $A_c(t)$  and  $\phi_c(t)$  take on fixed values, which depend on the frequency of that particular carrier, and so can be rewritten:

$$\begin{aligned} \phi_n(t) &\Rightarrow \phi_n \\ A_n(t) &\Rightarrow A_n \end{aligned} \quad (2.5)$$

If the signal is sampled using a sampling frequency of  $1/T$ , then the resulting signal is represented by:

$$S_s(kT) = \frac{1}{N} \sum_{n=0}^{N-1} A_n e^{j[\omega_0 + n\Delta\omega]kT + \phi_n} \quad (2.6)$$

At this point, the restriction of the time over which the analysis of the signal to  $N$  samples should be done. It is convenient to sample over the period of one data symbol, so that

$$T_s = NT \quad (2.7)$$

Simplifying equation (2.6), without a loss of generality by letting  $\omega_0=0$ , then the signal becomes:

$$S_s(kT) = \frac{1}{N} \sum_{n=0}^{N-1} A_n e^{j\phi_n} e^{j(n\Delta\omega)kT} \quad (2.8)$$

Now equation (2.8) can be compared with the general form of the inverse Fourier transform:

$$g(kT) = \frac{1}{N} \sum_{n=0}^{N-1} G\left(\frac{n}{NT}\right) e^{j2\pi nk/n} \quad (2.9)$$

In equation (2.8), the function  $A_n e^{j\phi_n}$  is no more than a definition of the signal in the sampled frequency domain, and  $S_s(kT)$  is the time domain representation. Equations (2.8) and (2.9) are equivalent if

$$\Delta f = \frac{\Delta\omega}{2\pi} = \frac{1}{NT} = \frac{1}{T_s} \quad (2.10)$$

This is the same condition that was required for orthogonality. Thus, one consequence of maintaining orthogonality is that the OFDM signal can be defined by using Fourier transform procedures.

The fast Fourier transform (FFT) is merely a rapid mathematical method for computer applications of DFT. It is the availability of this technique, and the technology that allows it to be implemented on integrated circuits at a reasonable price, that has permitted OFDM to be developed as far as it has. The process of transforming from the time domain representation to the frequency domain representation uses the Fourier transform itself, whereas the reverse process uses the inverse Fourier transform.

### 2.3.1 Create the OFDM symbol

The equation (2.11) is an essentially an Inverse FFT.

$$c(t) \sum_{n=1}^N m_n(t) \sin(2\pi mt) \quad (2.11)$$

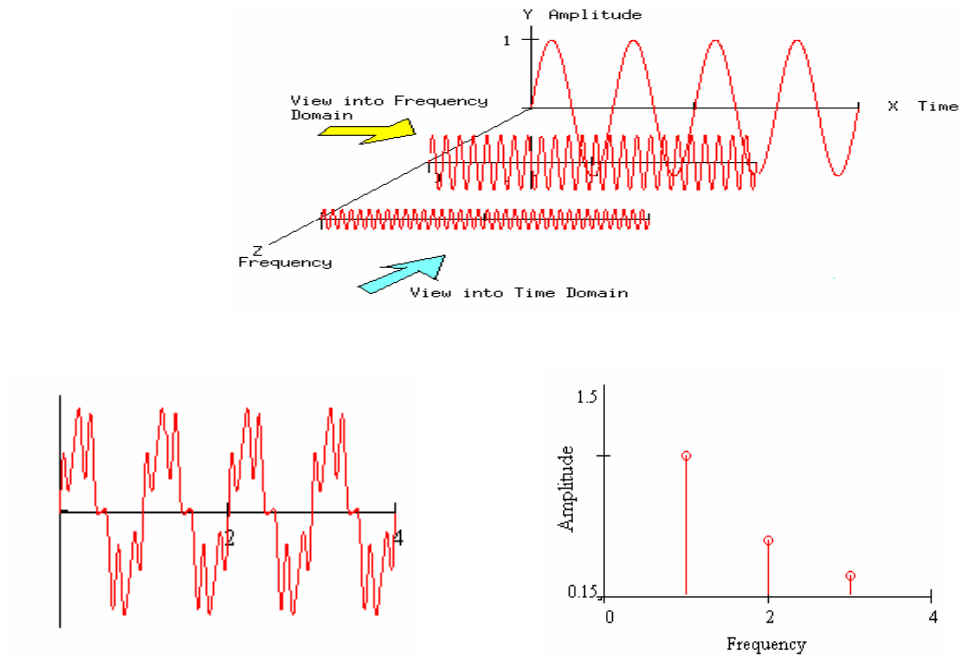


Figure 2.7(a) Time domain view (b) Frequency domain view

Forward FFT takes a random signal, multiplies it successively by complex exponentials over the range of frequencies, sums each product and plots the results as a coefficient of the frequency. The coefficients are called a spectrum and represent how much of that frequency is present in the input signal.

We can write FFT in sinusoids as

$$x(k) = \sum_{n=0}^{N-1} x(n) \sin\left(\frac{2\pi kn}{N}\right) + j \sum_{n=0}^{N-1} x(n) \cos\left(\frac{2\pi kn}{N}\right) \quad (2.12)$$

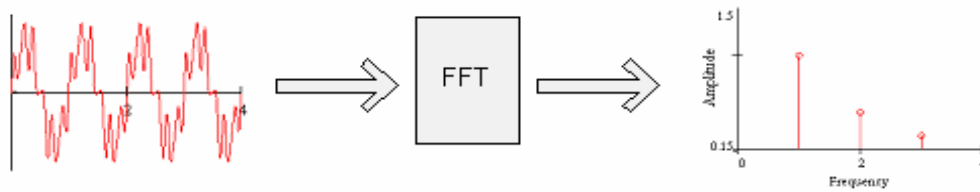
Here  $x(n)$  are the coefficients of the sines and cosines of frequency  $\frac{2\pi K}{N}$ , where  $k$  is the index of the frequencies over the  $N$  frequencies, and  $n$  is the time index

The inverse FFT takes this spectrum and converts the whole thing back to time domain signal by again successively multiplying it by a range of sinusoids

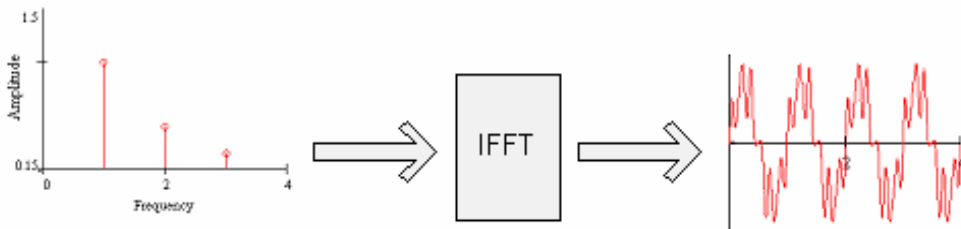
The equation for IFFT is

$$x(n) = \sum_{k=0}^{N-1} x(k) \sin\left(\frac{2\pi kn}{N}\right) - j \sum_{k=0}^{N-1} x(k) \cos\left(\frac{2\pi kn}{N}\right) \quad (2.13)$$

The difference between Eq. (2.12) and (2.13) is the type of coefficients the sinusoids are taking, and the minus sign, The coefficients by convention are defined as time domain samples  $x(k)$  for the FFT and  $X(n)$  frequency bin values for the IFFT



(a) A time domain signal comes out as a spectrum out of FFT



(b) A frequency domain signal comes out as a time domain signal out of IFFT

Figure 2.8

## 2.4 Basic OFDM Transmitter Analysis

In OFDM each carrier is orthogonal to each other. Figure (2.9) represents a simple block diagram of OFDM which is used here for the analysis [53].

$$\text{Here, } \frac{1}{T} \int_0^T e^{j2\pi(f_j - f_k)t} dt = \begin{cases} 1, & j = k \\ 0, & j \neq k \end{cases} \quad (2.14)$$

so,  $f_j - f_k = n/T$ , in this case the carriers are minimally separated with frequency spacing  $= 1/T$ . It is assumed that  $f_k = k/T = k/NT_s$ , then

$$x(t) = \frac{1}{\sqrt{T}} \sum_{k=0}^{N-1} S_k(n) e^{j2\pi f_k t} = \frac{1}{\sqrt{T}} \sum_{k=0}^{N-1} S_k(n) e^{j2\pi \frac{k}{NT_s} t}, \quad nT \leq t < (n+1)T \quad (2.15)$$

If the signal  $x(t)$  is sampled at time instances  $nT_s = nT/N$ , then

$$x(n) = c(nT_s) = \frac{1}{\sqrt{T}} \sum_{k=0}^{N-1} S_k(n) e^{j2\pi \frac{kn}{N}} \quad (2.16)$$

$x(n)$  is IDFT of  $S_k(n)$ . By taking the Fourier transform of  $x(t)$ , leads to:

$$X(f, nT) = \frac{1}{\sqrt{T}} \int_{nT}^{(n+1)T} x(t) e^{-j2\pi f t} dt = e^{-j\left[2\pi(n+1/2)fT - \frac{\pi}{2}\right]} \sum_{k=0}^{N-1} S_k(n) \text{sinc}(fT - k). \quad (2.17)$$

Notice that the symbol  $S_k(n)$  is obtained by sampling  $X(f, nT)$  at  $f = k/T$ ,

$$X\left(\frac{k}{T}, nT\right) = S_k(n). \quad k = 0, 1, 2, \dots, N-1 \quad (2.18)$$

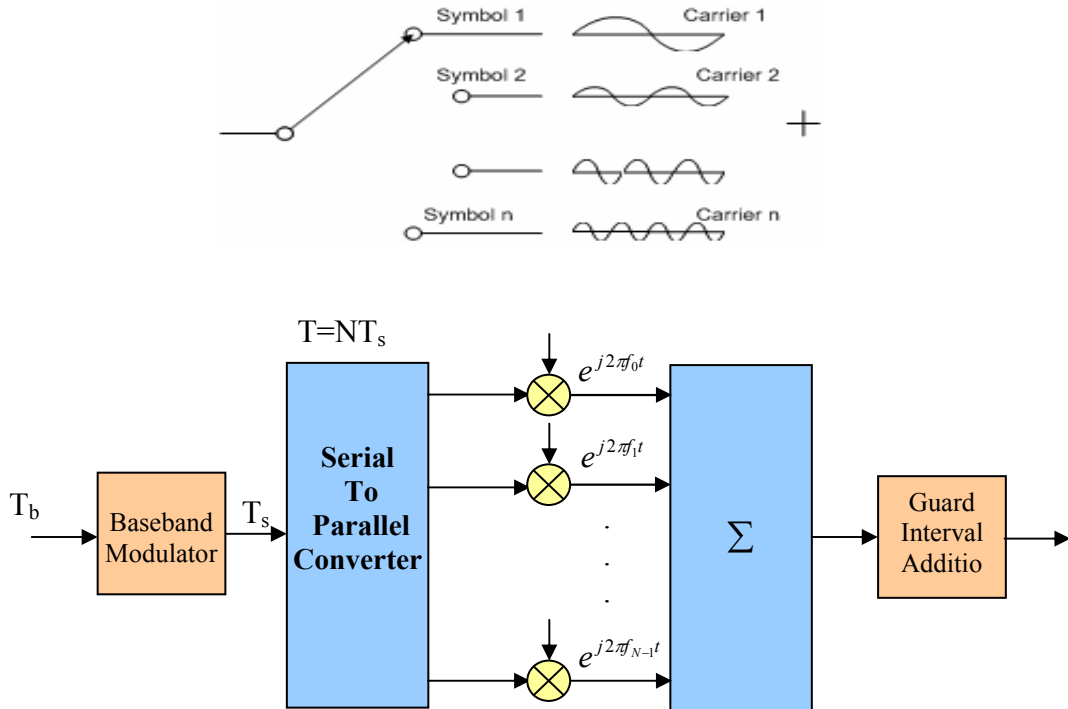


Figure (2.9) Basic OFDM transmitter system

## 2.5 Basic OFDM Receiver Analysis

The OFDM demodulator is composed of  $N$  correlators, and each is centered on a different sub-carrier frequency. The received sample at sub-carrier  $k$  can be written as:

$$y_k(n) = \frac{1}{\sqrt{T}} \int_{nT}^{(n+1)T} y(t) e^{-j2\pi\frac{k}{T}t} dt = x_k(n)h_k(n) + \eta_k(n) \quad (2.19)$$

Here  $x_k(n)$  is the transmitted signal,  $h_k(n)$  is the frequency response of channel,  $\eta_k(n)$  is the complex Gaussian random variable with zero mean. Figure (2.10) shows the block diagram of simple OFDM receiver.

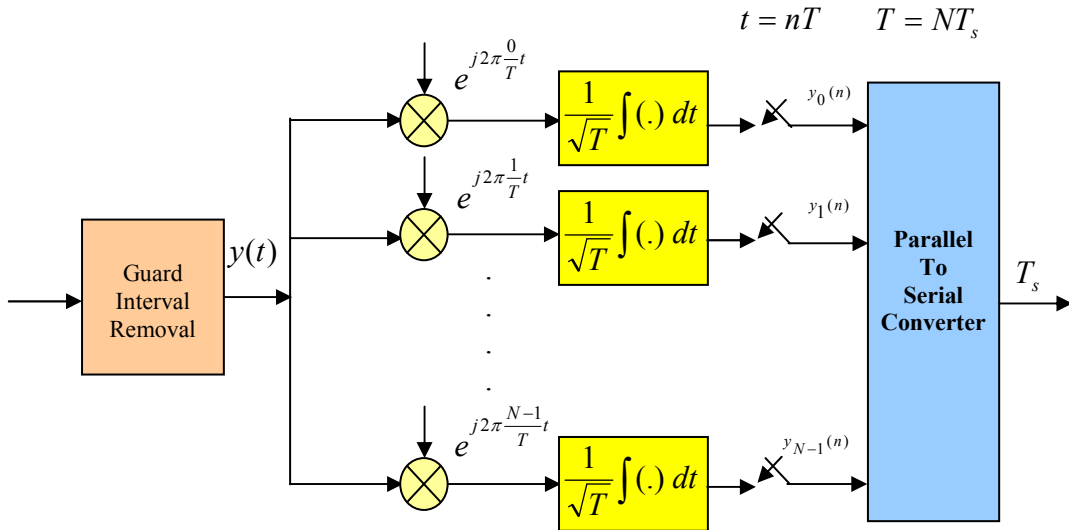


Figure (2.10) Basic OFDM receiver system

From fig. (2.11), it is easy to find that in an idealized OFDM system, sub-channels can be considered as parallel Gaussian channels under the assumption of perfect time and carrier synchronization and perfect suppression of multipath by guard interval. Thus after the equalization at the receiver, the output of  $k^{\text{th}}$  sub-carrier can be written as:

$$r_k(n) = x_k(n) + \frac{h_k^*(n)}{|h_k(n)|^2} \eta_k(n) \quad (2.20)$$

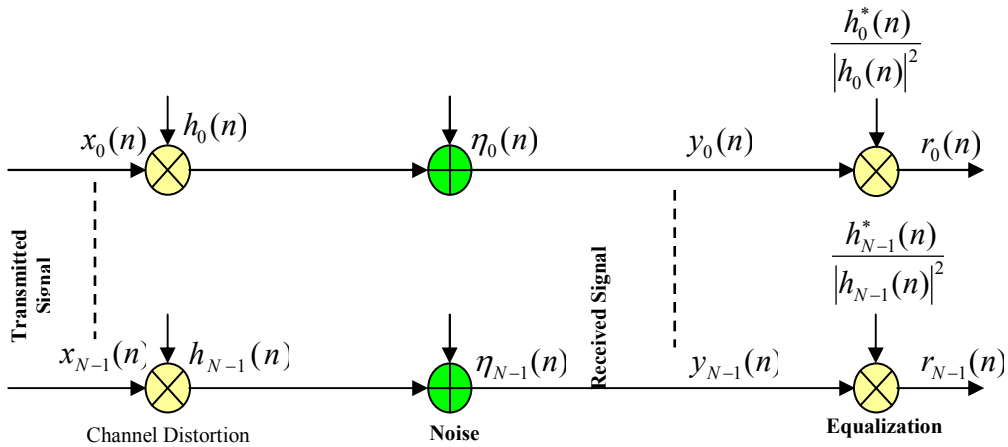


Figure (2.11) Transmitted OFDM symbol over sub-channels

OFDM has a strong ability to reduce ISI on frequency-selective channels, especially when data transmission is at a high bit-rate. Nowadays, OFDM is proposed to be applied in many fields, such as digital audio and video broadcasting systems (DAB and DVB), digital subscriber lines (DSL), and wireless local area networks (WLAN) [54], etc.

## 2.6 OFDM System Difficulties

While OFDM transmission over mobile communications channels can alleviate the problem of multipath propagation, recent research efforts have focused on solving a set of inherent difficulties regarding OFDM, namely the peak-to-mean power ratio, time and frequency synchronization, and on mitigating the effects of the frequency selective fading channel. These issues are addressed below in more depth [6].

### 2.6.1 Peak-to-Mean Power Ratio

It is plausible that the OFDM signal-which is the superposition of a high number of modulated sub-channel signals, may exhibit a high instantaneous signal peak with respect to the average signal level. Furthermore, large signal amplitude swings are encountered, when the time domain signal traverses from a low instantaneous power waveform to a high power waveform, which may result in a high Out-Of-Band (OOB) harmonic distortion power, unless the transmitter power amplifier exhibits an extremely high linearity across the entire signal level range, as discussed in [37]. Then this potentially contaminates the adjacent channels with adjacent channel interference.

Practical amplifiers exhibit a finite amplitude range, in which they can be considered near-linear. In order to prevent severe clipping of the high OFDM signal peaks, which is the main source of OOB emissions, the power amplifier must not be driven into saturation and hence it is typically operated with a certain so-called back-off, creating a certain “headroom” for the signal peaks, which reduces the risk of amplifier saturation and OOB emission. Two different families of solutions have been suggested in the literature, in order to mitigate these problems, either reducing the peak-to-mean power ratio, or improving the amplification stage of the transmitter. OFDM systems with increased robustness to non-linear distortion have been proposed [38, 39].

### **2.6.2 Synchronization**

Time and frequency synchronization between the transmitter and the receiver is not of crucial importance as regards the performance of an OFDM link [40, 41]. A wide variety of techniques have been proposed for estimating and correcting both timing and carrier frequency offsets at the OFDM receiver. Rough timing and frequency acquisition algorithms relying on known pilot symbols or pilot tones embedded into OFDM symbols have been suggested [42, 43].

## **2.7 OFDM System Model**

The simulation Model of OFDM is shown in Fig. (2.12). The input data stream is first mapped into Quadrature Amplitude Modulation (QAM) according to the QAM constellation map, then the output complex is converted from serial to parallel into N-points IFFT to generate the OFDM symbol. The output data from the IFFT is now converted from parallel to serial and a cyclic prefix is added. The data are sent to the receiver over the channel after being converted to a frame structure (serial data stream). The frame structure consists of modulated data and the pilot signal is used for estimation and compensation. The channel consists of a multipath fading (flat fading channel or frequency selective fading channel) with AWGN, at the receiver the inverse operation is employed. The cyclic prefix is removed and a serial to parallel conversion is done for the signal. A FFT with N points is used to convert the signal

from time to frequency domain. Then the effective channel is compensated after the OFDM demodulation, the signal de-mapper is used to recover the transmitted signal.

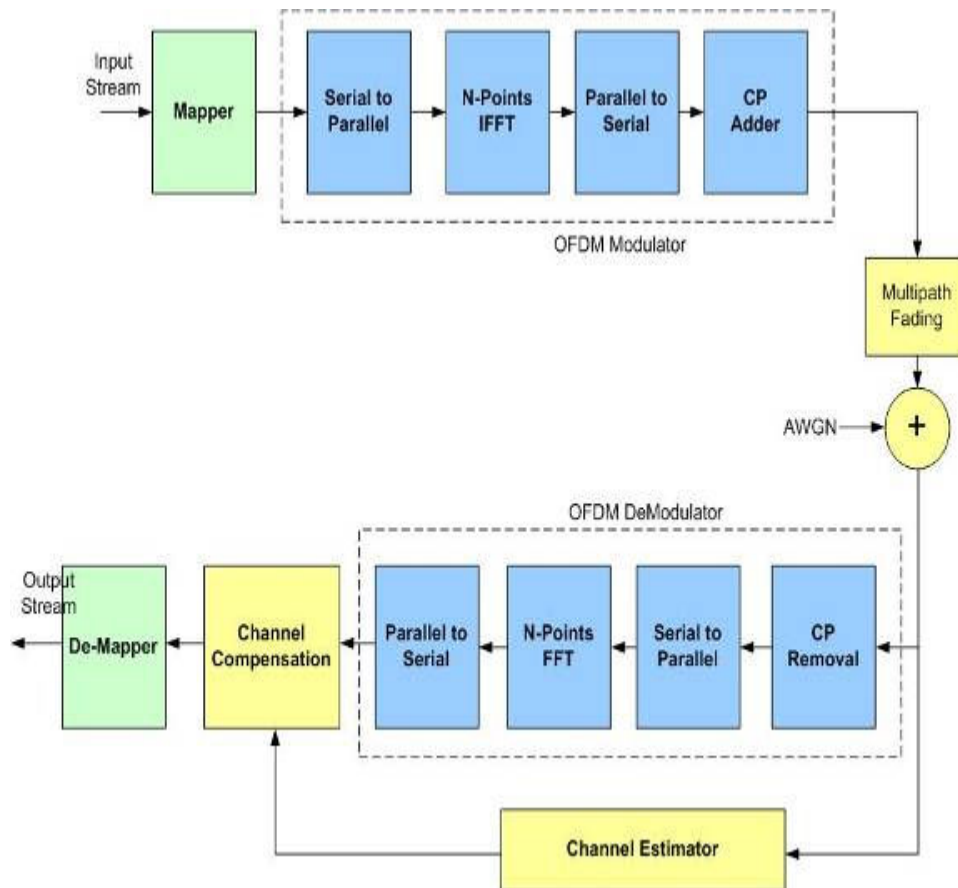


Figure (2.12) Simple block diagram of OFDM transceiver based FFT

### 2.7.1 Guard Interval

To preserve the orthogonality of each sub-channel and independence of subsequent OFDM symbols, a guard interval or cyclic prefix is needed. A guard interval must be greater than the maximum excess delay of the multipath channel, which not only ensures orthogonality between each sub-channel, but also provides an interval between adjacent OFDM symbols. A positive side effect is that the beginning and the end of each OFDM symbol are exact copies of each other, so that this structure can be used for synchronization [44]. The guard interval is removed by

OFDM demodulator at the receiver side. Figure (2.13) and Figure (2.14) show the time and frequency representation of OFDM symbols respectively.

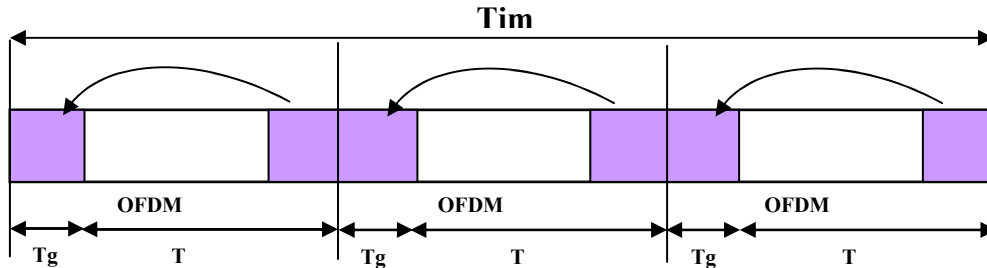


Figure (2.13) Time representation of OFDM

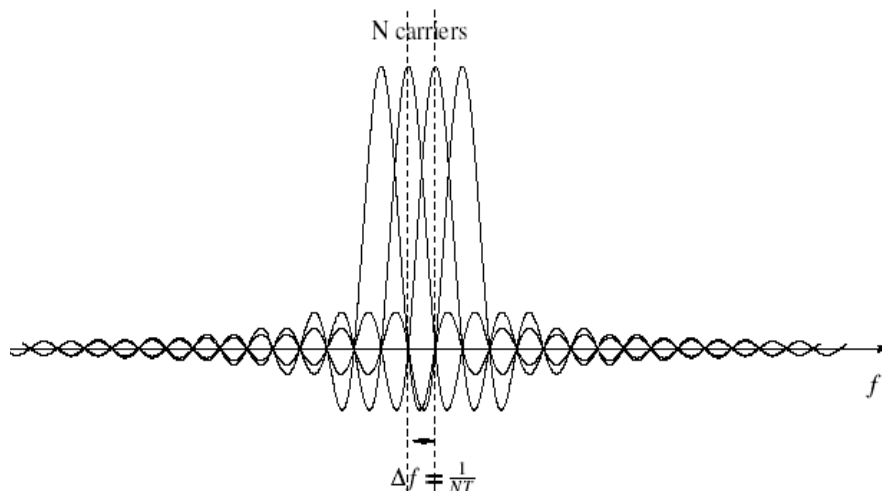


Figure (2.14) Frequency representation of OFDM

The guard interval is robustness against multipath delay spread. This is achieved by having a long symbol period, which minimizes the inter-symbol interference. The level of robust can in fact be increased even more by the addition of a guard period between transmitted symbols. The guard period allows time for multipath signals from the pervious symbol to die away before the information from the current symbol is gathered [45]. As long as the multipath delay echoes stay within the guard period duration, there is strictly no limitation regarding the signal level of the echoes, they may exceed the signal level of the shorter path, the signal energy from all paths just

adds at the input to the receiver, and the whole available power feeds the decoder. If the delay spread is longer than the guard intervals then they begin to cause inter-symbol interference. However, provided the echoes are sufficiently small they do not cause significant problems. This is true most of the times as multipath echoes are delayed longer than the guard period. There are several types of guard interval such that cyclic prefix, zero padded, and other variation of guard interval are possible.

### 2.7.2 Cyclic Prefix

The most effective guard period used is a cyclic extension of the symbol. If a mirror in time, of the end of the symbol waveform is put at the start of the symbol as the guard period, this effectively extends the length of the symbol, while maintaining the orthogonality of the waveform. Using this cyclic extended symbol the samples required for performing the FFT (to decode the symbol), can be taken anywhere over the length of the symbol. This provides multipath immunity as well as symbol time synchronization tolerance. After a combination of  $N$  input data (the desired number to be transmitted in parallel), a serial-parallel conversion takes place. The base band data block with rectangular pulse shaping of  $T_u$  duration, is processed by IFFT to obtain a time-domain waveform with the exact frequency content specified by the carrier weight. Each sub-carrier will be assigned one baseband data to transmit. Then a cyclic prefix of length  $\nu$  is inserted between consecutive symbols. The length of CP ( $\nu$ ) is determined by the length of the channel impulse response and is chosen to minimize ISI. The entries of the resulting redundant symbol are finally sent sequentially through the channel. The total number of time-domain samples per transmitted symbol is thus  $P=N+\nu$  [46]. At the receiver side, the inverse operations are performed in the reverse order to yield the received bit-stream. There is loss in the signal-to-noise ratio (SNR) due to the use of guard period insertion because of that the transmitted energy increases with the length guard interval  $T_g$  of cyclic prefix, while the received and sampled signal remains the same.

$$E_{T_n} = T / (T - T_g) \quad (2.21)$$

Where  $E_{T_n}$ : is the transmitted energy per sub-carrier, and the  $SNR_{Loss}$  due to remove CP in the receiver is

$$SNR_{Loss} = -10 \log_{10} [1 - T_g / T] \quad (2.22)$$

Typically, the relative length of the CP is kept small, Long symbol duration automatically results in long useful part of the OFDM symbol and therefore in reduced spacing between the individual carriers that leads to complex circuitry in the receiver. The efficiency of the transceivers is reduced by the factor  $N/(N+v)$ , so it is desirable to make  $v$  as small or  $N$  as large as possible.

### 2.7.3 Zero Padding

Another type of guard interval is zero padding. Instead of inducing the cyclic prefix, each IFFT processed block is zero padded, by many zeros depending on channels in order to eliminate ISI. If the number of zeros padded is equal to cyclic prefix length, then ZP-OFDM and CP-OFDM transmission have the same spectral efficiency. Other types of guard intervals are possible. One possible type is to have half the guard period cyclic prefix of the symbol, as in a cyclic prefix type, and the other half zero padded [47]. The training frame (pilot sub-carriers frame) will be inserted and sent prior to information frame. This pilot frame will be used to make channel estimation that is used to compensate the channel effects on the signal. To modulate spread data symbol on the orthogonal carriers, an  $N_F$ -points IFFT will be used.

The added zeros to some sub-carriers will limit the bandwidth of the system, while the system without zeros pad has a spectrum which is spread in frequency. The last case is unacceptable in communication systems, since one limitation of communication systems is the width of bandwidth. The addition of zeros to some sub-carriers means that not all the sub-carriers will be used; only subset ( $N_s$ ) of total sub-carriers ( $N_T$ ) will be used.

The received signal is converted to parallel version, after that discarding the interfered cyclic prefix. The FFT is used to transfer the signal back to the baseband frequency domain, and then the channel effects are compensated (by using pilot carrier to estimate the channel frequency response).

## 2.8 Inter-carrier Interference

The insertion of guard time is an effective means of eliminating the ISI in a dispersive fading channel. However, the time variations of the channel also disrupt the

orthogonality between the subcarriers and results in ICI. The extent to which the channel can vary within an OFDM block period decreases with increasing symbol rate. Hence, for some high data rate applications the literature often assumes that the channel doesn't change significantly within the OFDM block period. The effect of ICI is very prominent for mobile reception in vehicles such as trains or buses. If the channel impulse response can be estimated by using some pilot tones, then it is possible to reduce the ICI through proper equalization. In [48], some pilot tones are assisted, estimation and equalization is performed to compensate the ICI. In [49] theoretical expressions are derived for ICI variance by modeling the ICI as additive Gaussian random processes.

## **2.9 Combining OFDM and CDMA**

In the last section, it was explained how OFDM can be a robust scheme for wireless communication and mentioned the drawbacks of the OFDM scheme. By using this scheme, a system achieves both the desirable diversity from CDMA systems on frequency selective channels and without losing the ability of OFDM to combat inter-chip-interference. The diversity is obtained by spreading each modulation symbol, and chips are transmitted over multiple sub-carriers. Different fading on different sub-carriers causes the codeword to be attenuated and even if there is no inter-chip interference, orthogonality is still lost at the receiver. For a CDMA system, it is seen that the diversity can be obtained by the CDMA spreading scheme, in which each codeword spreads into many chips that is transmitted over frequency-selective channel. However, the spreading codes become correlated due to the effect of the channel; thus, there must be MAI between different users. Compared to single-carrier CDMA system, a significant advantage of OFDM-CDMA scheme system is that it reduces the cross-correlations between the spreading codes at the receiver [53]. The CDMA-OFDM appeared in 1993 [11], and up to now, several different schemes have been proposed, which differ mainly in the detectors used and in the mapping of the chips on the sub-carrier frequency. There are three schemes of OFDM symbol that are employed for transmitting a given chip. One is called multi-carrier CDMA (MC-CDMA). One codeword spreads into direct-sequence chips, which are transmitted on adjacent sub-carriers in one OFDM symbol in frequency domain [15, 44]. Another one is called multi-carrier direct sequence CDMA (MC-DS-CDMA). In this case, the

direct-sequence chips of one codeword are sent on the same sub-carrier in consecutive OFDM symbols, the symbols are spread in the time domain. The third scheme is time-frequency localized CDMA (TFL-CDMA), which means the direct-sequence chips of each CDMA codeword are transmitted on closely located time-frequency bins. This system achieves low cross-correlations between spreading codes of different users from OFDM feature, but without additional diversity by increasing length of spreading code.

### **2.10 Multicarrier Code Division Multiple Access (MC-CDMA)**

The basic idea to use multicarrier transmission in a CDMA system is to extend the symbol duration so that a frequency selective fading channel is divided into a number of narrow band flat fading channels, and the complex time domain equalization can therefore be replaced with a relatively simple frequency domain combining. Normally an inverse Fast Fourier Transform (FFT) block is used in the transmitter to modulate user data onto the subcarriers, and an FFT block is used in the receiver to demodulate the data so as to achieve fast computation. Frequency domain diversity can be easily achieved in multicarrier CDMA systems by means of frequency diversity combining schemes. Fast implementation and simple receiver design are especially important in wideband applications, where the data rate and consequently the processing burden are very high. However, sinusoid waveforms which are used as the subcarriers in the conventional multicarrier CDMA are not well localized in the time domain. Thus, time diversity within one chip duration is difficult to achieve. Therefore, in practice a cyclic prefix is inserted between consecutive symbols to eliminate residual Inter Symbol Interference (ISI) due to multipath. The length of the cyclic prefix is equal to or longer than the maximum channel delay spread. This method needs transmitting extra cyclic prefix, which introduces overhead and thus decreases bandwidth efficiency and data rate.

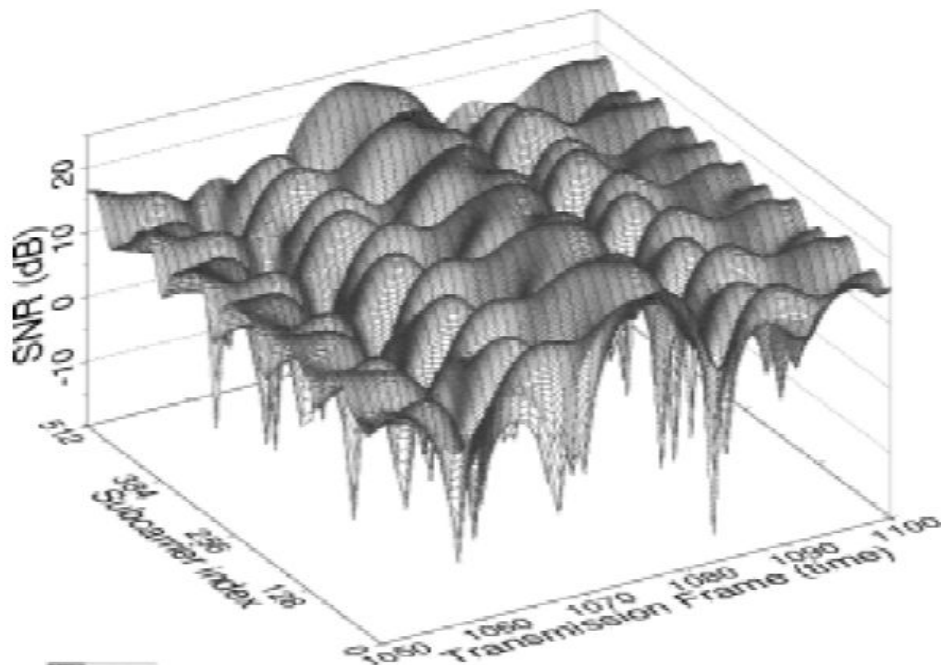


Figure 2.15 Instantaneous channel SNR for all 512 subcarriers versus time

MC-CDMA spreads each user symbol in the frequency domain. That is, each user symbol is carried over multiple parallel subcarriers, but it is phase shifted (typically 0 or 180 degrees) according to a code value. The code values differ per subcarrier and per user. The receiver combines all subcarrier signals, by weighing these to compensate varying signal strengths and undo the code shift. The receiver can separate signals of different users, because these have different (orthogonal) code values. Since each data symbol occupies a much wider bandwidth (in hertz) than the data rate (in bit/s), a signal-to-noise-plus-interference ratio (if defined as signal power divided by total noise plus interference power in the entire transmission band) of less than 0 dB is feasible.

This combination of OFDM-CDMA is a useful technique for 4G systems due to the need of variable data rates as well as provides reliable communication systems. In conventional DS-SS-CDMA each user symbol is transmitted in the form of sequential chips, each of which is narrow in time and hence wide in bandwidth. In contrast to this, in MC-CDMA due to the FFT transform along with OFDM the chips are longer in time duration and hence narrow in bandwidth. The multiple chips for a data symbol are not sequential but instead transmitted in parallel over many subcarriers. An

interesting feature of MC-CDMA is that the modulation and demodulation can be easily implemented using simple FFT and IFFT operators.

The combining of OFDM and CDMA has one major advantage though, it can lower the symbol rate in each subcarriers compared to OFDM so that longer symbol duration makes it easier to synchronize [58]. Kaiser [59] has shown that MC-CDMA suffers only slightly in presence of interference as opposed to DS-CDMA whose performance decreases significantly in presence of interference.

Multicarrier CDMA schemes can be broadly categorized into two groups [15, 60]. The first type spreads the original data stream using a spreading code and then modulates different carriers with each chip, i.e., spreading the chips in the frequency domain. This is usually referred to as MC-CDMA and is the technique of interest to us. The second type spreads the serial to parallel converted streams using a spreading code and then modulates different carriers with each data stream, i.e., spreading in the time domain. If the bit duration is denoted as  $T_b$  and the chip duration as  $T_c$ , then the subcarriers spacing in one system is  $1/T_c$  and the other is  $1/T_b$ . The former is called the Multicarrier DS-CDMA (MC-DS-CDMA) and the latter is called the Multitone CDMA (MT-CDMA). The performance of these two schemes has been studied for an uplink channel in [61]. Prasad and Hara [15] have shown that MC-CDMA outperforms MC-DS-CDMA and MT-CDMA in terms of downlink BER performance. MC-CDMA is thus an attractive technique for the downlink.

A simple block diagram of MC-CDMA system is shown in Fig. (2.16). The input data stream is spread using the spreading sequence which could be a Walsh-Hadamard code or a PN sequence. The resultant chips after spreading the symbols are modulated into different subcarriers using the IFFT operator. The few end symbols are appended at the beginning of the frame to act as the cyclic prefix. The cyclic prefix maintains orthogonality between the subcarriers in a multipath channel. The receiver first removes the cyclic prefix and then performs a FFT operation of the received symbols and brings them back to the frequency domain. Then despreading and decoding of the chips in frequency domain are performed.

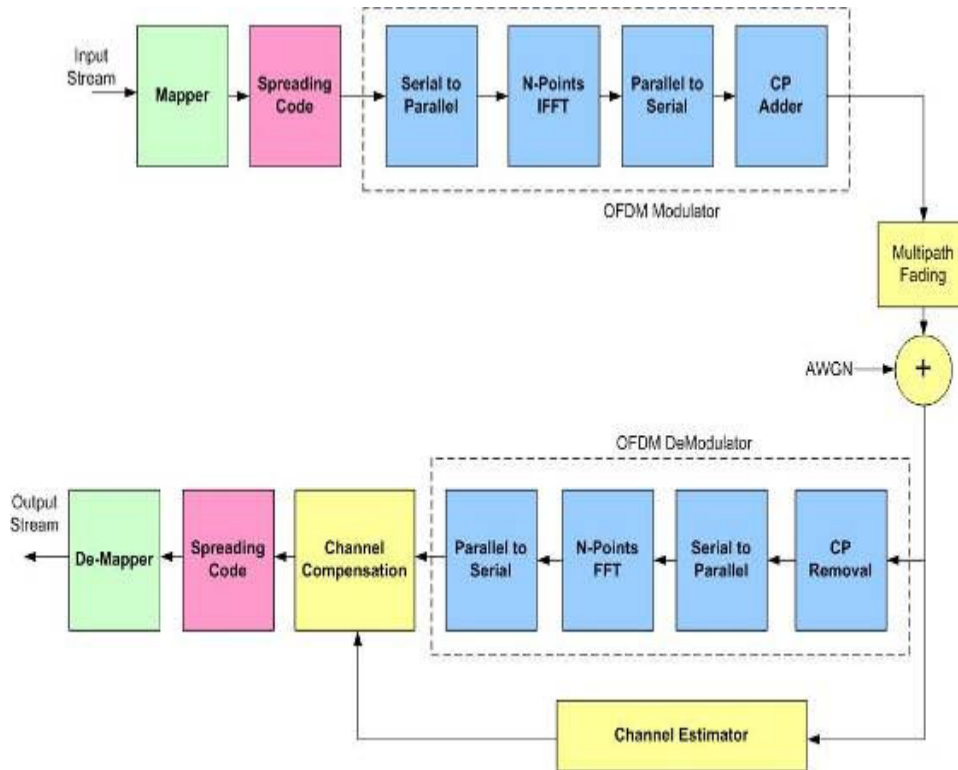


Figure (2.16) Block diagram of a MC-CDMA system

### 2.10.1 Spreading Sequences

A spread spectrum communication system spreads the transmitted signal using user-specific signature sequences. The receiver then correlates the synchronized replica of the signature sequences with the received signal, in order to recover the original information. Due to the noise-like properties of the spreading sequences, “eavesdropping” is not straightforward. DS-CDMA exploits the code’s autocorrelation properties in order to optimally combine the multipath signals of a particular user. By contrast, the different user codes exhibit a low cross-correlation, which can be exploited for separating each user’s signal. MC-CDMA also relies on this cross-correlation property in supporting multi-user communication. The characteristics of the spreading sequences play an important role in terms of the achievable system performance. Hanzo L. [62] shows that the multiple access interference (MAI) is largely dependent on the cross-correlation between the spreading code of the wanted user and the spreading codes of all the other interfering users. The ideal cross-correlation value is zero for all values of  $t \neq 0$ . Ideally, the auto-correlation of the spreading sequences should also be zero, in order to tolerate

inaccurate synchronization of the spreading sequences. Therefore, for the conventional CDMA receiver, the design of the set of spreading sequences to be used in a CDMA system is very important to its performance.

### 2.10.1.1 Walsh-Hadamard Code

Orthogonal codes have zero cross-correlation. They may appear attractive in terms of replacing Pseudo Noise (PN) codes, which have non-zero cross-correlation. However, the cross-correlation value is zero only, when there is no offset between the codes. In fact, they exhibit higher cross-correlation at non-zero offset, than PN codes. There are several so-called code expansion techniques that can be used in order to generate orthogonal codes. Probably the Hadamard transform [43] is the best-known technique. There are other types of orthogonal codes such as the multi-rate orthogonal codes which are attractive, since they can provide variable spreading factors depending on the information rate to be supported [6]. The orthogonal signaling could be used to optimize the detection process in a digital communications system. That is, a detector can be designed that makes the least errors on average if the signal set possesses the orthogonality property. A class of functions that has true orthogonality is the Walsh functions. Walsh functions have been known since 1923 [6] and are advantageous because they assume only values of  $\pm 1$  and therefore are easily generated by digital circuits. An XOR gate can be used to modulate a baseband information bit with a Walsh function. It turns out that a Walsh function is simply a row or column taken from a Hadamard matrix. A Hadamard matrix is a symmetric, square matrix composed of ones and zeros, with a dimension that is a power of two. Hadamard matrices are defined recursively by:

$$H_{n+1} = \begin{vmatrix} H_n & H_n \\ H_n & H_n \end{vmatrix} \quad (2.23)$$

As an example, let us consider the case of  $n=8$ , it can generate 8-bit Walsh codes, and  $H_8$ , applying the transform continuously from  $H_1$  three times. The resultant matrix is as in the following steps:

$$H_1 = \begin{vmatrix} 0 & 0 \\ 0 & 1 \end{vmatrix} \quad (2.24)$$

By definition

$$H_2 = \begin{pmatrix} H_1 & H_1 \\ H_1 & H_1 \end{pmatrix} = \begin{vmatrix} 0 & 0 & 0 & 0 \\ 0 & 1 & 0 & 1 \\ 0 & 0 & 1 & 1 \\ 0 & 1 & 1 & 0 \end{vmatrix} \quad (2.25)$$

Similarly

$$H_3 = \begin{pmatrix} H_2 & H_2 \\ H_2 & H_2 \end{pmatrix} = \begin{vmatrix} 0 & 0 & 0 & 0 & 0 & 0 & 0 & 0 \\ 0 & 1 & 0 & 1 & 0 & 1 & 0 & 1 \\ 0 & 0 & 1 & 1 & 0 & 0 & 1 & 1 \\ 0 & 1 & 1 & 0 & 0 & 1 & 1 & 0 \\ 0 & 0 & 0 & 0 & 1 & 1 & 1 & 1 \\ 0 & 1 & 0 & 1 & 1 & 0 & 1 & 0 \\ 0 & 0 & 1 & 1 & 1 & 1 & 0 & 0 \\ 0 & 1 & 1 & 0 & 1 & 0 & 0 & 1 \end{vmatrix} \quad (2.26)$$

Notice in 8x8 Hadamard matrix that any two rows or columns are mutually orthogonal, that is, for any two rows the number of columns in which they agree is equal to the number of columns in which they disagree. Similarly, pick any two columns and the number of rows in which they agree is equal to the number of rows in which they disagree. Because of the orthogonality property of Walsh-Hadamard code the detection at the receiver can be optimized [62, 63]. In the MC-CDMA system, the orthogonal Walsh code is used to separate the users. Each user is randomly allocated a Walsh code to spread the data to be transmitted. The transmitted signals from all the users are combined together, and then passed through a radio channel model. This allows for clipping of the signal, adding multipath interference, and adding Gaussian noise to the signal. The receiver uses the same Walsh code that was used by the transmitter to demodulate the signal and recover the data.

### 2.10.1.2 Gold Sequences

Pseudo-noise (PN) sequences are binary sequences, which exhibit noise-like properties. Maximal length sequences (m-sequences), Gold sequences and Kasami sequences are well-know PN sequences. One of the best-known binary sequences having relatively good correlation values is the Gold sequence set. A set of Gold sequences is constructed from a preferred pair of  $m$ -sequences,  $x$  and  $y$ , having

identical length  $Q$ , and the period of the Gold sequences generated by  $x$  and  $y$  is also  $Q$ . Each Gold sequence in a set is generated by a modulo-2 sum (XOR) of  $x$  and cyclic shifts of  $y$ . The set also includes the  $m$ -sequences  $x$  and  $y$ . The entire set of Gold sequences having a period of  $Q$  is given by

$$Sg = \{x, y, x \oplus y, x \oplus T^{-1}y, x \oplus T^{-2}y, \dots, x \oplus T^{-(Q-1)}y\} \quad (2.27)$$

where,  $T^q y$  for  $q=1, 2, \dots, Q-1$ , represents a cyclic shift of  $y$  by  $q$  chip intervals; and the symbol  $\oplus$  represents modulo-2 addition.

### 2.10.1.3 Maximal Length Sequences (m-Sequences)

Various pseudo random codes can be generated using linear feedback shift registers (LFSR). The so-called generator polynomial or connection polynomial governs all the characteristics of the generator. For a given generator polynomial, there are two ways of implementing LFSRs. Shift-register sequences having the maximum possible repetition period of  $2^n - 1$  for an  $n$ -stage shift register are referred to as maximal-length sequences or  $m$ -sequences. The  $m$ -sequences have three important properties, namely the so-called balance property, the run-length property as well as the shift-and-add properties. An important class of binary sequences is the binary maximal-length shift register sequences, commonly known as  $m$ -sequences. Sequences can be generated using the well-known linear generator polynomials of degree  $m$ , where:

$$g(x) = g_m x^m + g_{m-1} x^{m-1} + g_{m-2} x^{m-2} + \dots + g_1 x + g_0 \quad (2.28)$$

The  $m$ -sequence generated has a period of  $Q=2^m-1$ , where  $m$  is the degree of the generator polynomial.

### 2.10.2 MC-DS-CDMA

The block diagram of a MC-DS-CDMA transmitter is shown in Fig. (2.17). The incoming data stream is first converted to a parallel stream and then spread in time using spreading codes. This ensures that the resulting spectrum has orthogonal subcarriers. The spreading code is represented as  $C(t)$  and the processing gain is  $N$ . The receiver block is shown in Fig. (2.18), the de-spreading is done in time after the

FFT is followed by a low pass filter and demodulation. The figures are adapted from [15, 22, and 58].

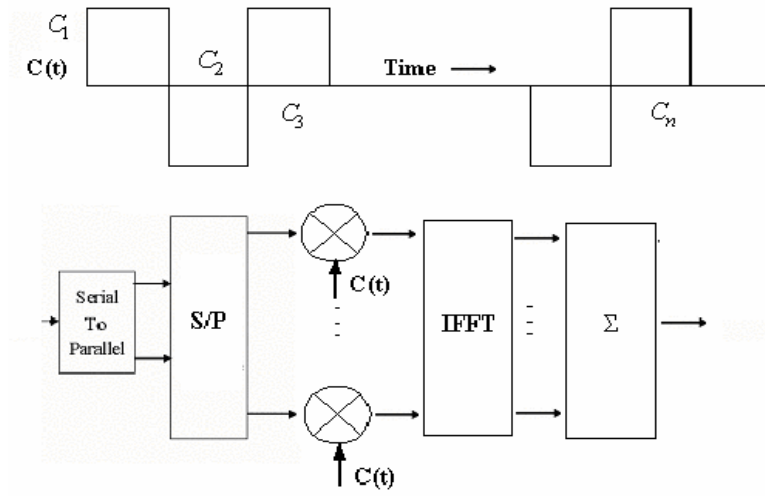


Figure (2.17)

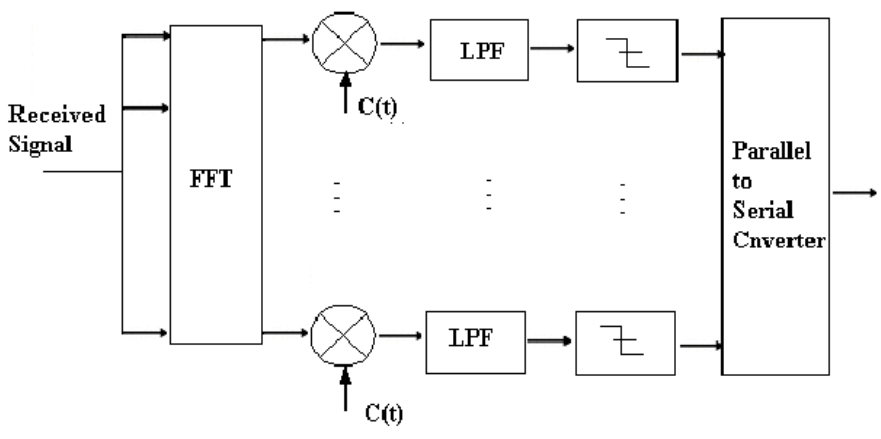


Figure (2.18)

(a) MC-DS-CDMA Transmitter, (b) MC-DS-CDMA Receiver

### 2.10.3 Multi-Tone Code Division Multiple Access (MT-CDMA)

Multi-Tone CDMA transmitter spreads the serial parallel converted data streams using a spreading code in time domain so that the spreading operation can satisfy the Orthogonality condition. The MT-CDMA uses spreading codes in multiples of the number of subcarriers as compared to MC-DS-CDMA. The transmitter block is shown in Fig. (2.19), the receiver employs Rake combining to effectively utilize the diversity due to multipath as shown in fig. (2.20), the figures are adapted from [15, 22, and 58].

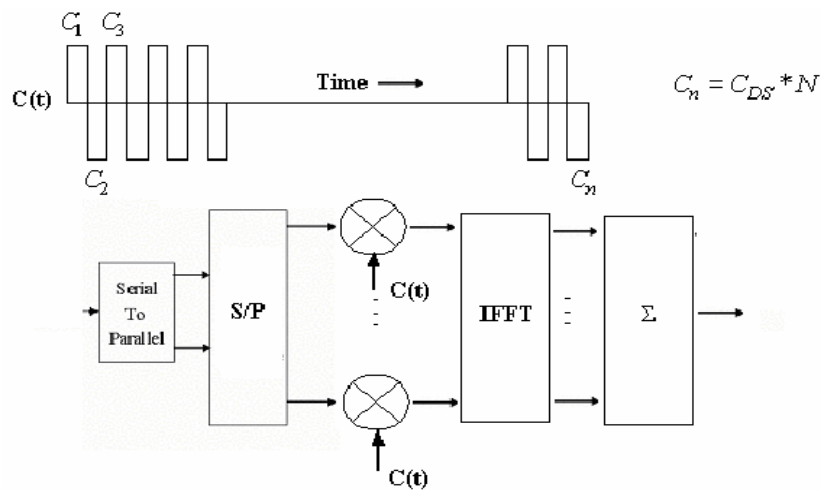


Figure (2.19)

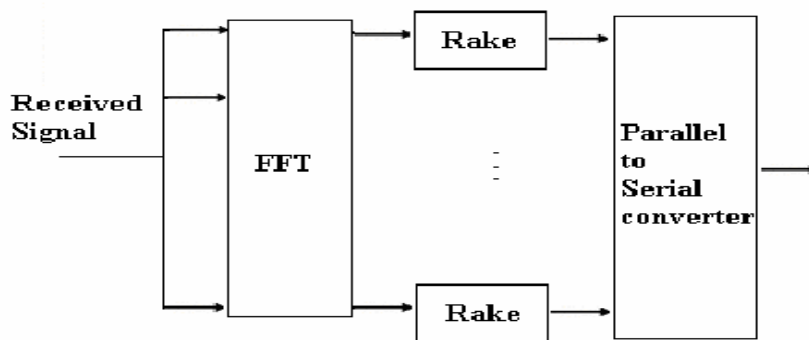


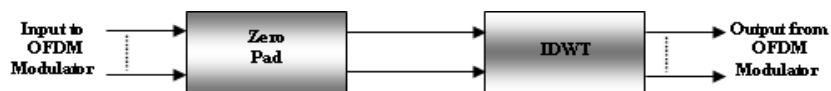
Figure (2.20)

(a) MT-CDMA transmitter, (b) MT-CDMA receiver

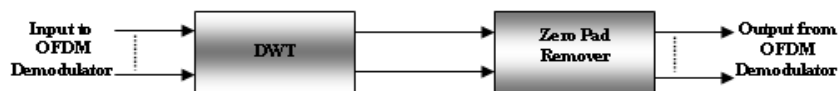
### 3 OFDM System Model Based Wavelet Transform

The wavelet based OFDM modulator and demodulator used are shown in fig. (3.1), the block diagram of the system for DWT-OFDM is depicted in fig. (3.2).

The processes of the S/P converter, the signal de-mapper and the insertion of training sequence are the same as in the system of FFT-OFDM. Also the zeros will be added as in the FFT based case and for the same reasons. After that the inverse discrete wavelet transform (IDWT) will be applied to the signal. The main and important difference between FFT based OFDM and DWT based OFDM is that the wavelet based OFDM will not add a cyclic prefix to OFDM symbol. Therefore, the data rates in wavelet based OFDM can surpass those of the FFT implementation. After that the P/S converter will convert the OFDM symbol to its serial version and will be sent through the channel. At the receiver, the S/P converts the OFDM symbol to parallel version. After that the DWT will be done. Also the zero pads will be removed and the other operations of the channel estimation, channel compensation, signal demapper and P/S will be performed.



(a) WT-OFDM modulator



(b) WT-OFDM demodulator

Figure (3.1) WT-OFDM modem system

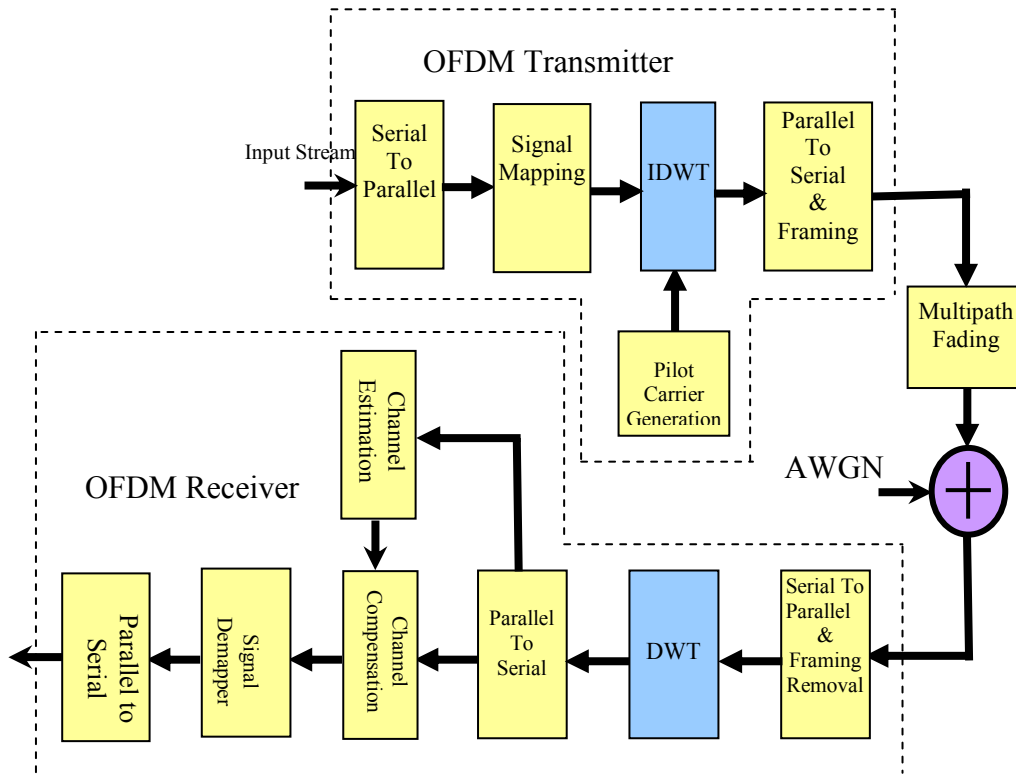


Figure (3.2) Block diagram of DWT-OFDM system

### 3.1 Wavelet Transform

A cyclic prefix (CP) which is the last part of the OFDM symbol to be transmitted prefixed to the transmitted symbol, is the standard method to combat types of interference. If the delay spread of the channel is shorter than the cyclic prefix, all intersymbol interference (ISI) and interchannel interference (ICI) can be avoided at the expense of noise enhancement.

The fundamental assumption that the CP is used to mitigate interference, that the delay spread of the channel is shorter than the cyclic prefix, generally is not true. Practical channels have energy lying outside CP. As a result, neither ISI nor ICI is eliminated. Wavelet-based OFDM has gained popularity in the literature recently. Due to very high spectral containment properties of wavelet filters, wavelet-based OFDM can be better in combating narrowband interference and is inherently more

robust with respect to ICI than traditional FFT filters. The classic notion of a guard band does not apply DWT-OFDM, hence data rates can enhance those of FFT implementations [55].

In OFDM based wavelet transform, the IFFT and FFT blocks are simply replaced by an inverse discrete wavelet transform (IDWT) and discrete wavelet transform (DWT), respectively. Fig. (3.3) illustrates 5 adjacent wavelet subchannels. These channels remain orthogonal to one another, inspite of the significant overlap in the frequency domain. Due to the higher spectral containment between subchannels, wavelet-based OFDM is better in ameliorating the effects of narrowband interference and is inherently more robust with respect to ICI than traditional Fourier filters. Wavelets OFDM is implemented via overlapped waveforms to preserve data rate. Without the CP, the data rate in wavelet systems can surpass those of Fourier implementations, one of its key motivating factors.

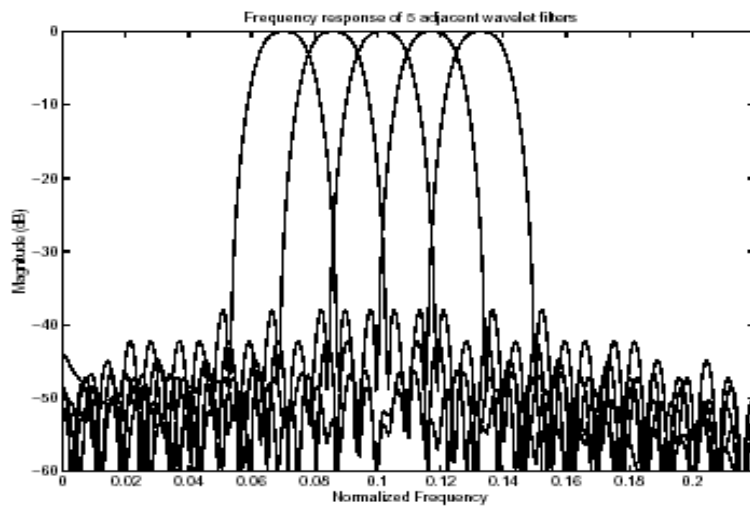


Figure (3.3) Five-adjacent overlapped and orthogonal wavelet subchannels

It was found here that the great reduction in side lobe levels is the main motivation behind the recent trend of using wavelet filters in OFDM systems. Wavelet filters provide better spectral containment than their Fourier counterparts. When orthogonality between carriers is lost, after the transmitted signal passes through a non-uniform channel, the amount of interference between carriers in wavelet systems is much lower than in Fourier systems, since the side lobes contain much less energy. As a result of the improved spectral containment it will be hopefully in reducing the ICI.

### 3.1.1 Haar Wavelet Transform

The wavelet transform is a mathematical transform similar to the commonly known Fourier transform. Wavelet analysis is a form of “multiresolution analysis”, which means that wavelet coefficients for a certain function contain both frequency and time-domain information [56]. This fact makes wavelets useful for signal processing applications where knowledge of both frequency information and the location in time of that frequency information is useful.

There are many different wavelet transforms, each based on different functions for low and high-pass transformation. The Haar wavelet transform, sometimes called the Haar 4-2 wavelet transform, is the simplest of the wavelet transforms. Because of the method used to calculate the transform coefficients, it is also sometimes known as the averaging/differencing transform.

The low-pass wavelet coefficient is generated by averaging the two adjacent values, and the high-pass coefficient is generated by taking half of their difference. Figure (3.4) shows the conversion for an 8-coefficient row.

The inverse transform can be calculated from the wavelet coefficients very easily. Adding the corresponding average and difference coefficients and then subtracting these, leads to restoring the original two coefficients. Fig.(3.5) shows the inverse transform procedure.

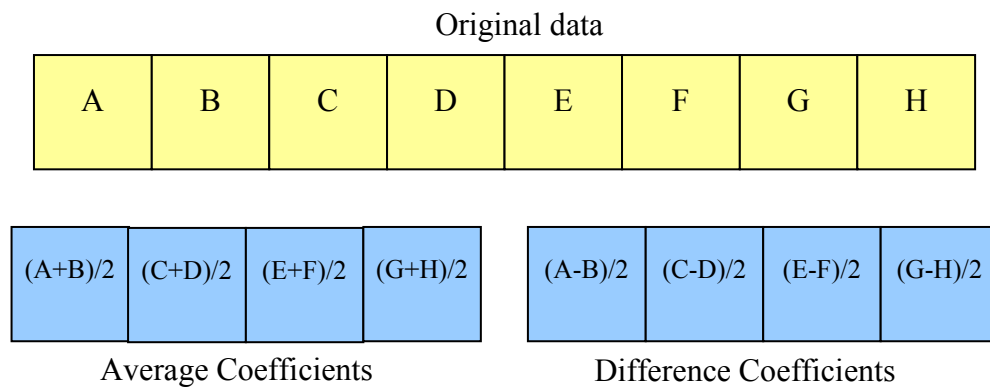


Figure (3.4) Forward Haar transform for an 8-coefficient row

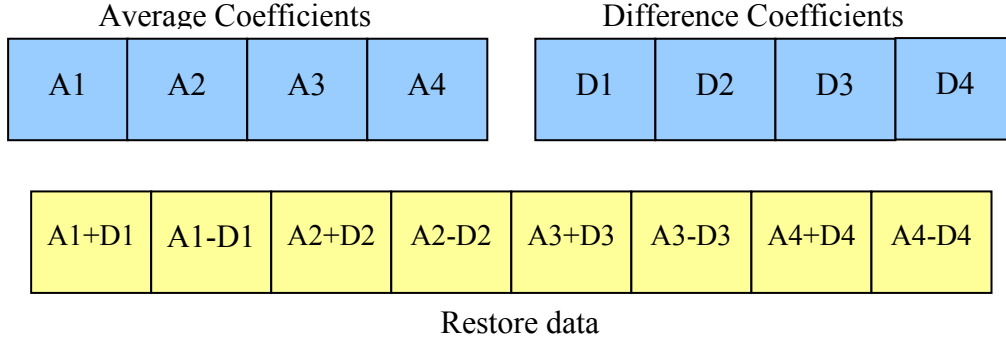


Figure (3.5) Inverse Haar transform example

The basic Haar transform expresses the approximating function  $\tilde{f}$  with wavelets by replacing an adjacent pair of steps via one wider step and one wavelet. The wider step measures the average of the initial pair of steps, while the wavelet, formed by two alternating steps, measures the difference of the initial pair of steps. The shifted and dilated wavelet  $\psi_{[u,w]}$  is defined by the midpoint  $v = (u + w) / 2$  [57],

$$\psi_{[u,w]}(t) = \begin{cases} 1 & \text{if } u \leq t < v \\ -1 & \text{if } v \leq t < w \\ 0 & \text{otherwise} \end{cases} \quad (3.1)$$

For all numbers  $u$  and  $w$ , the notation  $[u,w[$  represents the interval of all numbers from  $u$  included to  $w$  excluded,

$$[u, w[ = \{t : u \leq t < w\} \quad (3.2)$$

The sum and the difference of the narrower steps give a wider and a wavelet

$$\varphi_{[u,w]} = \varphi_{[u,v]} + \varphi_{[v,w]} \quad (3.3)$$

$$\psi_{[u,w]} = \varphi_{[u,v]} - \varphi_{[v,w]} \quad (3.4)$$

Adding and subtracting the last two equations yields the inverse relation, expressing the two narrower steps in terms of the wider step and the wavelet,

$$\frac{1}{2}(\varphi_{[u,w]} + \psi_{[u,w]}) = \varphi_{[u,v]} \quad (3.5)$$

$$\frac{1}{2}(\varphi_{[u,w]} - \psi_{[u,w]}) = \varphi_{[u,v]} \quad (3.6)$$

The basic Haar wavelet transform with the shifts and dilations are applied to all the consecutive pairs of measured signals.

### 3.1.2 The Ordered Fast Haar Wavelet Transform

To analyze a signal or function in terms of wavelets, begins with the initialization of an array with entries, and then proceeds with  $n$  iterations of the basic transform explained in the preceding section.

For each index  $l \in \{1, \dots, n\}$ , before iteration number  $l$ , the array will consist of  $2^{n-(l-1)}$  coefficients of  $2^{n-(l-1)}$  step functions  $\varphi_k^{(n-(l-1))}$ , defined below. After iteration number  $l$ , the array will consist of half as many,  $2^{n-l}$ , coefficients of  $2^{n-l}$  step functions  $\varphi_k^{(n-l)}$ , and  $2^{n-l}$  coefficients of wavelets  $\psi_k^{(n-l)}$ .

- **Initialization:** in Haar wavelet transform, the initialization consists only in establishing a one-dimensional array  $\vec{a}^{(n)}$ , also called a *vector* or a *finite sequence*, of sample values, of the form

$$\vec{a}^{(n)} = (a_0^{(n)}, a_1^{(n)}, \dots, a_j^{(n)}, \dots, a_{2^n-2}^{(n)}, a_{2^n-1}^{(n)}) \quad (3.7)$$

$$= \vec{S} = (S_0, S_1, \dots, S_j, \dots, S_{2^n-2}, S_{2^n-1}) \quad (3.8)$$

With a total number of sample values equal to an integral power of two,  $2^n$ , as indicated by the superscript <sup>(n)</sup>. Though indices ranging from 1 through  $2^n$  would also serve the same purpose, indices ranging from 0 through  $2^n-1$  will accommodate a binary encoding with only  $n$  binary digits, and will also offer notational simplifications in the exposition. The array corresponds to the sampled step function

$$\tilde{f}^{(n)} = \sum_{j=0}^{2^n-1} a_j^{(n)} \varphi_j^{(n)} \quad (3.9)$$

In general the  $l^{\text{th}}$  sweep of the basic transform begins with an array of  $2^{n-(l-1)}$  values

$$\vec{a}^{(n-[l-1])} = (a_0^{(n-[l-1])}, \dots, a_{2^{n-(l-1)}-1}^{(n-[l-1])}) \quad (3.10)$$

and applies the basic transform to each pair  $(a_{2k}^{(n-[l-1])}, a_{2k+1}^{(n-[l-1])})$  which gives two new wavelet coefficients

$$a_k^{(n-l)} = \frac{a_{2k}^{(n-[l-1])} + a_{2k+1}^{(n-[l-1])}}{2} \quad (3.11)$$

$$c_k^{(n-l)} = \frac{a_{2k}^{(n-[l-1])} - a_{2k+1}^{(n-[l-1])}}{2} \quad (3.12)$$

These  $2^{(n-l)}$  pairs of new coefficients represent the result of the  $l^{th}$  sweep, a result that can also be reassembled into two arrays.

$$\bar{a}^{(n-l)} = (a_0^{(n-l)}, a_1^{(n-l)}, \dots, a_k^{(n-l)}, \dots, a_{2^{n-l}-1}^{(n-l)}) \quad (3.13)$$

$$\bar{c}^{(n-l)} = (c_0^{(n-l)}, c_1^{(n-l)}, \dots, c_k^{(n-l)}, \dots, c_{2^{n-l}-1}^{(n-l)}) \quad (3.14)$$

The arrays related to the  $l^{th}$  sweep have the following significance.

$\bar{a}^{(n-[l-1])}$ ; The beginning array:

$$\bar{a}^{(n-[l-1])} = (a_0^{(n-[l-1])}, \dots, a_{2^{n-[l-1]}-1}^{(n-[l-1])})$$

Lists the values  $a_k^{(n-[l-1])}$  of a simple step function  $\tilde{f}^{(n-[l-1])}$  that approximates the initial function  $f$  with  $2^{n-(l-1)}$  steps of narrower width  $2^{(l-1)-n}$ :

$$\tilde{f}^{(n-[l-1])} = \sum_{j=0}^{2^{n-(l-1)}-1} a_j^{(n-[l-1])} \varphi_j^{(n-[l-1])} \quad (3.15)$$

$\bar{a}^{(n-l)}$ : the first array produced by the  $l^{th}$  sweep,

$$\bar{a}^{(n-l)} = (a_0^{(n-l)}, a_1^{(n-l)}, \dots, a_k^{(n-l)}, \dots, a_{2^{n-l}-1}^{(n-l)})$$

Lists the values  $a_k^{(n-l)}$  of a simple step function  $\tilde{f}^{(n-l)}$  that approximates the initial function  $f$  with  $2^{n-l}$  steps of wider width  $2^{l-n}$ ,

$$\tilde{f}^{(n-l)} = \sum_{j=0}^{2^{n-l}-1} a_j^{(n-l)} \varphi_j^{(n-l)} \quad (3.16)$$

$\bar{c}^{(n-l)}$ : the second array produced by the  $l^{th}$  sweep,

$$\bar{c}^{(n-l)} = (c_0^{(n-l)}, c_1^{(n-l)}, \dots, c_k^{(n-l)}, \dots, c_{2^{n-l}-1}^{(n-l)}) \quad (3.17)$$

Lists the coefficients  $c_k^{(n-l)}$  of simple wavelets  $\psi_j^{(n-l)}$  also of wider width  $2^{l-n}$ ,

$$\tilde{f}^{(n-l)} = \sum_{j=0}^{2^{n-l}-1} c_j^{(n-l)} \psi_j^{(n-l)} \quad (3.18)$$

The wavelet given by the second array,  $\bar{c}^{(n-l)}$ , represents the difference between the finer steps of the initial approximation  $\tilde{f}^{(n-[l-1])}$  and the coarser steps of  $\tilde{f}^{(n-l)}$ . Thus, each sweep of basic transforms expresses the previous finer approximation as the sum of a new, coarser approximation and a new lower-frequency, set of wavelets.

Nevertheless, because the basic step of Haar's transform does not alter the sampled function but merely expresses it with different wavelets. It follows that the initial approximation,  $\tilde{f}^{(n-[l-1])}$  and  $\dot{f}^{(n-[l-1])}$

$$\tilde{f}^{(n-[l-1])} = \tilde{f}^{(n-l)} + \dot{f}^{(n-l)} \quad (3.19)$$

### 3.1.3 The Wavelet Packet Transform (WPT)

As a generalization of wavelets, wavelet packets were introduced first for data analysis and compression. They are functions well localized in both time and frequency domains. The construction of a wavelet packet basis starts from a pair of quadrature mirror filters (QMF),  $g_l$  and  $g_0$ , satisfying the following conditions [23],

$$\sum_{n=-\infty}^{\infty} g_1(n) = 2 \quad (3.20)$$

$$\sum_{n=-\infty}^{\infty} g_1(n) g_1(n-2k) = 2\delta(k) \quad (3.21)$$

$$g_0(n) = (-1)^n g_1(L-n-1) \quad (3.22)$$

The sequence of functions  $\varphi_n(x)$ , called wavelet packets, are *recursively* defined by the QMF  $g_l(n)$  and  $g_0(n)$  as

$$\varphi_{2n}(x) = \sum_{k \in \mathbb{Z}} g_1(k) \varphi_n(2x-k) \quad (3.23)$$

$$\varphi_{2n+1}(x) = \sum_{k \in \mathbb{Z}} g_0(k) \varphi_n(2x-k) \quad (3.24)$$

The first two functions of this sequence  $\varphi_0(x)$  and  $\varphi_1(x)$  are exactly the scaling function and its corresponding wavelet function from a multiresolution analysis. Since the two functions  $\varphi_{2n}(x)$  and  $\varphi_{2n+1}(x)$  are generated from the same function  $\varphi_n(x)$ , they are called the "children" functions of the "parent"  $\varphi_n(x)$ . Two operators, also known as filtering-down sampling processes using the QMF  $g_l(n)$  and  $g_0(n)$ , are defined as

$$G_1\{x\}(2n) = \sum_{k \in \mathbb{Z}} x(k) g_1(k-2n) \quad (3.25)$$

$$G_0\{x\}(2n) = \sum_{k \in \mathbb{Z}} x(k) g_0(k-2n) \quad (3.26)$$

These two operators can be used to decompose (analyze) any discrete function  $x(n)$  on the space  $l^2(Z)$  into two orthogonal subspaces  $l^2(2Z)$ . In each step the resulting two coefficient vectors has a length half of the input vector so that the total data length remains unchanged. The process can continue and stop at any desired step. For the deepest decomposition the output coefficient vectors become scalars. This decomposition process is called Discrete Wavelet Packet Transform (DWPT). The DWPT transform is orthogonal and the original signal  $x(n)$  can be recovered from the coefficients by the inverse transform, which is defined as a series of up-sampling-filtering processes using the reversed filters  $g_l(-n)$  and  $g_0(-n)$ . The wavelet packet function set defined in (2.32) and (2.33) can also be constructed using the Inverse DWPT (IDWPT) with the dual operators of (2.34) and (2.35) defined as,

$$G_1^{-1}\{x\}(2n) = \sum_{k \in Z} x(k)g_1(n-2k) \quad (3.27)$$

$$G_0^{-1}\{x\}(2n) = \sum_{k \in Z} x(k)g_0(n-2k) \quad (3.28)$$

The process of constructing a wavelet packet function set can be more clearly seen via the wavelet packet construction tree shown in fig. (3.6). Each wavelet packet function is constructed by starting from a leaf of this binary tree with an impulse  $\delta(n)$ , going up node by node until reaching the root of the tree. The operator from one node to an upper layer node is one of the above operators  $G_l^{-1}$  and  $G_0^{-1}$  depending on the left/right direction.

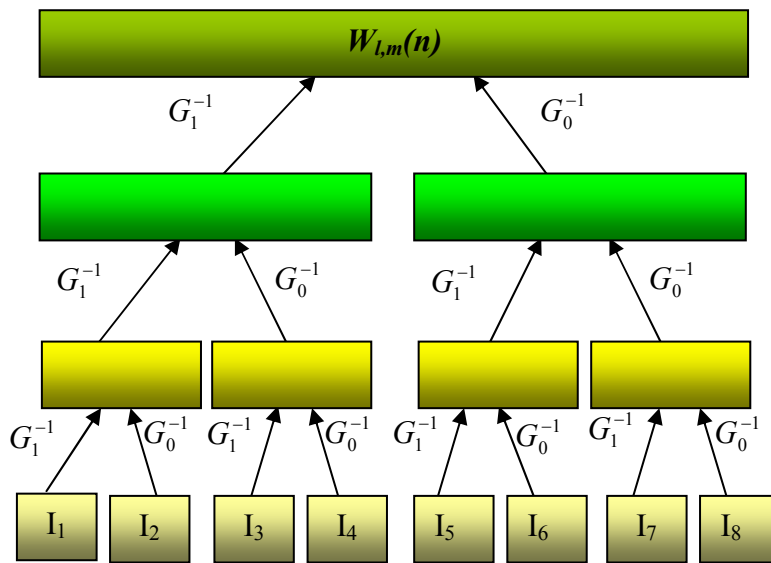


Figure (3.6) Wavelet packet construction tree

In the transmitter part, the data symbols design a block of  $N$  subcarriers that are first converted from serial to parallel to decrease symbol rate by a factor of  $N$  that is equal to the number of sub-carriers. These symbols are modulated to different subcarriers through an IDWPT (Inverse Discrete Wavelet Packet Transform) block. This modulation/mapping is equivalent to the Inverse Discrete Fourier Transform block in the conventional sinusoid waveform based multicarrier system. The inverse wavelet packet construction tree for two levels is shown in fig. (3.7),

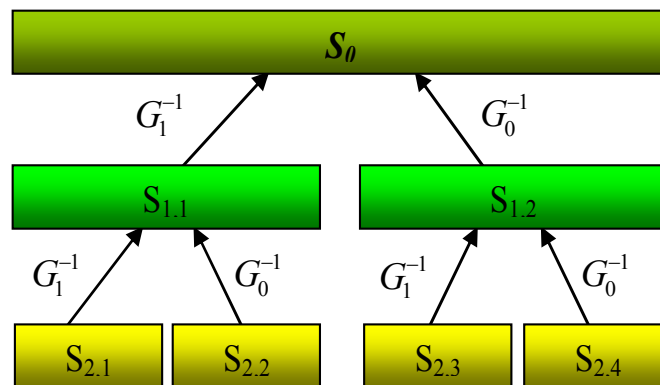


Figure (3.7) Inverse wavelet packet construction tree for two levels

### 3.2 A proposed Model ‘1’ of OFDM based In-Place Wavelet Transform Algorithm

A number of different schemes have been proposed in the literature, the MC-CDMA can be categorized mainly into two groups. The first one make to spreads the user symbols in the frequency domain and the second one make to spreads in the time domain. Accordingly, the detection algorithms for these two different multicarrier systems also fall into time domain and frequency domain signal processing. The description of different proposed models. As illustrated before, wavelet packets have the property of both time and frequency localization. In this chapter a description of models of MC-CDMA lying wavelet transform will be suggested and analyzed [74].

The overall system of OFDM based In-Place wavelet transform that is used in this simulation is shown in fig. (3.8). From this figure, it can be seen that the IFFT and the FFT blocks in the conventional system are replaced by the In-Place Inverse Wavelet Transform (IP-IWT) and the In-Place Wavelet Transform (IP-WT) blocks and the other blocks at the transmitter and receiver parts are staying in the same as in the traditional model.

The processes of the S/P converter, the signal demapper and the insertion of training sequence are the same as in the OFDM system based FFT. The main and important difference between OFDM based FFT and the OFDM based DWT or based IP-WT is that the OFDM model based wavelet transform will not add a cyclic prefix to the OFDM symbols. Therefore, the data rates in this system can surpass those of the FFT implementation model. After that the P/S converter will convert the OFDM symbol to its serial version and the signals (data and training) will be sent through the channel to the receiver. At the receiver, the S/P converts the OFDM symbol to parallel version, then, the IP-WT will be applied on the received symbols. Also the zero pads will be removed and the other operations of the channel estimation, channel compensation, signal demapper and P/S will be performed in a similar manner to that of the OFDM based FFT. The training sequence will be used to estimate the channel frequency response as follows [8, 57]:

$$H(k) = \frac{\text{Received Training Sample}(k)}{\text{Transmitted Training Sample}(k)} \quad (3.29)$$

The channel frequency response will be used to compensate the channel effects on the data, and the estimated data can be found using the following equation:

$$\text{Estimate. data} = H^{-1} \text{estimate}(k) * \text{Re ceived. data}(k) \quad (3.30)$$

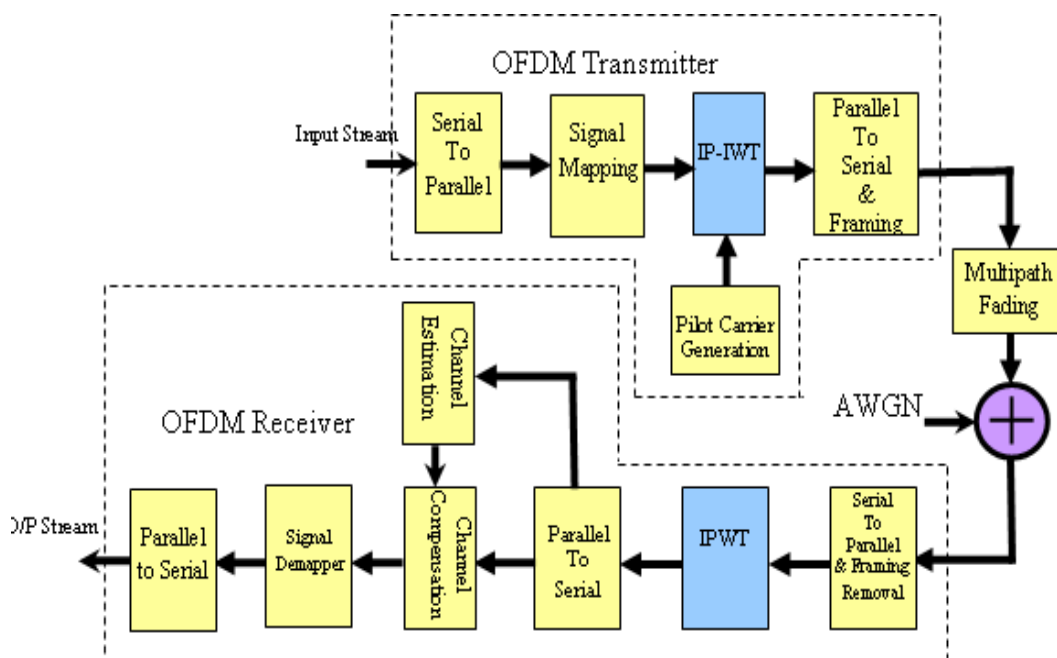


Figure (3.8) Block diagram of a proposed model of MC-CDMA based In-Place wavelet transform

### 3.2.1 In-Place Fast Haar Wavelet Transform

In this section the fundamental study of the In-Place Fast Haar wavelet transform (IP-WT) is introduced. The basic Haar transform expresses the approximating function with wavelets by replacing an adjacent pair of steps via one wider step and one wavelet. The wider step measures the average of the initial pair of steps, while the

wavelet, formed by two alternating steps, measures the difference of the initial pair of steps. Whereas the presentation in section (3.1) conveniently lays out all the steps of the Fast Haar Wavelet transform, it requires additional arrays at each sweep, and it assumes that the whole sample is known at the start of the algorithm. In contrast, some applications require real-time processing as the signal proceeds, which precludes any knowledge of the whole sample, and some applications involve arrays so large that they do not allow sufficient space for additional arrays at each sweep. The two problems just described, lack of time or space, have a common solution in the In-Place Fast Haar wavelet transform presented here [57], which differs from preceding algorithm only in its indexing scheme.

- **In-Place Basic Sweep**

For each pair  $a_{2k}^{(n-[l-1])}, a_{2k+1}^{(n-[l-1])}$ , instead of placing its results in two additional arrays, the  $l^{\text{th}}$  sweep of the in-place transform merely replaces the pair  $a_{2k}^{(n-[l-1])}, a_{2k+1}^{(n-[l-1])}$  by the new entries  $a_k^{(n-l)}, c_k^{(n-l)}$ :

Initialization. Consider the pair  $a_{2k}^{(n-[l-1])}, a_{2k+1}^{(n-[l-1])}$ .

Calculation. Perform the basic transform

$$a_k^{(n-l)} = \frac{a_{2k}^{(n-[l-1])} + a_{2k+1}^{(n-[l-1])}}{2}, \quad (3.31)$$

$$c_k^{(n-l)} = \frac{a_{2k}^{(n-[l-1])} - a_{2k+1}^{(n-[l-1])}}{2}. \quad (3.32)$$

Replacement. Replace the initial pair  $a_{2k}^{(n-[l-1])}, a_{2k+1}^{(n-[l-1])}$  by the transform  $a_k^{(n-l)}, c_k^{(n-l)}$ .

Example: for the initial array  $\vec{S} = \vec{S}^{(3)} = (3, 1, 0, 4, 8, 6, 9, 9)$ , the first sweep yields

$$\vec{S}^{(3-1)} = \left( \frac{3+1}{2}, \frac{3-1}{2}, \frac{0+4}{2}, \frac{0-4}{2}, \frac{8+6}{2}, \frac{8-6}{2}, \frac{9+9}{2}, \frac{9-9}{2} \right) = (2, 1, 2, -2, 7, 1, 9, 0).$$

### 3.2.2 The In-Place Fast Haar Wavelet Transform Analysis (IP-WT)

The In-Place basic sweep explained in the preceding subsection extends to a complete algorithm through mere record-keeping. The first few sweeps proceed as follows.

- **Initialization**

$$\vec{S}^{(n-1)} = \vec{S} = (S_0, S_1, S_2, \dots, S_{2k}, S_{2k+1}, \dots, S_{2^{n-2}}, S_{2^{n-1}}) \quad (3.33)$$

- **First Sweep**

$$\begin{aligned} \vec{S}^{(n-1)} &= \left( \frac{S_0 + S_1}{2}, \frac{S_0 - S_1}{2}, \frac{S_2 + S_3}{2}, \frac{S_2 - S_3}{2}, \dots, \frac{S_{2k} + S_{2k+1}}{2}, \frac{S_{2k} - S_{2k+1}}{2}, \dots \right. \\ &\quad \left. \dots, \frac{S_{2^{n-2}} + S_{2^{n-1}}}{2}, \frac{S_{2^{n-2}} - S_{2^{n-1}}}{2} \right) \\ &= \left( \mathbf{a}_0^{(n-1)}, c_0^{(n-1)}, \mathbf{a}_1^{(n-1)}, c_1^{(n-1)}, \mathbf{a}_2^{(n-1)}, c_2^{(n-1)}, \mathbf{a}_3^{(n-1)}, c_3^{(n-1)}, \dots \right. \\ &\quad \left. \dots, \mathbf{a}_k^{(n-1)}, c_k^{(n-1)}, \dots, \mathbf{a}_{2^{n-1}-1}^{(n-1)}, c_{2^{n-1}-1}^{(n-1)} \right) \end{aligned} \quad (3.34)$$

- **Second Sweep**

In the new array  $\vec{S}^{(n-1)}$ , keep but skip over the wavelet coefficients  $c_k^{(n-1)}$ , and perform the basic sweep on the array  $\mathbf{a}_k^{(n-1)}$  at its new location, now occupying every

other entry in  $\vec{S}^{(n-1)}$ :

$$\begin{aligned} \vec{S}^{(n-2)} &= \left( \frac{\mathbf{a}_0^{(n-1)} + \mathbf{a}_1^{(n-1)}}{2}, c_0^{(n-1)}, \frac{\mathbf{a}_0^{(n-1)} - \mathbf{a}_1^{(n-1)}}{2}, c_1^{(n-1)}, \frac{\mathbf{a}_2^{(n-1)} + \mathbf{a}_3^{(n-1)}}{2}, c_2^{(n-1)}, \frac{\mathbf{a}_2^{(n-1)} - \mathbf{a}_3^{(n-1)}}{2}, c_3^{(n-1)}, \dots \right. \\ &\quad \left. \dots, \frac{\mathbf{a}_{2^{n-1}-2}^{(n-1)} + \mathbf{a}_{2^{n-1}-1}^{(n-1)}}{2}, c_{2^{n-1}-2}^{(n-1)}, \frac{\mathbf{a}_{2^{n-1}-2}^{(n-1)} - \mathbf{a}_{2^{n-1}-1}^{(n-1)}}{2}, c_{2^{n-1}-1}^{(n-1)} \right) \\ &= \left( \mathbf{a}_0^{(n-2)}, c_0^{(n-1)}, c_0^{(n-2)}, c_1^{(n-1)}, \mathbf{a}_1^{(n-2)}, c_2^{(n-1)}, c_1^{(n-2)}, c_3^{(n-1)} \right. \\ &\quad \left. , \mathbf{a}_2^{(n-2)}, c_4^{(n-1)}, c_2^{(n-2)}, c_5^{(n-1)}, \dots, c_{2^{n-2}-1}^{(n-2)}, c_{2^{n-1}-1}^{(n-1)} \right) \end{aligned} \quad (3.35)$$

In general, the In-Place  $l^{\text{th}}$  sweep begins with an array

$$\vec{S}^{\rightarrow(n-[l-1])} = \left( \mathbf{a}_0^{(n-[l-1])}, \mathbf{c}_0^{(n-1)}, \mathbf{c}_0^{(n-2)}, \mathbf{c}_1^{(n-1)}, \mathbf{c}_0^{(n-3)}, \mathbf{c}_2^{(n-1)}, \mathbf{c}_1^{(n-2)}, \mathbf{c}_3^{(n-1)}, \dots, \mathbf{c}_{2^{n-2}-1}^{(n-2)}, \mathbf{c}_{2^{n-1}-1}^{(n-1)} \right) \quad (3.36)$$

This contains the array

$$\vec{\mathbf{a}}^{\rightarrow(n-[l-1])} = \left( \mathbf{a}_0^{(n-[l-1])}, \mathbf{a}_1^{(n-[l-1])}, \dots, \mathbf{a}_{2^{n-(l-1)}-1}^{(n-[l-1])} \right) \quad (3.37)$$

At the locations  $\mathbf{a}_k^{(n-[l-1])} = S_{2^{l-1}k}^{(n-[l-1])}$ , in other words, at multiples of  $2^{l-1}$  apart in

$\vec{S}^{\rightarrow(n-[l-1])}$ , and which the  $l^{\text{th}}$  sweep replaces by

$$a_j^{(n-l)} = \frac{a_{2j}^{(n-[l-1])} + a_{2j+1}^{(n-[l-1])}}{2} = \frac{S_{2^{l-1}2j}^{(n-[l-1])} + a_{2^{l-1}(2j+1)}^{(n-[l-1])}}{2} \quad (3.38)$$

$$c_j^{(n-l)} = \frac{a_{2j}^{(n-[l-1])} - a_{2j+1}^{(n-[l-1])}}{2} = \frac{S_{2^{l-1}2j}^{(n-[l-1])} - a_{2^{l-1}(2j+1)}^{(n-[l-1])}}{2}, \quad (3.39)$$

$$S_{2^{l-1}2j}^{(n-l)} = a_j^{(n-l)}, \quad S_{2^{l-1}(2j+1)}^{(n-l)} = c_j^{(n-l)} \quad (3.40)$$

So that the new array  $\vec{a}^{\rightarrow(n-l)}$  occupies entries at multiples of  $2^l$  apart in  $\vec{S}^{\rightarrow(n-l)}$ , becomes  $a_j^{(n-l)} = S_{2^{l-1}2j}^{(n-l)} = S_{2^l j}^{(n-l)}$ .

### 3.2.3 The In-Place Fast Inverse Haar Wavelet Transform Analysis (IP-IWT)

As described in the preceding section, the Fast Haar Wavelet Transform neither alters nor diminishes the information contained in the initial array  $\vec{S} = (S_0, S_1, \dots, S_{2^n-1})$ , because each basic transform

$$a_k^{(l)} = \frac{a_{2k}^{(n-1)} + a_{2k+1}^{(n-1)}}{2}, \quad c_k^{(l)} = \frac{a_{2k}^{(n-1)} - a_{2k+1}^{(n-1)}}{2}$$

admits an inverse transform:

$$a_{2k+1}^{(l-1)} = a_k^l - c_k^l. \quad (3.41)$$

Repeat the applications of the basic inverse transform just given, beginning with the wavelet coefficients

$$\vec{S}^{\rightarrow(0)} = \left( a_0^{(n)}, c_0^{(1)}, \dots, c_{2^{n-1}-1}^{(1)} \right),$$

Reconstruct the initial array  $\vec{S}^{\rightarrow(n)} = \vec{S} = (S_0, S_1, \dots, S_{2^n-1})$

### 3.2.4 Simulation Results

In this section, the combination of conventional OFDM based FFT with the proposed OFDM based IP-WT will be studied, A simulation of the two systems has been made using MATLAB 7. And the BER performance of the two systems will be studied in different models of channels which are AWGN, AWGN & flat fading channel, and AWGN & frequency selective fading channel [64], with a bit rate of 5 Mbps, 32 subcarriers are used in this simulation, and 8-bit cyclic prefix was added to the OFDM symbols for the conventional system based FFT. The simulation parameters are given in table (3.9).

<b>Modulation Type</b>	QAM, 8 Points and 64 Points
<b>Doppler frequency</b>	5, 100 Hz
<b>Number of sub-carriers</b>	32
<b>Number of bits per Symbol</b>	32
<b>Number of FFT points</b>	32
<b>Channel model</b>	AWGN
	Flat fading+AWGN
	Selective Fading+AWGN

Table (3.9) Simulation Parameters

### 3.2.5 Performance of the Proposed System in AWGN Channel

The channel here is modeled as an Additive White Gaussian Noise for wide range of SNR from 0 dB to 40 dB, from Fig. (3.10), it is found that the proposed system does worked with SNR=19.5 dB at BER= $10^{-4}$  and 8 constellation points, while in the traditional OFDM the bit error rate of  $10^{-4}$  at SNR=38 dB, which means a gain of 18.5 dB was obtained by the proposed model. As the number of constellation mapping increased to 64 point, the BER was increased for both systems even the proposed model is less affected by this variation. The loss is about 8 dB for the proposed model while the BER is about  $10^{-2}$  at SNR=40 dB for the conventional model.

### 3.2.6 Performance of the Proposed System in Flat Fading Channel

In this section, the performance of proposed models in flat fading channel will be shown under two values of Doppler frequencies as in the previous subsection, these are: 5 Hz, and 100 Hz. It can be seen from fig. (3.11) that there exists a wide difference in BER curves between the suggested and the traditional OFDM model, where the BER= $10^{-4}$  at SNR=24.5dB, while the traditional OFDM system was failed to work in this type of model of channel, it has high BER in all simulated SNR range. As the number of constellation point increases the losses for both models were also increases, in all cases the proposed model has better performance than the conventional one. Figure (3.12) shows the performance of these models as the Doppler frequency increases to 100 Hz. The BER for both models was increased; the proposed model based on IP-WT outperforms the conventional system in all range of SNR.

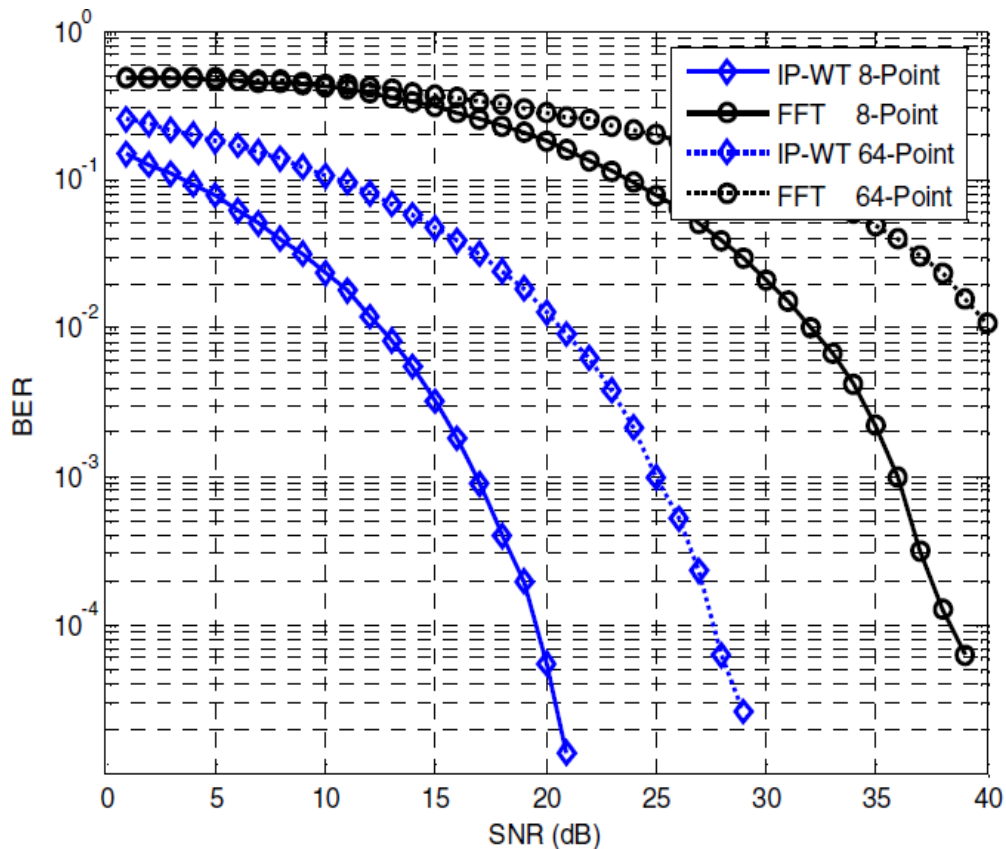


Figure (3.10) BER performance of the proposed OFDM based IP-WT and the traditional model based FFT in AWGN channel

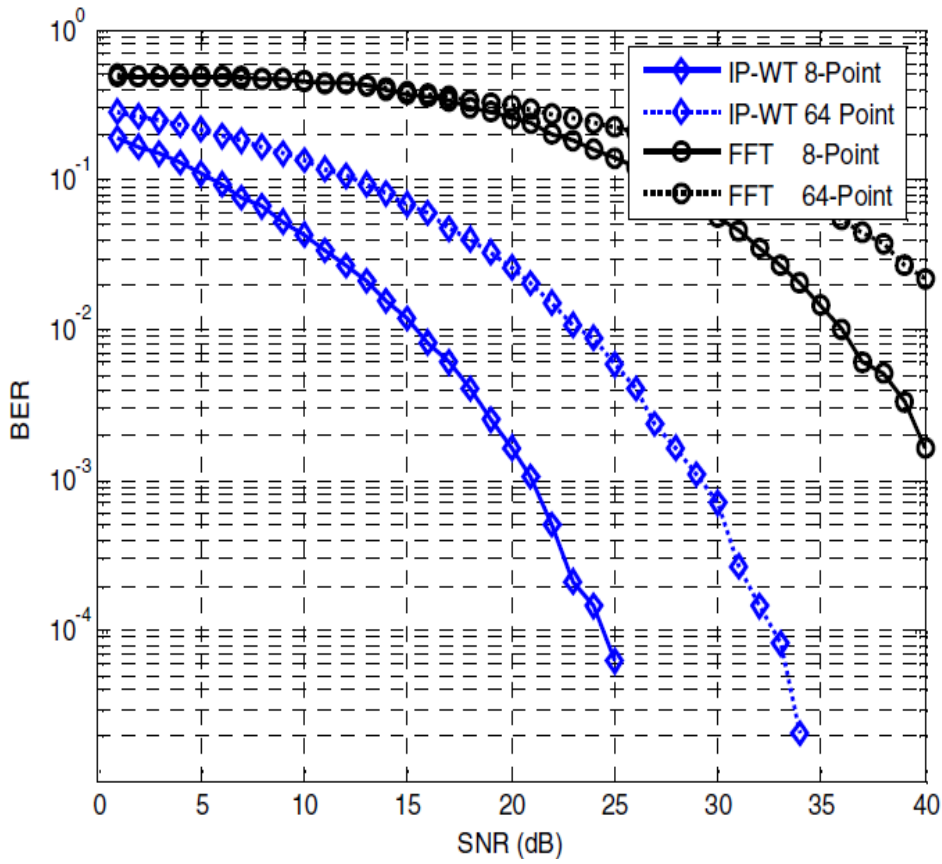


Figure (3.11) Performance of the proposed and traditional OFDM in flat fading channel (maximum Doppler shift =5 Hz)

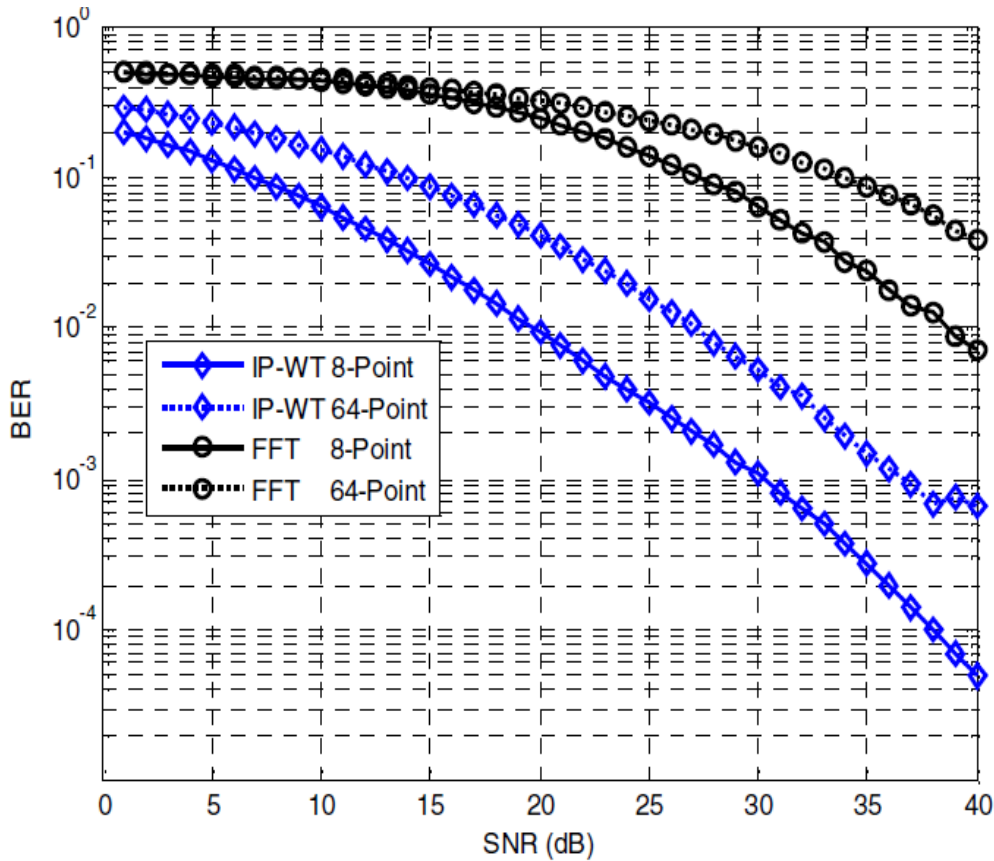


Figure (3.12) Performance of the proposed and traditional OFDM in flat fading channel (maximum Doppler shift =100 Hz)

### 3.2.7 Performance of the Proposed System in Selective Fading Channel

In this type of channel, the frequency components of the transmitted signal are affected by uncorrelated changes, where the parameters of the channel in this case corresponding to multipath, the two paths chosen are, the direct path and the reflected path. In selective fading channel many models can be taken into consideration to compare the BER performance of the systems, the influence of the attenuation, delay and maximum Doppler shift of the echo. Now, set the Doppler shift to 5 Hz, the path delay has been set to 1 sample and the path gain to -8 dB. It is seen that from Fig. (3.13) at Doppler frequency=5 Hz, the proposed model has better performance at the lower values of SNR. As the SNR increases for more than 20 dB, the BER will be constant for this model while it is reduces for the conventional model based FFT. As the number of constellation mapping increased to 64 points, the BER will increase for both systems. OFDM may be combined with antenna arrays at the transmitter and receiver to increase the diversity gain and/or to enhance the system capacity on time-

variant and frequency-selective channels, resulting in a Multiple-Input Multiple-Output (MIMO) configuration [65], this method can enhance the system performance in selective fading channel by using MIMO-OFDM structure with the proposed algorithm that require a minimum memory size for each sweep in the IP-WT.

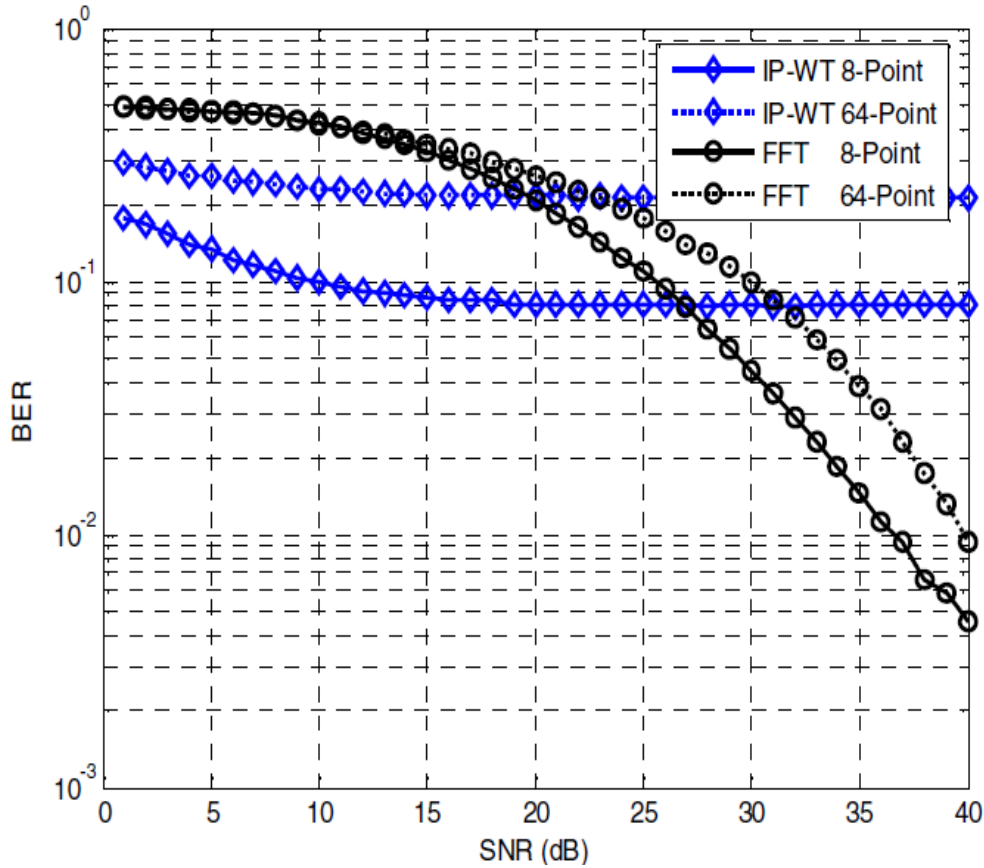


Figure (3.13) Performance of the proposed and traditional OFDM in frequency selective fading channel (maximum Doppler shift =5 Hz, path gain =-8dB, 1 sample delay)

### 3.3.8 A Demonstrated Graphical Example for Model ‘1’

Let us consider the input data binary sequence generated at the transmitter side of logic ‘1’, user code number 20 of length 32 bits, 32 zero bits are added after spreading. As in Fig. (3.14), the location of zero padding appears in subplot (3,3,3), then, the signal is processed by the In-Place Inverse Wavelet Transform before transmitting it over the channel of AWGN type with SNR=10 dB. At the receiver the inverse procedures is done to extract the transmitted data. The signal is normalized to mean value of 0.5 by dividing the transmitted frame by (2\*1.125). An additive white

Gaussian noise is added to the transmitted signal which makes it be fluctuating. Note that the main power of transmitted signal are concentrated at the edge of the transmitted vector, this nature of distribution makes this model to be affected more by the multipath effect, but in general, this model worked well in AWGN, flat fading, and frequency selective fading channel in compared with ordered fast Haar wavelet transform and wavelet packet transform. The performance of this model can be improved more by using the phase matrix rotation which is described in chapter three.

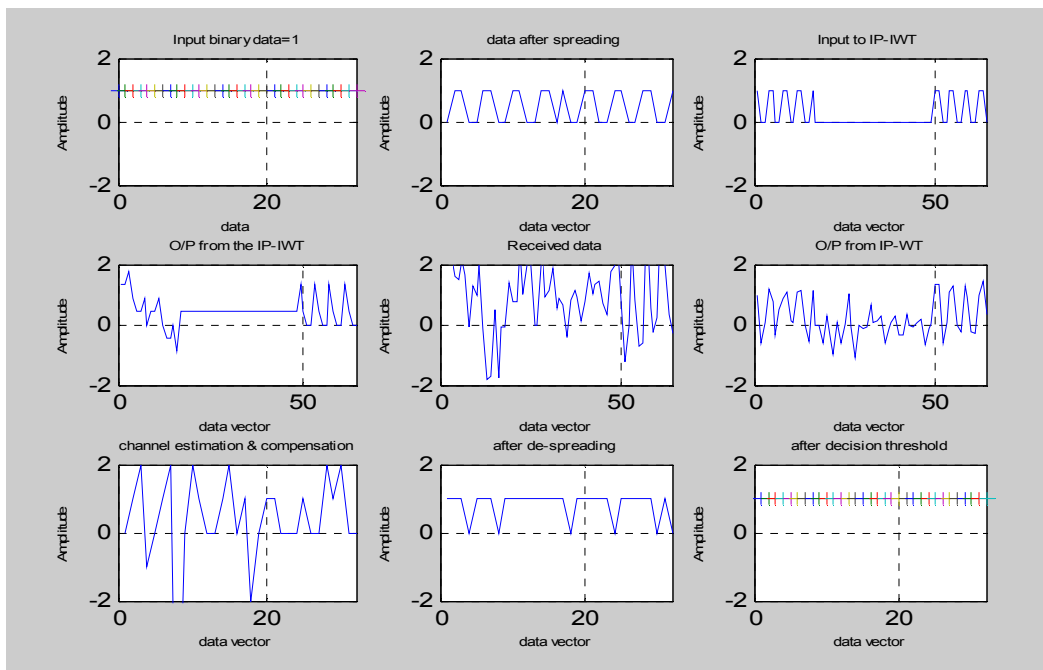


Figure (3.14) Time envelope of the proposed model '1'

### 3.2.9 Conclusions

The simulation of the proposed and the conventional OFDM systems has been investigated. It has been shown that the new algorithm is widely active to work under the AWGN and flat fading channel characteristics. The proposed and the conventional models have poor performance in selective fading channel. The suggested model can be considered as an alternative technique to the conventional system where it does not require additional arrays at each sweep which makes the transform faster and enable it for using in telecommunication systems, where low processing delays are required.

### **3.3 A proposed Model '2' based In-Place Wavelet Transform Algorithm and Phase Matrix**

MC-CDMA transmitter spreads the original signal using a given spreading code in the frequency domain. In other words, a fraction of the symbol corresponding to a chip of the spreading code is transmitted through different subcarriers. For multicarrier transmissions, it is essential to have frequency nonselective fading over each subcarrier. Therefore, if the original symbol rate is high enough to become subject to frequency selective fading, the signal needs to first be converted from serial to parallel before spreading over the frequency domain.

The relative motion between receiver and transmitter, or mobile medium among them, would result in the Doppler Effect. The Doppler Effect would influence the quality of a cell phone conversation in a moving car. On the other word, the path delay causes a fluctuation in the received signal and leads to an inter-symbol interference.

Now, if the transmitted data are modulated on different phase values then it is expected that many phase values of the received signal are changed due to fluctuations, but it will stay lying within the same generated phase values or near to its values. This property is related to MC-CDMA, because the same bits or symbols are modulated in different subcarriers, so, it is possible to transmit each bit on different phases. At the same time, if the data vectors are modulated directly by multiplying them by a phase vector, then any fluctuation in any bit of these vectors can make an increasing loss due to mixing property of the IP-WT algorithm. This means the symbols cannot be multiplied by a phase vector, because the needing here is to make every bit out of IP-IWT has different sharing phase values with the other bits. If this is possible then, if a single fluctuation occurs to this bit due to channel effect, then it will be slowly affected by these variations, which means the algorithm must be able to block the error in any bit from spreading or affecting the other bits as shown later.

In this model, the processing of signal and training here will be done for single level (first level), then the output data and training are multiplied by the phase matrix of size  $(N*N)$  ( $N=WT$  size) [76]. This model is simpler than the traditional model based wavelet packet transform or fast ordered Haar wavelet transform. Where, the ability of fast processing time that can be obtained from comparing with the original

models based FFT and wavelet transform. Since the first level alone will be used, then it is normal that the size of memory will be reduced.

A Phase Matrix (PM) which can be simply generated as in Eq. (3.42) and Eq. (3.43)

$$x(n,i) = \sum_{v=0}^N x(n * N - (N - 1) + v, i) e^{-j(2\pi / N)i.v} \quad (3.42)$$

Where:

n: is the data bit number which is equal to the frame number.

i: is the frequency bin of the wavelet transform (from 1 to N)

N: is the window size of wavelet transform.

x( . ) : is the output signal from the inverse wavelet transform

It can be seen that the Phase Matrix in Eq. (3.3.1) is a square matrix with a dimension of N\*N points. The phase of this matrix will change as the frequency bin of the W.T changes.

The Phase Matrix in Eq.(3.42) can be formulated for N=64 in the following fashion :

$$PM = \begin{bmatrix} e^{-j(2\pi/64)*0} & e^{-j(2\pi/64)*1} & e^{-j(2\pi/64)*2} & \dots & e^{-j(2\pi/64)*63} \\ e^{-j(2\pi/64)*0} & e^{-j(2\pi/64)*2} & e^{-j(2\pi/64)*4} & \dots & e^{-j(2\pi/64)*126} \\ e^{-j(2\pi/64)*0} & e^{-j(2\pi/64)*3} & e^{-j(2\pi/64)*6} & \dots & e^{-j(2\pi/64)*189} \\ \cdot & \cdot & \cdot & \dots & \cdot \\ \cdot & \cdot & \cdot & \dots & \cdot \\ \cdot & \cdot & \cdot & \dots & \cdot \\ \cdot & \cdot & \cdot & \dots & \cdot \\ e^{-j(2\pi/64)*0} & e^{-j(2\pi/64)*64} & e^{-j(2\pi/64)*128} & \dots & e^{-j(2\pi/64)*4032} \end{bmatrix} \quad 3.43$$

The phase values in degree can be written in the form:

$$\theta_{\text{degree}} = \begin{vmatrix} 0 & -5.625 & -11.25 & -16.8750 & -22.5 & \dots & 16.875 & 11.25 & 5.625 \\ 0 & -11.25 & -22.5 & -33.7500 & -45 & \dots & 33.75 & 22.5 & 11.25 \\ 0 & -16.875 & -33.75 & -50.6250 & -67.5 & \dots & 50.625 & 33.75 & 16.875 \\ \vdots & \vdots \\ 0 & 5.625 & 11.25 & 16.875 & 22.5 & \dots & -16.875 & -11.25 & -5.625 \\ 0 & 0 & 0 & 0 & 0 & \dots & 0 & 0 & 0 \end{vmatrix} \quad (3.44)$$

If the signal is multiplied by this PM at the transmitter side then it must be multiplied by the Inverse of Phase Matrix (IPM) at the receiver side in order to retrieve it, or in other form:

$$y_{\text{receiver-side}} = y_{\text{received}} * IPM \quad (3.45)$$

Note that the last equation is a general equation, which means it depends on the location of the received signal that must be processed, and the location depends on the transmitter side, because at the receiver the inverse procedure will be done to process the signal.

### 3.3.1 Phase Matrix Performance Analysis

For illustrating the effect of phase matrix on the performance of suggested models, let us consider a simple circuit shown in fig. (3.15), Assume that the input data is logic '1' with a Walsh-Hadamard spreading code number 20 for this simulation. The spreading signal is processed by the (N=32) and the output vector is multiplied by PM with a dimension (32\*32). The transmitted signal over the channel is assumed to be subjected to a phase variation  $45^0$  at bit 14 and 15 due to channel noise effect respectively. Fig. (3.16) describes these steps. The subplot (3,8,1) represents the input signal to the W.T which it has zero phase shift and the second subplot (3,8,2) represents the phase values for the signal out from IP-W.T Now let us consider that the signal is transmitted over the channel to the receiver with phase values shown in subplot (3,8, 3). Note that there is a phase difference between

subplots (3,8,3) and (3,8,4) by the value of  $45^{\circ}$  at bits 14 and 15, the phase angle about  $-150^{\circ}$  at these bits is decreased to about  $105^{\circ}$  after the channel. The IPM redistributes the phases before converting the signal to frequency domain by the block IP-WT. The important thing here that the random phase generated by the channel only appeared at the output of the block compared with the phases of the input signal to the IW.T block. If the phase matrix was not used as in the original model of MC-CDMA, then any variation in any bit will lead to loss, approximately all bits as in (Fig 3.17), because, the W.T will mix the phases and the amplitudes values of the received signal and training.

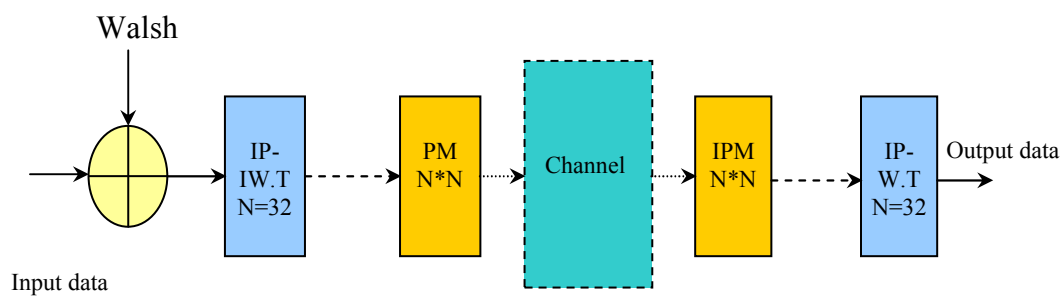


Figure (3.15) Simple demonstration circuit for phase matrix method

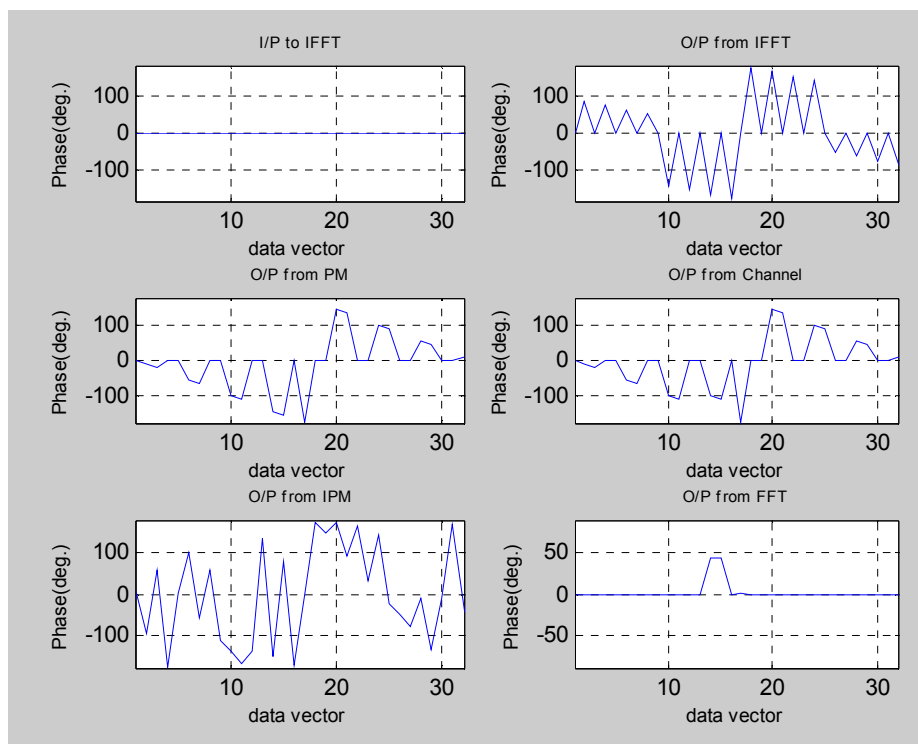


Figure (3.16) Phase values for the demonstrated circuit, with a phase matrix

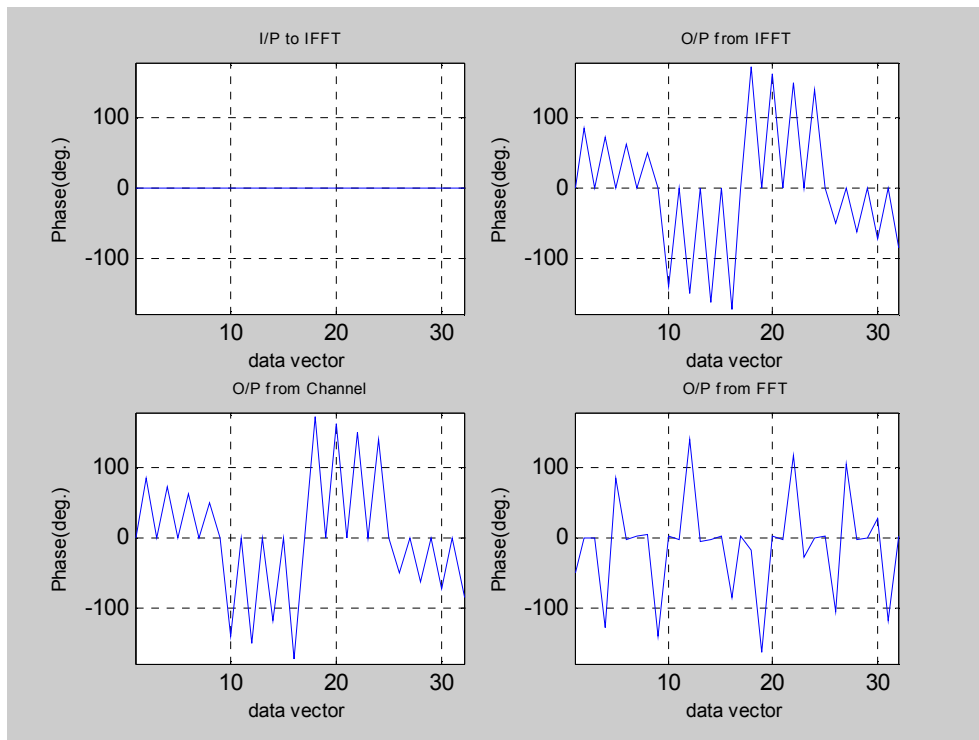


Figure (3.17) Phase values for the demonstrated circuit, without phase matrix

### 3.3.2 Properties and Advantages of Phase Matrix

- 1) The output signal mean value will be reduced due to using the IP-IWT at the transmitter side, the phase matrix is able to keep the output signal power to its normal level according to the same input mean value to the IP-IWT. At the receiver side the IP-WT will increase the mean value of the received signal then, the use of IPM will keep the received mean value of the signal to its normal level.
- 2) It is able to keep the location of each input value to the IP-IWT to its normal value, if it is zero then the output of phase matrix at this location will be zero, else it has another value. This property inhibits the bit error in any location to be transferred or affects the other bits that do not contain any error, as in the last example the phase values exist in the same bins of user specific code that has a unity value.
- 3) Ability to arrange the phases of the transmitted signal to be ordered in a constant form.
- 4) It is flexible phase rotation matrix which makes us be able to use it by vector or column

5) It can be used for multiple stages with the IP-IWT. The multiplication of row phase matrix by column signal vector will cause a circular shift of one bit for each stage from bit one to bit N, which means the signal value at bin number 1 will be the value of bin number N in the next stage.

### 3.3.3 The Mean Value of the Transmitted Symbols

In the Matlab simulation at the channel, the noise is generated randomly between -1 to 1 for real values, or in the absolute mean value it has values between 0 and 1. So, if the researchers need to make a simulation by Matlab tool for the channel, then, the transmitted symbols must have average mean values between zero and one, but in general the generated mean value of the noise by Matlab tools is approximately equal to 0.5. For example if the instruction `rand(10000, 1)` run by Matlab then it gives us 10000 values between zero and one. The mean value is approximately equal to 0.5. Many researchers used the mean value of the transmitted symbols at unity or more than 0.5 which means the transmitted signal power is more than the average noise power, even they were worked in the acceptable range but a better simulation is to take place the mean value of the transmitted signal and training at 0.5 or less, that mean the signal and noise have the same average mean value. This leads to giving us more acceptable performance simulation results related with a strong noise effect on the signal. In all results of this thesis the mean value is set at 0.5 or less. For example, if the mean value is less than 0.5 which has a mean value of 0.25 for the data then, it will be fixed without variation. If it is more than 0.5 or one then the signal is divided by its mean value, the output absolute mean value of signal is about 2.5111, This signal is scaled to 0.5 by dividing it on its (absolute mean value\*2). For any proposed model the output mean value of the transmitted signal or training was scaled to 0.5 as given by Eq. (3.46) and (3.47).

$$Absolute\ Mean\ Value_{Data\ or\ Training}(k) = \left( Real_k^2 + Imag_k^2 \right)^{1/2}, \quad k = 1, 2, 3, \dots, N \quad (3.46)$$

$$Transmitted\ Symbols_{Data\ or\ Training} = Transmitted_{Data\ or\ Training} / (2 * mean(Eq.(3.46))) \quad (3.47)$$

At the receiver, the signal and training are multiplied by (2\*mean value) that are divided by it at the transmitter side

### 3.3.4 Performance Analysis of Model '2'

In this section, the proposed MC-CDMA transceiver based on In-Place Haar wavelet transform for the first level with a phase matrix will be described, and its performance will be discussed. The proposed model is shown in fig. (3.18). Also there are new two blocks added to the proposed model, the first block added at the transmitter side which is the Phase Matrix (PM) block and the other block at the receiver side which is the Inverse of Phase Matrix block.

The wavelet transform is commonly used in the time domain. For example, wavelet noise filters are constructed by calculating the wavelet transform for a signal and then applying an algorithm that determines wavelet coefficients should be modified. Wavelet coefficients are the result of the high pass filter applied to the signal or to combinations of low pass filters of the signal. Although these coefficients are associated with frequency components, they are modified in the time domain (each coefficient corresponds to a time range). In contrast to the wavelet transform, the Fourier transform takes a signal in the time domain (e.g., a signal sampled at some frequency) and transforms it into the frequency domain, where the Fourier transform results represent the frequency components of the signal. Once the signal is transformed into the frequency domain, then all information about time are lost, only frequency remains. The Wavelet Transform is flexible algorithm compared with FFT. At the first decomposition level, the signal is passed through the high pass and low pass filters, followed by sub sampling by 2. The flexibility comes from the ability to use it at different levels.

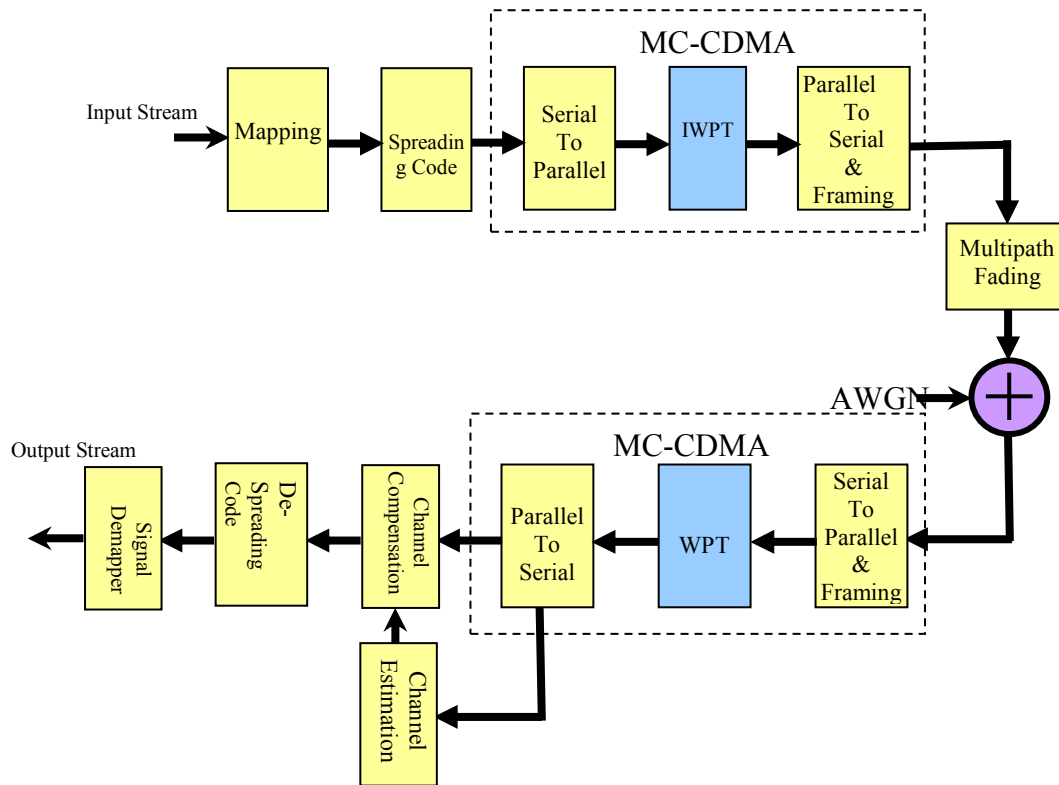
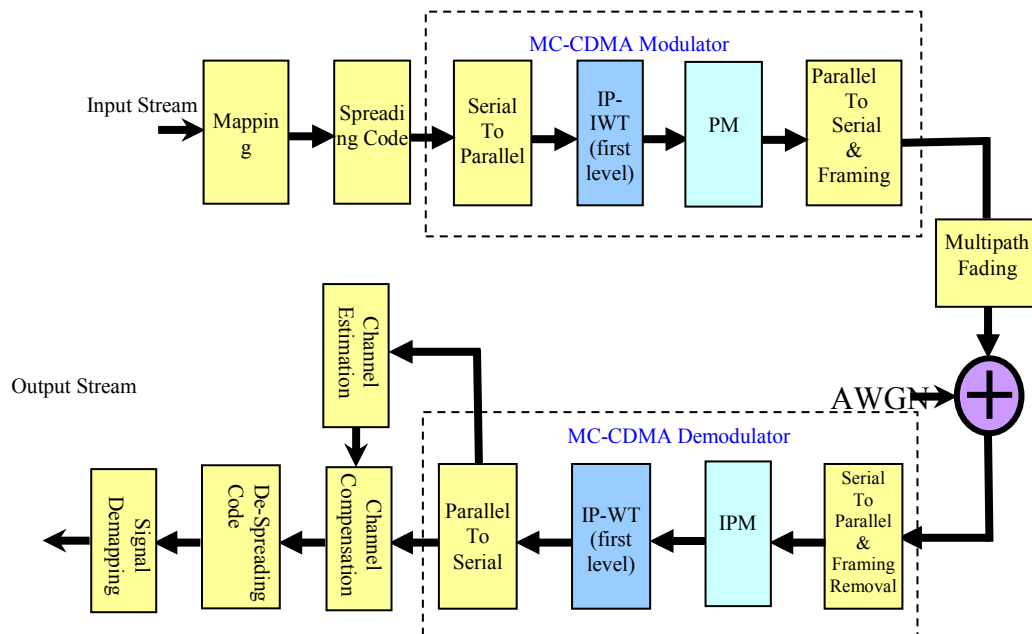


Fig. (3.18a) Traditional Block diagram of MC-CDMA based WPT



(3.18) In-Place Wavelet Transform (IP-WT) blocks for first level

To check the performance of this system, let us consider the data and training processed by the first level of the In-Place Haar wavelet transform alone, and directly the signal is transmitted to the receiver over the channel without multiplying it by the phase matrix, 64 subcarriers, user code 20, path delay=1 sample, path gain=-8 dB, Doppler frequency=1100 Hz and selective fading channel type. Also the proposed model is checked under the same conditions (with Phase Matrix). The results are shown in fig. (3.19). From this curve it can be seen that the In-Place Haar wavelet transform (first level) has a very poor performance in selective fading channel in comparing with the proposed model that is worked with a phase Matrix. The proposed model has a high improved performance under the same conditions. The wavelet packet or normal fast Haar wavelet transform also cannot be used in single level for selective fading channel.

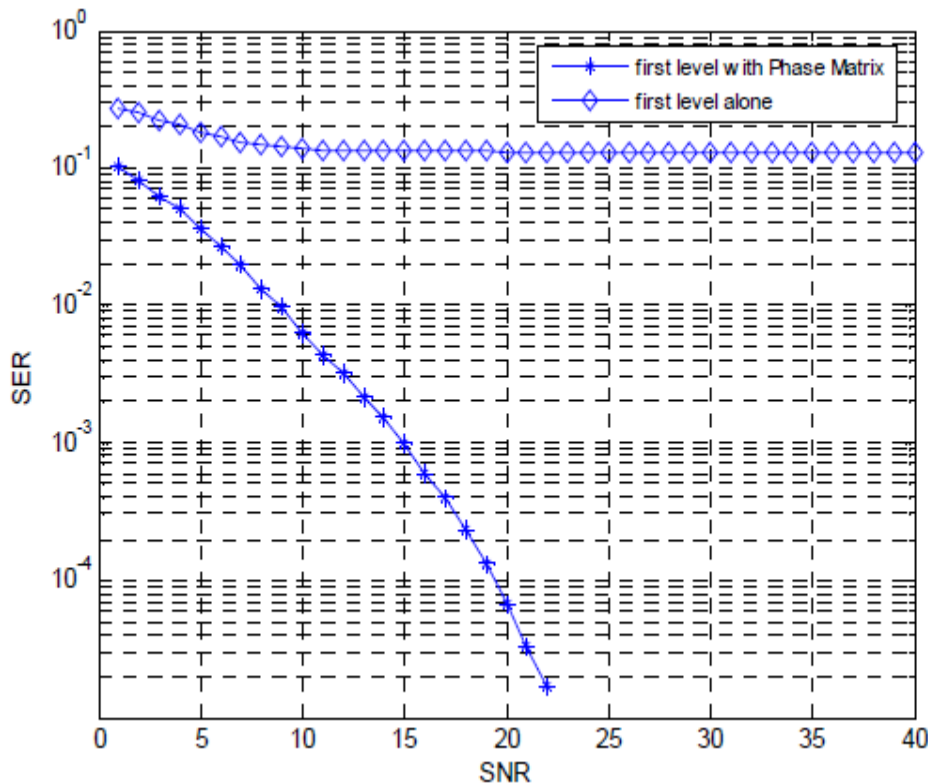


Figure 3.19 Performance of the proposed model with and without phase matrix in frequency selective fading channel. (path delay=1 sample, Doppler frequency=1100 Hz, path gain=-8 dB)

From the block diagram of the transceiver shown in fig.(3.10), its assume that a binary data sequence are generated and modulate one bit for each packet of length (128 bit) that transmitted over the channel.

A brief description of the simulation model shown in fig.(3.18) is described by the following steps:

1. A random bits are generated by a random source generator and every one bit is spreads at the second block with a user-specified spreading code [66]; (in this design every one bit copied 32 times [67], which is equal to the Walsh-Hadamard code that used here (32 bits) and the output is the result of the Exclusive-OR of Walsh-Hadamard and the input bit. The output is a vector of length (1\*32).
2. A zero padding of length (32 bits) is added to this vector to yields an output of (1\*64) bits.
3. A pilot signal is generated of length (1\*32) bits and zeros are padded to it of length (1\*32) and the total pilot vector will be of length (1\*64). For both of data and the pilot signal the zero padding is added at the middle of the vector, namely the zeros are added from 17:48 bits.
4. The data and training are processed by In-Place Inverse Wavelet Transform (IP-IWT) which is not found in the traditional MC-CDMA (fig (3.18a)) to yields 64\*2 output data.
5. Now, the data and training signal are multiplied by a phase Matrix of size 64\*64 to give an output of 64\*1 for each one as in the following equation:

$$x(n,i) = \sum_{v=0}^N x(n*N-(N-1)+v,i) e^{-j(2\pi/N)i.v} \quad (3.48)$$

6. The data and the pilot signal are now being converted to a frame structure; the total frame will be of length 1\*128 bit transmitted over the channel. Before transmit the signal and pilot carrier through the channel it must be scaled to the mean value of both of them to be less than or equal to unity, such that the absolute mean value of them are more nearest the absolute mean value of the generated random noise by the Matlab program. In this paper the transmitted mean value scaled to 0.5 by dividing the transmitted vector by (2\*absolute mean value of vector). This step leads to the best simulation results by Matlab tool, where both of the transmitted signal and noise have the same mean value. The signal power is scaled to 0.5 because the using of phase matrix will lead to increase the transmitted signal mean value to high amplitude (more than unity). At the receiver the signal and training are multiplied by (2\*mean value)

that are divided by it at the transmitter side. In this simulation two types of statistical model of fading channels which are frequently used in the analysis and design of a communication systems, namely AWGN, and selective fading channel. For more information reference [31, 25] had analyzed these types of channels

7. At the receiver, a serial to parallel conversion is done for the received signals, each vector of length 64\*1.
8. The data and the pilot signal are multiplied by the Inverse of Phase Matrix (IPM).
9. The output signal from the IPM is processed by the In-Place wavelet transform with a vector of length 64\*1 for each of data and training signal.
10. Remove the zeros that added at the transmitter for both of data and pilot signal.
11. The training sequence will be used to estimate the channel frequency response as follows:

$$H(k) = \frac{\text{Received Training Sample}(k)}{\text{Transmitted Training Sample}(k)}, \quad k = 0,1,2,\dots,\text{length of Walsh code} \quad (3.49)$$

12. The channel frequency response will be used to compensate the channel effects on the data, and the estimated data can be found using the following equation:

$$\text{Estimate. data} = H^{-1} \text{estimate}(k) * \text{Re ceived .data}(k) \quad (3.50)$$

13. Finally the signal is Exclusive Ored (XOR) with a Walsh-Hadamard of the same transmitter user code, and the detection threshold decision is used to decide the value of signal.

### 3.3.5 Demonstration of Graphical Example

Let us consider the data and training signal are processed by the IP-IWT for first level. The parameter values are: SNR=10 dB, code number=20, input value =1 and AWGN channel type (Fig 3.20) shows the time envelope of the proposed model. Note that in (subplot 3,12,4) which represents the output values from phase matrix, it has a maximum negative value at the centre of frame, the maximum value at the centre exists for all other spreading codes except the distribution is different at the edge or other bits of this vector. The maximum value at the centre of data frame in subplot

(3,12,4) represents not only the data at the centre bit alone but also this value is a sharing value from the other (N-1) bit due to the mixing property of the phase matrix, and the same thing for the other bits. This value at the centre of frame can be considered it as the dominant point for the transmitted data, which is less affected by the noise, because it has high amplitude in comparing with the other bits. The main advantage of the using of phase matrix here is related with its ability to redistribute the received signal power in such way that be able to reduce the noise effect, or in other form for example if a single error occurred in any transmitted bit of the data vector the additional noise energy will be equally distributed to the other most bits. This will ensure that the noise generated at the channel has the same effect on all bits, this will lead to reduce the error.

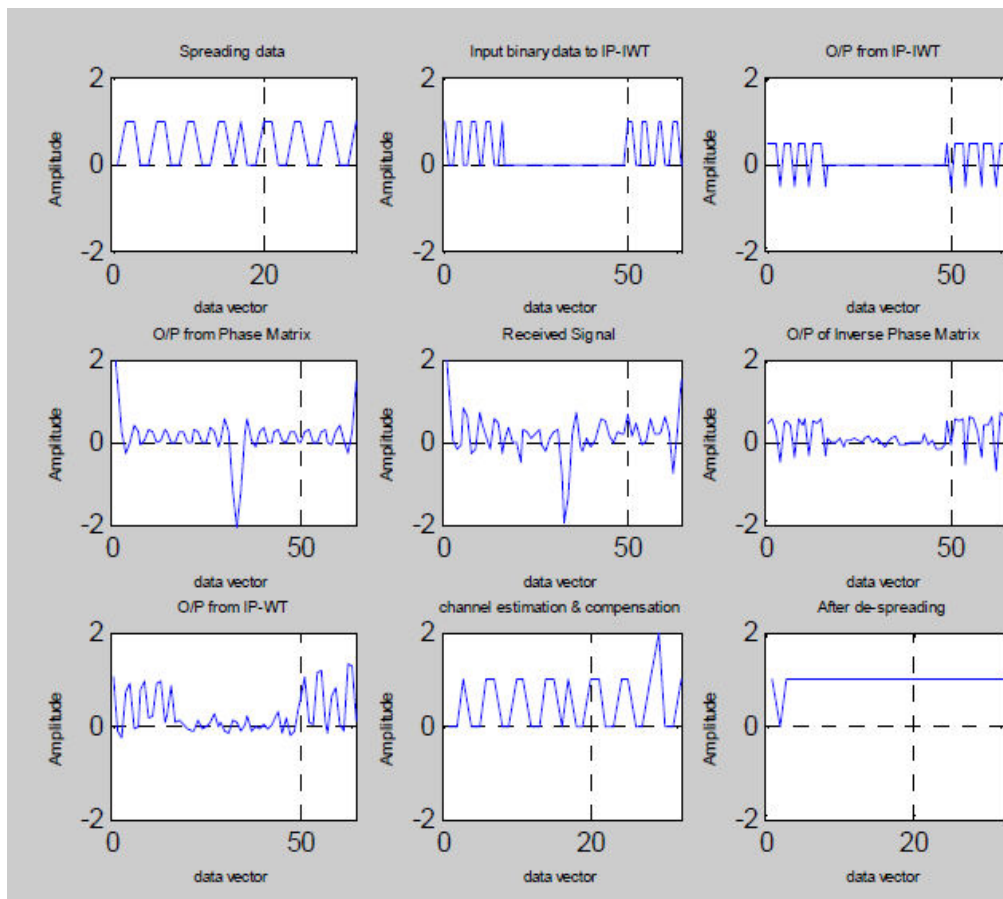


Figure (3.20) Time envelope of the proposed model, (Code number 20, SNR=10 dB, AWGN channel type)

### **3.3.6 Simulation Results**

In this section, the combination of the conventional MC-CDMA based wavelet packet transform with the proposed MC-CDMA based on the first level IP-WT will be studied, the Walsh-Hadamard (code 20) has been used with 32 bits of zeros are added. A simulation of the two systems has been made using MATLAB 7. And the BER performance of the two systems will be studied in two types of channel models, these are AWGN, and AWGN+ selective fading channel, with a bit rate of 5 Mbps and 64 subcarriers are used in this simulation.

### **3.3.7 Performance of the Proposed System in AWGN Channel**

In this section, the channel is modeled as an Additive White Gaussian Noise for wide range of SNR from 0 dB to 40 dB, from Fig. (3.21), it is found that the proposed system MC-CDMA based on first level IP-WT does worked with SNR=3.5 dB at BER= $10^{-4}$  compared with SNR=8 dB for the traditional MC-CDMA based wavelet packet transform, which means a gain of 4.5 dB is obtained by the proposed model. Also the error is started to be appeared at BER= $10^{-2}$  when SNR=1 dB.

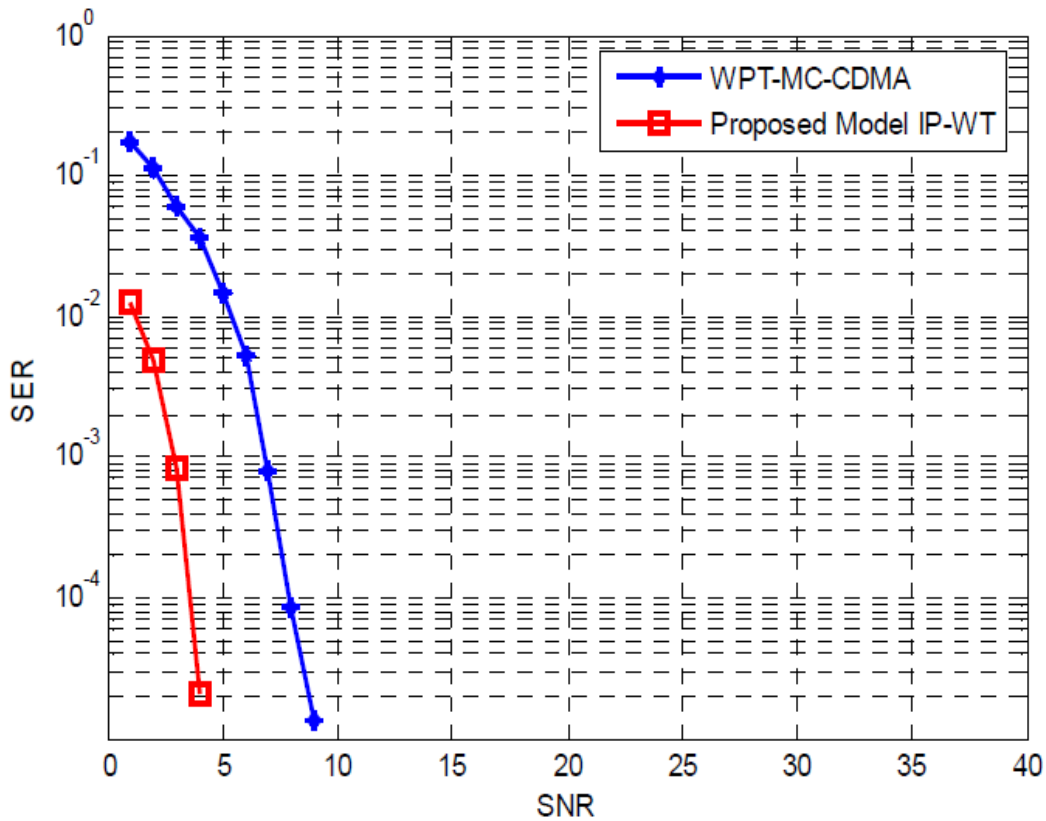


Figure (3.21) Performance of the proposed model in AWGN channel

### 3.3.8 Performance of the Proposed System in Selective Fading Channel

In this type of channel, the frequency components of the transmitted signal are affected by uncorrelated changes, where the parameters of the channel in this case correspond to multipath, the two paths chosen are, the Line Of Sight (LOS) and second path (reflected path). In selective fading channel many models have been taken into consideration to compare the BER performance of the systems, the influence of the attenuation, delay and maximum Doppler shift of the echo is successfully discussed. First, the Doppler shift parameter has been taken out of interest; set the Doppler shift to 5 Hz, 500, and 1100 Hz. The path delay has been set to 1 sample and the path gain to -8 dB.

It is seen that from Fig. (3.22) at Doppler frequency=5 Hz, the proposed MC-CDMA has SNR=16 dB at BER= $10^{-4}$ , while the traditional model was not approach this value of BER at any simulated SNR range. As the Doppler frequency increases to 500 Hz, the BER will increase for both systems and the same value of gain can be obtained by the proposed model as shown in figure (3.23) figure (3.24) is plotted for

the proposed and the traditional model at Doppler frequency=1100 Hz, the same performance approximately is obtained in this figure compared with fig. (3.24).

The last parameter that can be checked is the path gain for the reflected path, the values are checked at maximum Doppler shift of 5 Hz, and the path gains are -1 and -8 dB respectively. The results are shown in fig. (3.25). It is clear from the results, the effect of increasing the path gain for the reflected path on the performance of both systems (as in dotted lines). The SNR required achieving a BER at  $10^{-4}$  is decreased by 6 dB for the proposed system as the path gain increased from -8 dB to -1 dB, for the traditional system the error is slowly increased as shown in the same figure.

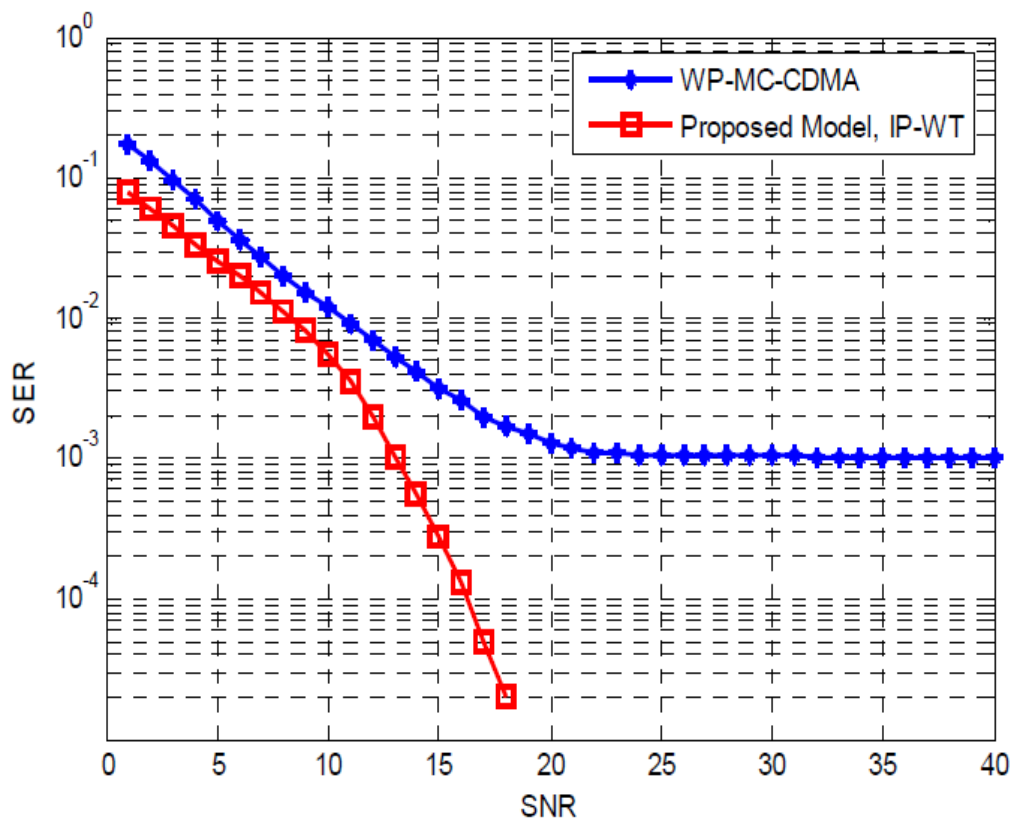


Figure (3.22) Performance of the proposed model in selective fading channel (path delay=1 sample, path gain=-8 dB, and the Doppler frequency=5 Hz)

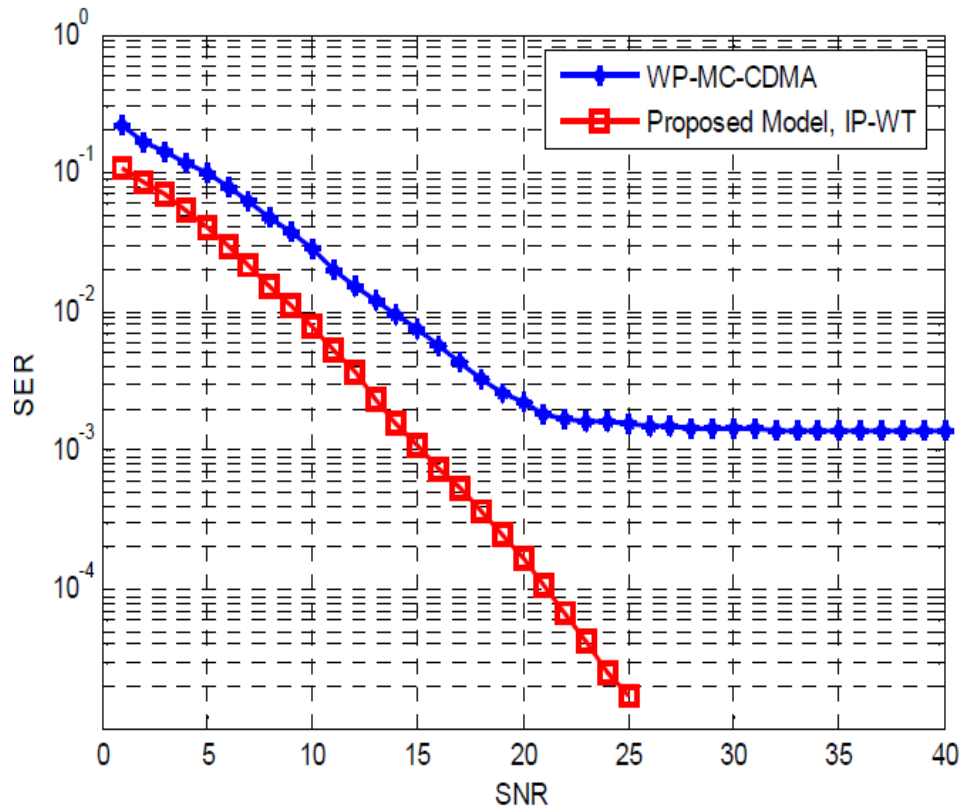


Figure (3.23) Performance of the proposed model in selective fading channel (path delay=1 sample, path gain=-8 dB, and the Doppler frequency=500 Hz)

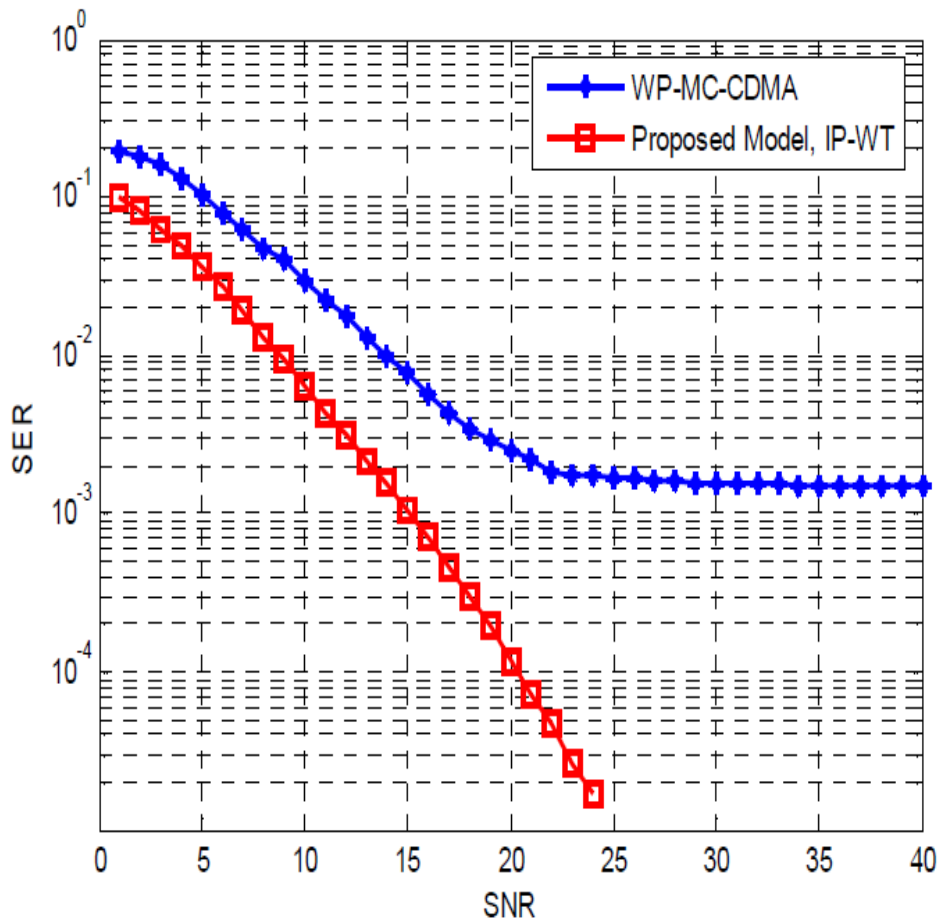


Figure (3.24) Performance of the proposed model in selective fading channel (path delay=1 sample, path gain=-8 dB, and the Doppler frequency=1100 Hz)

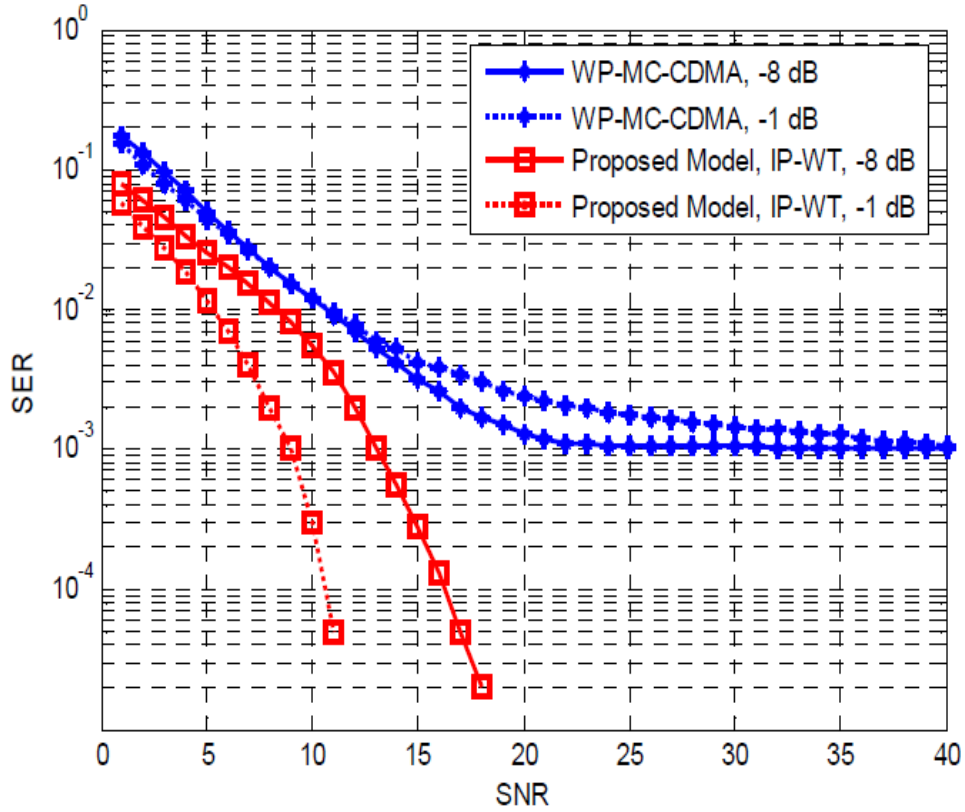


Figure (3.25) Performance of the proposed model in selective fading channel (path delay =1 sample, path gain =-8 and -1 dB, and the Doppler frequency=5 Hz)

### 3.3.9 A Demonstration Numerical Example for Model ‘2’

To illustrate the operation of model ‘2’ let us consider the input data binary uence  $T_{data}$  consisting of bit logic ‘1’, and assume that there are 8 sub-channels

$$T_{Data} = [1] \quad (3.51)$$

Step 1: Spreading Walsh-Hadamard Code

Each data symbol is multiplied with a spreading sequence, Walsh-Hadamard code of length 8 bits. The user specific code number 4 is used in this example whose sequence code is:

$$C_8 = [1 \quad -1 \quad -1 \quad 1 \quad 1 \quad -1 \quad -1 \quad 1] \quad (3.52)$$

This code is converted to unipolar signal in order to correlate it by XOR gate with the random generated signal from the source, the output signal with an input value of logic ‘0’ will be:

$$T_{spreaded} = T_{Data} x C_8 = [0 \quad 1 \quad 1 \quad 0 \quad 0 \quad 1 \quad 1 \quad 0] \quad (3.53)$$

### Step 2: Generation and Insertion of Pilot Carriers

A pilot-carrier (training sequence) is generated as a bipolar sequence  $\{\pm 1\}$ . The training sequence in this demonstrated example is:

$$Training \ Sequence = [1 \quad -1 \quad 1 \quad 1 \quad 1 \quad -1 \quad -1 \quad 1] \quad (3.54)$$

### Step 3: *The MC-CDMA Modulator*

1. Apply the IP-IWT for the first level to the produced sequence. The resultant IP-IWT coefficients will be two row vectors (2\*8) (row 1 for pilot and row 2 for data), the two output vectors are:

$$IP - IWT_{output} = \begin{bmatrix} 0 & 2 & 2 & 0 & 0 & 2 & 0 & -2 \\ 1 & -1 & 1 & 1 & 1 & -1 & 1 & 1 \end{bmatrix} \quad (3.55)$$

Note that the output values are all real values for data and training.

2. The data and the pilot signal are multiplied by the generated phase matrix of size (8\*8), the multiplication will be as a *row vector by column of phase matrix*. The output vectors of data and training from the phase matrix are:

$$PM_{out[ut]} = \begin{bmatrix} 4 & 4 \\ -3.4142 - 1.4142i & 0 \\ -6 + 2i & 4 \\ -0.5858 - 1.4142i & 0 \\ 0 & -4 \\ -0.5858 + 1.4142i & 0 \\ -6 - 2i & 4 \\ -3.4142 + 1.4142i & 0 \end{bmatrix} \quad (3.56)$$

The signal power was increased after applying the PM, these values are scaled to 0.5, and serial to parallel conversion is applied before the transmission through the channel. The total frame structure is:

$$Transmitted\ Signal = \begin{bmatrix} 0.5904 \\ -0.5039 - 0.2087i \\ -0.8856 + 0.2952i \\ -0.0865 - 0.2087i \\ 0 \\ -0.0865 + 0.2087i \\ -0.8856 - 0.2952i \\ -0.5039 + 0.2087i \\ 1 \\ 0 \\ 1 \\ 0 \\ -1 \\ 0 \\ 1 \\ 0 \end{bmatrix} \quad (3.57)$$

#### Step 4: *The Channel Effect*

The signal are fluctuated to a random amplitude and phase due to the effect of channel, it is assumed that an error will occur for the first bit of data and training (for example), and the value is  $0.7071+0.7071i$  or any other value, then the received vectors after removing the frame structure, multiplication by the mean value and serial to parallel conversion are:

$$Received\ Signal_{data+training} = \begin{bmatrix} 8.7909 + 1.1566i & 6.8284 + 0.6828i \\ -3.4142 - 1.4142i & 0 \\ -6 + 2i & 4 \\ -0.5858 - 1.4142i & 0 \\ 0 & -4 \\ -0.5858 + 1.4142i & 0 \\ -6 - 2i & 4 \\ -3.4142 + 1.4142i & 0 \end{bmatrix} \quad (3.58)$$

In the last equation the noise was added as a complex value because the training sequence has complex values.

#### Step 5: *The MC-CDMA Demodulator*

1. Multiply the vectors by the inverse of phase matrix of size (8\*8), the multiplication will be as *row vector by column of Inverse of phase matrix*. The output two vectors, out of the inverse of phase matrix are:

$$IPM_{output} = \begin{bmatrix} 0.5989 + 0.1446i & 1.3536 + 0.0854i \\ 2.5989 + 0.1446i & -0.6465 + 0.0854i \\ 2.5989 + 0.1446i & 1.3536 + 0.0854i \\ 0.5989 + 0.1446i & 1.3536 + 0.0854i \\ 0.5989 + 0.1446i & 1.3535 + 0.0854i \\ 2.5989 + 0.1446i & -0.6465 + 0.0854i \\ 0.5989 + 0.1446i & 1.3536 + 0.0854i \\ -1.4011 + 0.1446i & 1.3536 + 0.0854i \end{bmatrix} \quad (3.59)$$

In general the real and the imaginary parts are varied due to random channel effect on the transmitted signal, also the values for data vector above are different from the values in (3.55) due to spreading the error to other bits. It can be easily compare (3.59) with (3.55), for training vector the values that be less than unity in the last equation are matches or represents the values of zeros in the training vector of (3.55) and the other values represents the values of 2 in the training vector, also the last value above is negative value (-1.4011+0.1446i) which represents the last negative value in (3.55) which is -2, this means the phase matrix are able to redistribute the error in such way that guarantee the efficient distribution for this error to other all bits instead of spreading it to some bits, the same property can be discriminating it for the data vector by comparing (3.55) with the last equation.

2. The output vectors after applying the first sweep for IP-WT will be:

$$IP - WT_{output} = \begin{bmatrix} 1.5989 + 0.1446i & 0.3535 + 0.0854i \\ -1 & 1 \\ 1.5989 + 0.1446i & 1.3536 + 0.0854i \\ 1 & 0 \\ 1.5989 + 0.1446i & 0.3535 + 0.0854i \\ -1 & 1 \\ -0.4011 + 0.1446i & 1.3536 + 0.0854i \\ 1 & 0 \end{bmatrix} \quad (3.60)$$

In this matrix, it can be noted that the additional signal noise power will not appear at the same bit infected location (bit 1), instead of that the noise signal power was distributed on the other bits, the values which have a value of one for data or more represents logic '1' else it will be zero in comparing with the spreading data as in (3.53). Since most of bits are varied at the channel and this model is able to redistribute the additional noise power to other bits in an ordered form, then it expected that the effect of variation on the transmitted data will be reduced. Also the output training sign vector in the last equation are matches the training sign in Eq. (3.54).

Step 6: The Channel Estimation and Compensation

The training sequence will be used to estimate the channel frequency response as in Eq (3.49), and then the channel compensation is used to compensate the channel effects on the data.

#### Step 7: Data De-Spreading and Decision Threshold

Convert the data from parallel to serial and multiply the real values by the same user specific code that is used at the transmitter side. The decision threshold is used to determine the value of the received data.

If the system worked in AWGN channel, then in general all values are varied to both data and pilot signal as in the following received matrix for SNR=10 dB. From the next equation it can be seen that even the signal is randomly varied due to the channel effect but it also has the same shape of the spreading signal or it has the same last mentioned properties for both of data and training.

$$IP - WT_{output} = \begin{bmatrix} 1.5079 - 0.8528i & 1.0298 + 0.0392i \\ -1.1821 - 0.7830i & 0.1876 + 0.2139i \\ 0.5345 - 0.1842i & -0.1238 + 0.5440i \\ 1.5584 + 0.0044i & 1.1394 + 0.0236i \\ 0.7650 - 0.2704i & 1.2580 + 0.1743i \\ -0.6458 + 0.2574i & -0.0270 + 0.1860i \\ -1.1063 - 0.0522i & 0.0861 + 0.1181i \\ 1.6450 + 0.2437i & 1.2961 - 0.0653i \end{bmatrix} \quad (3.61)$$

The absolute mean values of these vectors are:

$$ABS_{Eq.(3.22)} = \begin{bmatrix} 1.7323 & 1.0305 \\ 1.4179 & 0.2845 \\ 0.5653 & 0.5579 \\ 1.5584 & 1.1396 \\ 0.8114 & 1.2700 \\ 0.6952 & 0.1879 \\ 1.1075 & 0.1462 \\ 1.6630 & 1.2977 \end{bmatrix} \quad (3.62)$$

The values that are more than 0.5 represent logic '1' else it will be zero. For frequency selective fading channel at Doppler frequency =1100 Hz and SNR=10 dB, one sample path delay, path gain=-8 dB, then the output data from the IP-WT will be:

$$IP - WT_{output} = \begin{bmatrix} -1.4691 - 0.5179i \\ 0.1073 + 0.3820i \\ -0.1303 - 0.2829i \\ -0.5851 - 0.4806i \\ -0.6617 - 0.7545i \\ -0.1633 - 0.3282i \\ 0.1178 - 0.1776i \\ -0.9534 - 0.2069i \end{bmatrix} \quad (3.63)$$

In this matrix, the values of logic '1' can be discriminate it from those of logic '0', if it's more than 0.5 or not. The data values have mostly negative values if the transmitted bits are zero or one; this property makes the channel estimation and compensation to be more active for recovering the transmitted signal.

### 3.3.10 Conclusion

The simulation of the proposed and traditional MC-CDMA systems has been investigated. It has been shown that the new algorithm is widely active to work under different channel characteristics. Approximately a gain of 4.5 dB was obtained at the AWGN channel, wide gain was obtained in selective fading channel at different Doppler frequency shift. As the path gain increased, the gain of the proposed system also increased. The new model is simpler than the traditional model and it has a fast processing time than the traditional one.

### 3.4 Multi-wavelet Theory

As a natural extension of wavelet, Multi-wavelet are designed to be simultaneously symmetric, orthogonal and having short supports with high approximation power, which cannot be achieved at the same time for wavelet using only one scaling function. The trick is to increase the number of scaling functions to raise the approximation power rather than one scaling function. It enhances the performance of many wavelet applications such as image coding and de-noising.

The multi-wavelet coefficients that the low pass filter  $H$  and high pass filter  $G$  consists of are  $r$  by  $r$  matrices, and during the convolution step they must multiply vectors (instead of scalars). This means that multifilter banks need  $r$  input rows. In the present case  $r = 2$  and two data streams enter the multifilter. To create them from an ordinary single-stream input of length  $N$ , there are several possibilities:

- i. Separate odd and even samples (in one dimension), or use adjacent rows of the image (in two dimensions).
- ii. Repeat the input stream to produce two length  $N$  streams.
- iii. Create consistent approximation based equations that yield two length  $N/2$  streams and a “de-approximation” that returns a length  $N$  stream.

Method (i) constrains the design of the multifilter and, in the case of images, introduces nontrivial two-dimensional processing. This method doesn't work well because it destroys the assumed characteristics of the input signal. Method (ii) introduces oversampling of the data by a factor of two. Oversampled representations require more calculation than critically-sampled representations.

In the case of one-dimensional signals the “repeated row” scheme is convenient to implement. In two-dimensions the oversampling factor increases to four, making this scheme useful only for applications such as denoising which does not require critically-sampled or near-critically-sampled representation of the data. Method (iii) maintains a critically sampled representation. The multifilter processes two  $N/2$  point data streams using an approximation method suggested by Geronimo.

### 3.4.1 A Proposed Model '3' of MC-CDMA Based Multiwavelet Transform

The Multiwavelet transform was introduced later and finds wide spread application in several fields due to the orthogonality of basis functions and their greater suitability for use in communication systems. This high degree of suitability is related to the finite support and self-similarity of the basis functions. The replacement of the Fast Fourier Transform (FFT) with the Multiwavelet transform will lead to overcome several limitations and improves performance efficiency. In fig (3.26) explain many types of wavelet and called as Wavelet Zoo.

In this paper, a new structure for MultiCarrier-Code Division Multiple Access (MC-CDMA) was proposed based on the Discrete Multiwavelet Transform (DMWT) [75]. The new proposed model based on multifilters called Multiwavelets. It has two or more low pass and high pass filters.

A very important multiwavelet filter is the GHM filter proposed by Geronimo, Hardian, and Massopust. The GHM basis offers a combination of orthogonality, symmetry, and compact support, which can not be achieved by any scalar wavelet basis. The GHM will be used in the MC-CDMA system block. In Multiwavelets setting, GHM multiscaling and multiwavelets functions coefficients are  $2 \times 2$  matrices, and during transformation step they must multiply vectors (instead of scalars) [70]. This means that multifilter bank need 2 input rows. The aim of preprocessing is to associate the given scalar input signal of length  $N$  to a sequence of length-2 vectors in order to start the analysis algorithm, and to reduce the noise effects. In the one dimensional signals the "repeated row" scheme is convenient and powerful to

implement.

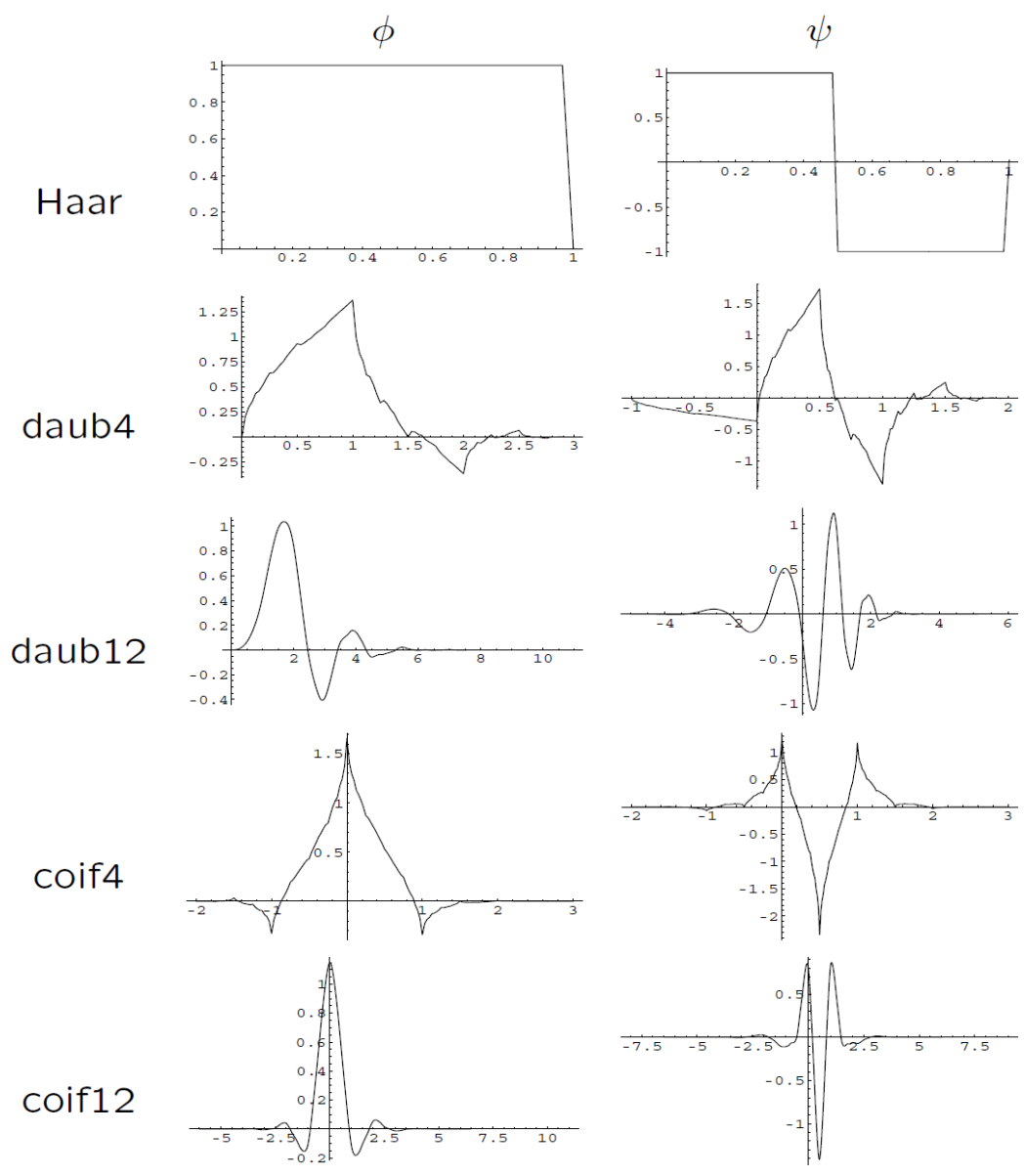


Figure (3.26) Wavelet Zoo

### 3.4.2 Proposed System For MC-CDMA Based On DMWT

The block diagram of the proposed system for MC-CDMA based on DMWT is depicted in figure (3.27). The modulator and demodulator of MC-CDMA based on DMWT are shown in figure (3.28).

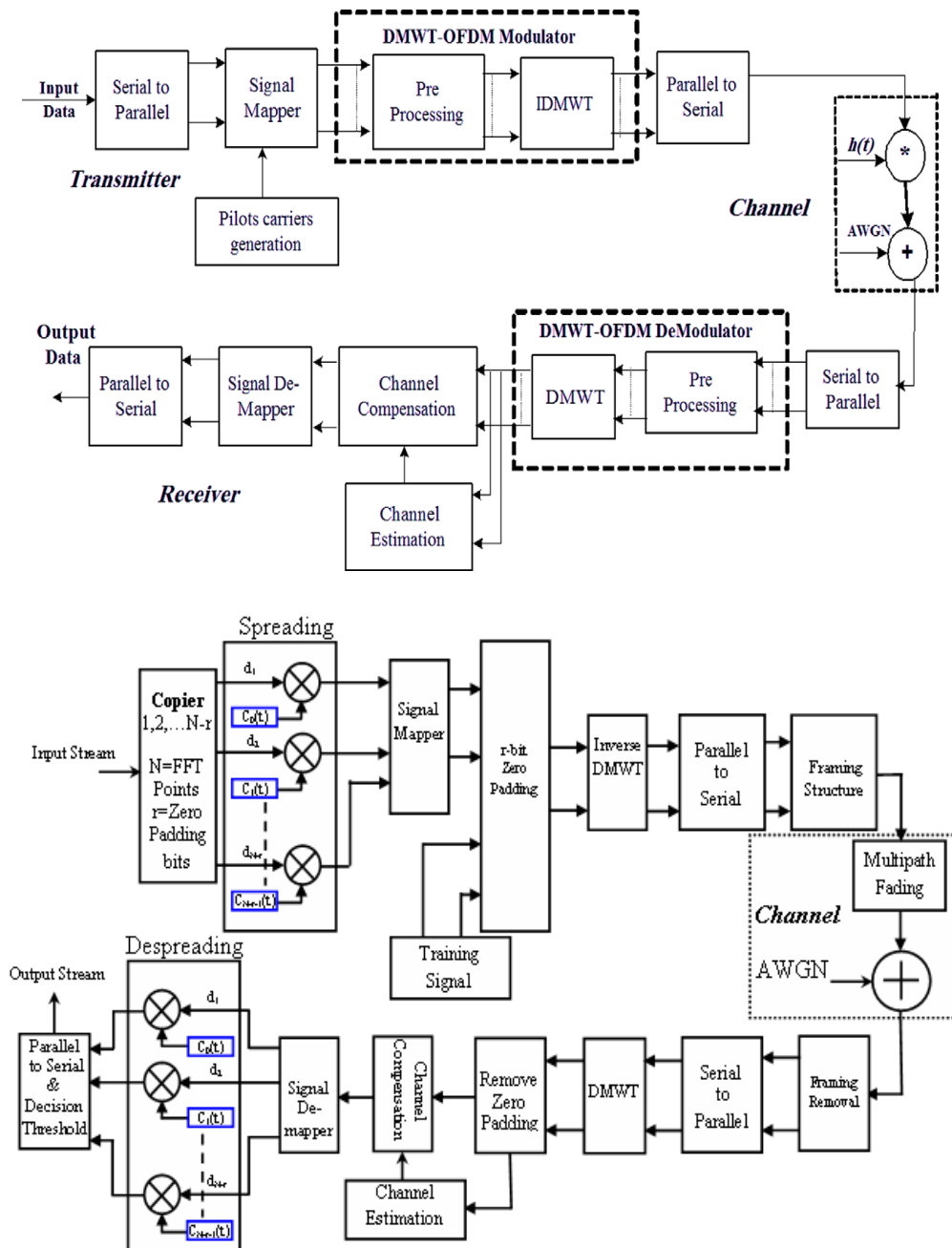
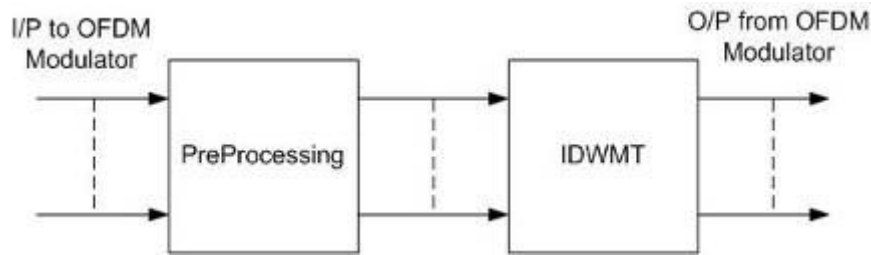
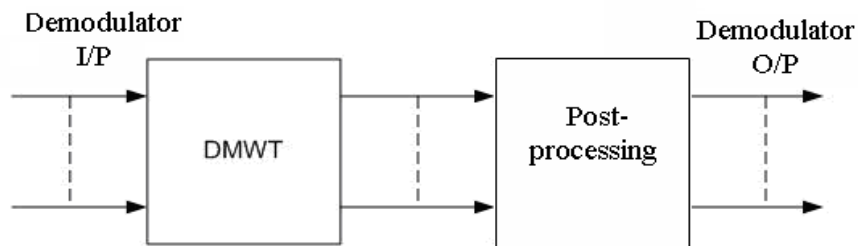


Figure (3.27) Block Diagram of MC-CDMA based on DMWT



**(a) DMWT Modulator**



**(b) DMWT-Demodulator**

Figure (3.28) DMWT modem system

The processes of the S/P converter, the signal mapper and the insertion of training sequence are the same as in the system of MC-CDMA based on FFT. After that a computation of IDMWT for 1-D signal is achieved. By using an over-sampled scheme of preprocessing (repeated row), the Inverse Discrete Multiwavelet Transform (IDMWT) matrix is doubled in dimension compared with that of the input, which should be a square matrix  $N \times N$  where  $N$  must be power of 2. Transformation matrix dimensions equal input signal dimensions after preprocessing. Scaling functions and orthogonal wavelets are created from the coefficients of a lowpass and highpass filter (in a two-band orthogonal filter bank). For “multifilters” those coefficients are matrices. This gives a new block structure for the filter bank, and leads to multiple scaling functions and wavelets. Geronimo, Hardin, and Massopust constructed two scaling functions that have extra properties not previously achieved [71, 72].

- The functions  $\phi_1$  and  $\phi_2$  are symmetric.
- All integer translates of the scaling functions are orthogonal.

- Compact Short support.
- Perfect reconstruction.
- Fast algorithms.

In particular, whereas wavelets have an associated scaling function  $\phi(t)$  and wavelet function  $\psi(t)$ , multiwavelets have two or more scaling and wavelet functions. For notational convenience, the set of scaling functions can be written using the notation  $\Phi(t) = [\phi_1(t) \ \phi_2(t) \ \dots \ \phi_r(t)]^t$ , where  $\Phi(t)$  is called the multiscaling function. Likewise, the multiwavelets function is defined from the set of wavelet functions as  $\Psi(t) = [\psi_1(t) \ \psi_2(t) \ \dots \ \psi_r(t)]^t$ .

When  $r=1$ ,  $\Psi(t)$  is called a scalar wavelet, or simply wavelet. While in principle,  $r$  can be arbitrarily large, the multiwavelets studied to date are primarily for  $r=2$ . The wavelet two-scaled below equations has nearly identical multiwavelet equivalents [73]:

$$\Phi(t) = \sqrt{2} \sum_{k=-\infty}^{\infty} H_k \Phi(2t - k) \quad (3.64)$$

$$\Psi(t) = \sqrt{2} \sum_{k=-\infty}^{\infty} G_k \Phi(2t - k) \quad (3.65)$$

Note, however, that  $H_k$  and  $G_k$  are matrix filters, i.e  $H_k$  and  $G_k$  are  $rxr$  matrices for each integer  $k$ . the matrix elements in these filters provide more degrees of freedom than a traditional scalar wavelet. These extra degrees of freedom can be used to incorporate useful properties into the multiwavelets filters, such as orthogonality, symmetry and high order of approximation. However, the multi-channel nature of multiwavelets also means that the subband structure resulting from passing a signal through a multifilter bank is different.

The two-scale equations (3.64) and the two wavelet equations (3.65) can be realized as a matrix filter bank (see fig. (3.29)) operating on  $r$  input data stream and filtering them into  $2r$  output data streams, each of which is down sampled by a factor two. In the scalar-valued expression  $v_{j,k}^l$ ,  $j$  refers to the scale,  $k$  refers to the translation, and  $l$  refers to the sub-channel or vector row. The equations are:

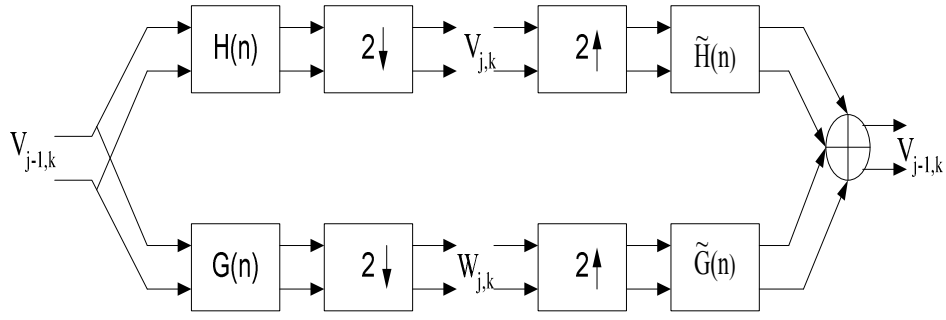


Figure (3.29) Analysis and Synthesis stages of 1-D single level DMWT

$$v_{j-1,k} = \sum_m H(m-2k)v_{j-1,k} \quad (3.66)$$

$$w_{j-1,k} = \sum_m G(m-2k)v_{j-1,k} \quad (3.67)$$

### 3.4.3 Choice of Multi-filter

In practice, multiscaling and wavelet functions often have multiplicity  $r=2$ . A very important multiwavelet system was constructed by Geronimo, Hardian and Massopust (GHM). Their system contains the two scaling functions  $\phi_1(t), \phi_2(t)$  shown in figure (3.30) and the two wavelets  $\omega_1(t), \omega_2(t)$  which shown in figure (3.31). according to equations (3.64) and (3.65) the GHM two scaling and wavelet functions satisfy the following two-scale dilation equations [12]:

$$\begin{bmatrix} \phi_1(t) \\ \phi_2(t) \end{bmatrix} = \sqrt{2} \sum_k H_k \begin{bmatrix} \phi_1(2t-k) \\ \phi_2(2t-k) \end{bmatrix} \quad (3.68)$$

$$\begin{bmatrix} \Psi_1(t) \\ \Psi_2(t) \end{bmatrix} = \sqrt{2} \sum_k G_k \begin{bmatrix} \Psi_1(2t-k) \\ \Psi_2(2t-k) \end{bmatrix} \quad (3.69)$$

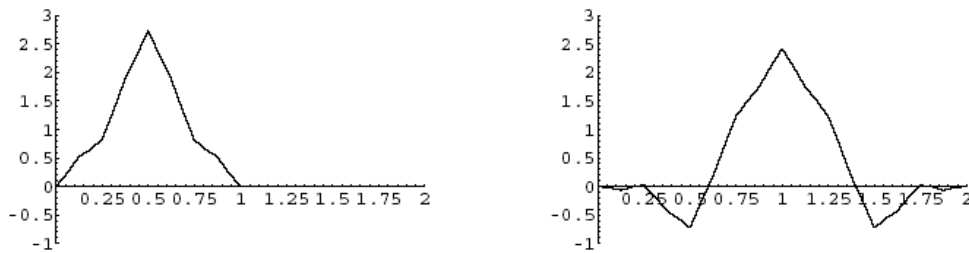


Figure (3.30) GHM scaling functions  $\phi_1(t), \phi_2(t)$

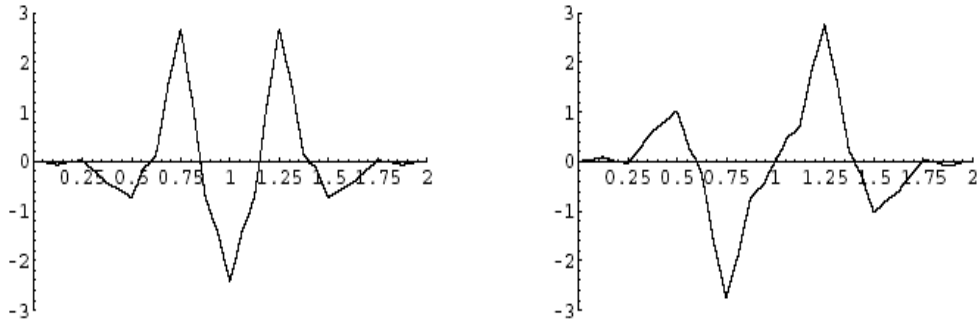


Figure (3.31) Wavelet functions  $\omega_1(t), \omega_2(t)$

To compute a single-level 1-D discrete multiwavelet transform, the following steps should be followed:

1. Checking input dimensions: input vector should be of length  $N$ , where  $N$  must be power of 2.
2. Constructing a transformation matrix,  $W$ , using GHM low and high pass filters matrices given in (1) and (2), the transformation matrix can be written as in (3.70). After substituting GHM matrix filter coefficients values, a  $2N \times 2N$  transformation matrix results.

For computing discrete Multiwavelet transform, scalar wavelet transform matrices (3.68) and (3.69) can be written as follows:

$$W = \begin{bmatrix} H_0 & H_1 & H_2 & H_3 & 0 & 0 & \dots & 0 & 0 & 0 & 0 \\ 0 & 0 & H_0 & H_1 & H_2 & H_3 & \dots & 0 & 0 & 0 & 0 \\ \vdots & \vdots \\ H_2 & H_3 & 0 & 0 & 0 & 0 & \dots & 0 & 0 & H_0 & H_1 \\ G_0 & G_1 & G_2 & G_3 & 0 & 0 & \dots & 0 & 0 & 0 & 0 \\ 0 & 0 & G_0 & G_1 & G_2 & G_3 & \dots & 0 & 0 & 0 & 0 \\ \vdots & \vdots & \vdots & \vdots & \vdots & \vdots & \dots & \vdots & \vdots & \vdots & \vdots \\ 0 & 0 & 0 & 0 & 0 & 0 & \dots & G_0 & G_1 & G_2 & G_3 \\ G_2 & G_3 & 0 & 0 & 0 & 0 & \dots & 0 & 0 & G_0 & G_1 \end{bmatrix} \quad (3.70)$$

Where  $H_i$  and  $G_i$  are the low and high-pass filter impulse response. They are  $2 \times 2$  matrices.

1. Preprocessing the input signal by repeating the input stream with the same stream multiplied by a constant  $\alpha$ , for GHM system functions  $\alpha = 1/\sqrt{2}$ .
2. Transformation of input vector which can be done by applying matrix multiplication to the  $2N \times 2N$  constructed transformation matrix by the  $2N \times 1$  preprocessing input vector.

Where  $H_k$  for GHM system are four scaling matrices  $H_0, H_1, H_2$  and  $H_3$

$$\begin{aligned}
 H_0 &= \begin{bmatrix} \frac{3}{5\sqrt{2}} & \frac{4}{3} \\ \frac{1}{20} & -\frac{3}{10\sqrt{2}} \end{bmatrix} & H_1 &= \begin{bmatrix} \frac{3}{5\sqrt{2}} & 0 \\ \frac{9}{20} & \frac{1}{\sqrt{2}} \end{bmatrix} \\
 H_2 &= \begin{bmatrix} \frac{0}{9} & \frac{0}{3} \\ \frac{1}{20} & -\frac{3}{10\sqrt{2}} \end{bmatrix} & H_3 &= \begin{bmatrix} \frac{0}{1} & \frac{0}{0} \\ -\frac{1}{20} & 0 \end{bmatrix}
 \end{aligned} \tag{3.71}$$

Also  $G_k$  for GHM system are four wavelet matrices  $G_0, G_1, G_2$  and  $G_3$ .

$$\begin{aligned}
 G_0 &= \begin{bmatrix} -\frac{1}{20} & -\frac{3}{10\sqrt{2}} \\ \frac{1}{10\sqrt{2}} & \frac{3}{10} \end{bmatrix} & G_1 &= \begin{bmatrix} \frac{9}{20} & -\frac{1}{\sqrt{2}} \\ \frac{9}{10\sqrt{2}} & 0 \end{bmatrix} \\
 G_2 &= \begin{bmatrix} \frac{9}{20} & -\frac{3}{10\sqrt{2}} \\ \frac{9}{10\sqrt{2}} & -\frac{3}{10} \end{bmatrix} & G_3 &= \begin{bmatrix} -\frac{1}{20} & 0 \\ \frac{1}{10\sqrt{2}} & 0 \end{bmatrix}
 \end{aligned} \tag{3.72}$$

There are three remarkable properties of the GHM scaling functions [71]:

1. They each have short support (the interval  $[0, 1]$  and  $[0, 2]$ ).
2. Both scaling functions are symmetric, and the wavelets form a symmetric/anti-symmetric pair.
3. All integer translates of the scaling functions are orthogonal.
4. The system has second order of approximation.

The scalar system with one scaling function cannot combine symmetry, orthogonality and second order approximation, moreover, a solution of a scalar dilation in equation with four coefficients is supported on the interval  $[0, 3]$ . The GHM multiscaling and Multiwavelet are also quite smooth.

Another example of symmetric orthogonal Multiwavelet with approximation order 2 is due to Chui and Lian, which is slightly longer than GHM. For the CL system, only three coefficients matrices are required [70, 73].

$$\begin{aligned}
 H_0 &= \frac{1}{2\sqrt{2}} \begin{bmatrix} 1 & -1 \\ \sqrt{7} & -\sqrt{7} \end{bmatrix} & H_1 &= \frac{1}{2\sqrt{2}} \begin{bmatrix} 2 & 0 \\ 0 & 1 \end{bmatrix} & H_2 &= \frac{1}{2\sqrt{2}} \begin{bmatrix} 1 & -1 \\ -\sqrt{7} & \sqrt{7} \end{bmatrix} \\
 G_0 &= \frac{1}{4\sqrt{2}} \begin{bmatrix} 3 & -2 \\ -1 & 1 \end{bmatrix} & G_1 &= \frac{1}{4\sqrt{2}} \begin{bmatrix} -4 & 0 \\ 0 & 2\sqrt{7} \end{bmatrix} & G_2 &= \frac{1}{4\sqrt{2}} \begin{bmatrix} 2 & 2 \\ 1 & 1 \end{bmatrix} \quad (3.73)
 \end{aligned}$$

CL scaling functions and wavelets are less smooth than GHM as shown in figure (3.32) and figure (3.33).

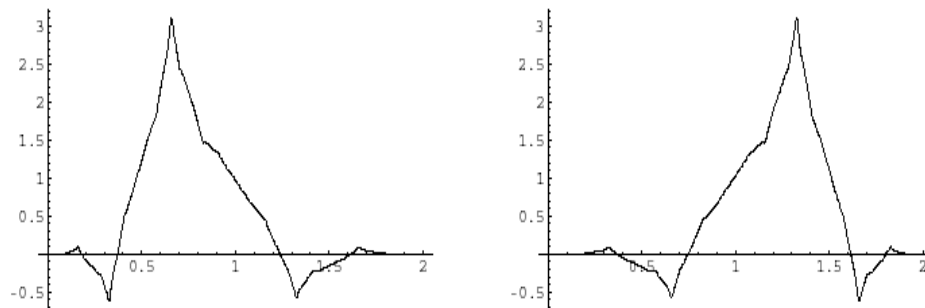


Figure (3.32) CL scaling functions  $\phi_1(t), \phi_2(t)$

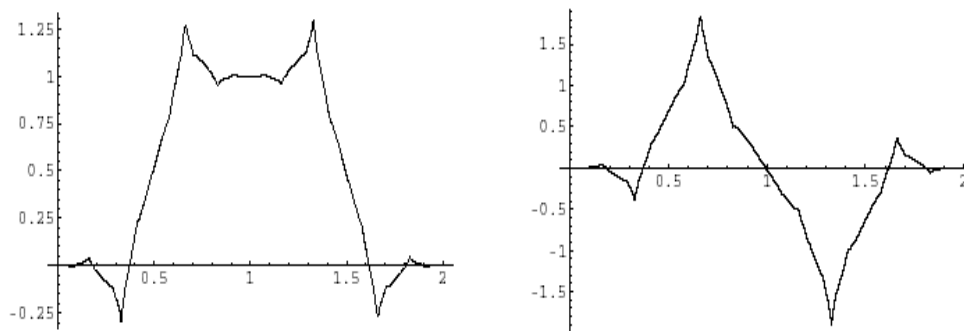


Figure (3.33) CL wavelet functions  $\omega_1(t), \omega_2(t)$

### 3.4.4 Preprocessing

The low pass filters  $H$  and high pass filter  $G$  consists of coefficients corresponding to the dilation (3.5.5) and wavelet (3.5.6) But in the Multiwavelet setting these coefficients are  $r$  by  $r$  matrices, and during the convolution step they must multiply vectors (instead of scalars). This means that multifilter banks need  $r$  input rows. In the present case,  $r=2$  and two data streams enter the multifilter.

The aim of preprocessing is to associate the given scalar input signal of length  $N$  to a sequence of length-2 vectors in order to start the analysis algorithm. Here  $N$  is assumed to be a power of 2, and so is of even length. If the preprocessing produces  $N$  length  $N/2$  length-2 vectors the result is a critical sampling [71]. In this case the input length-2 vectors are formed from the original time series via [71].

$$v_{0,k} = \begin{bmatrix} v_{0,k}^0 \\ v_{0,k}^1 \end{bmatrix} = \begin{bmatrix} X_k \\ \alpha X_k \end{bmatrix}, \quad k=0, 1, \dots, N-1 \quad (3.74)$$

Here  $\alpha$  is a constant, for the GHM case  $\alpha = 1/\sqrt{2}$ .

Obviously, repeated row preprocessing doubles the number of input data points, and preserves only one approximation order. If the preprocessing step is represented by a matrix multiplication:

$$PX = V_0 \quad (3.75)$$

Where  $P$  is  $2NXN$ ,  $X$  is  $NX1$ , and  $V_0$  is  $2NX1$ , then in detail

$$\begin{bmatrix} 1 & 0 & 0 & \cdots \\ \alpha & 0 & 0 & \cdots \\ 0 & 1 & 0 & \cdots \\ 0 & \alpha & 0 & \cdots \\ & & \ddots & \end{bmatrix} \begin{bmatrix} X_0 \\ X_1 \\ X_2 \\ X_3 \\ \vdots \end{bmatrix} = \begin{bmatrix} X_0 \\ \alpha X_0 \\ X_1 \\ \alpha X_1 \\ \vdots \end{bmatrix} = \begin{bmatrix} v_{0,0}^0 \\ v_{0,0}^1 \\ v_{0,1}^0 \\ v_{0,1}^1 \\ \vdots \end{bmatrix} \quad (3.76)$$

### 3.4.5 The Results of The Proposed System

In this section a simulation of the three systems for MC-CDMA based on FFT, MC-CDMA based on WT and MC-CDMA based on DMWT has been made by using MATLAB 7. and the BER performance of the three systems was studied in different channel models which are AWGN, flat fading and selective fading channel. Table (3.34) shows the parameters of the system that used in the simulation, the simulation work on a bitrates of 5 Mbps.

<b>Modulation Type</b>	BPSK
<b>Spreading Code</b>	Walsh-Hadamard
<b>Number of sub-carriers</b>	64
<b>Number of DMWT points</b>	64
<b>Channel model</b>	AWGN
	Flat fading+AWGN
	Frequency selective fading+AWGN

Table (3.34) Simulation Parameters

### 3.4.6 Performance of the Proposed Systems in AWGN Channel

In this section, the channel is modeled as Additive White Gaussian Noise for wide range of SNR from 0dB to 40dB; from figure (3.25), it was found that the MC-CDMA which is based on Multiwavelet is better and more significant than the two other systems based on the FFT transform and Wavelet transform. At BER  $10^{-2}$  the MC-CDMA based on Multiwavelet has SNR=5dB, while it has an SNR=21dB in FFT model, therefore the gain of MC-CDMA based on Multiwavelet is about 16dB in reference to the MC-CDMA based on FFT. For wavelet transform model the BER= $10^{-3}$  is found at SNR=7.5dB, and it is also a significant, and the gain achieved by using Wavelet transform model is about 15dB in proportion to the FFT model.

### 3.4.7 Performance of the Proposed Systems in Flat Fading Channel

In this section, the channel model that was considered is the flat fading channel that assumed all the frequency components of the transmitted signal are changed correlated in phase and magnitude. Maximum Doppler Shift taken in two different cases is 5 Hz, and 500 Hz, as shown in figure (3.26), and figure (3.27).

The simulation results in figure (3.26) showed that Multiwavelet transform model is still better than the other MC-CDMA systems based on FFT and WT. Where the MC-CDMA based on Multiwavelet transform has  $BER=10^{-3}$  at  $SNR=25dB$ , while in MC-CDMA system based on FFT, the  $BER=10^{-3}$  achieved approximately at SNR more than 40dB, this means a gain of more than 15 dB. In MC-CDMA based on wavelet transform the  $BER=10^{-3}$  showed at  $SNR=25dB$  that mean it is also significant; the relative gain to the FFT model is the same as in Multiwavelet transform model.

The effect of changing the Doppler shift value is shown in figure (3.27) The MC-CDMA based on WT is more sensitive to Doppler shift than Multiwavelet transform model, at 500Hz the BER performance of Multiwavelet transform model perform well compared to the others. The BER for WT model at  $SNR=40dB$  is approximate for  $2*10^{-4}$ ; while the Multiwavelet transform model still has the same BER performance which is  $10^{-4}$ , so the proposed model based on DMWT is less sensitive to the Doppler frequency variations.

### 3.4.8 Performance of the Proposed Systems in Selective Fading Channel

In this type of channel, the frequency components of the transmitted signal are affected by uncorrelated changes, where the parameters of the channel in this case corresponding to multipath the two paths are chosen, the Line Of Sight (LOS) and second path. In selective fading channel many models have been taken to compare the BER performance of the three systems, the influence of the attenuation, delay and maximum Doppler shift of an echo is successfully discussed.

First, the Doppler shift parameter has been taken in interest, the model that have been used in the simulation set the Doppler shift to 5Hz, and 500Hz. The path delay has been set to 1 sample and the path gain to -8dB. From figure (3.28), it was shown that multiwavelet transform model is still performs better than WT and FFT models,

where the performance of WT and FFT models is more degraded with increasing Doppler shift as in figure (3.29).

After Doppler shift parameter has been depicted, the second parameter is path gain, the other parameter is set to 1 sample for path delay, path gain=-1dB and 5Hz for Doppler shift. The BER performance is shown in figure (3.30) At this case the WT model perform better to the change in path gain rather than changing in Doppler shift. In overall cases the DMWT model has BER performance better than the FFT and WT models.

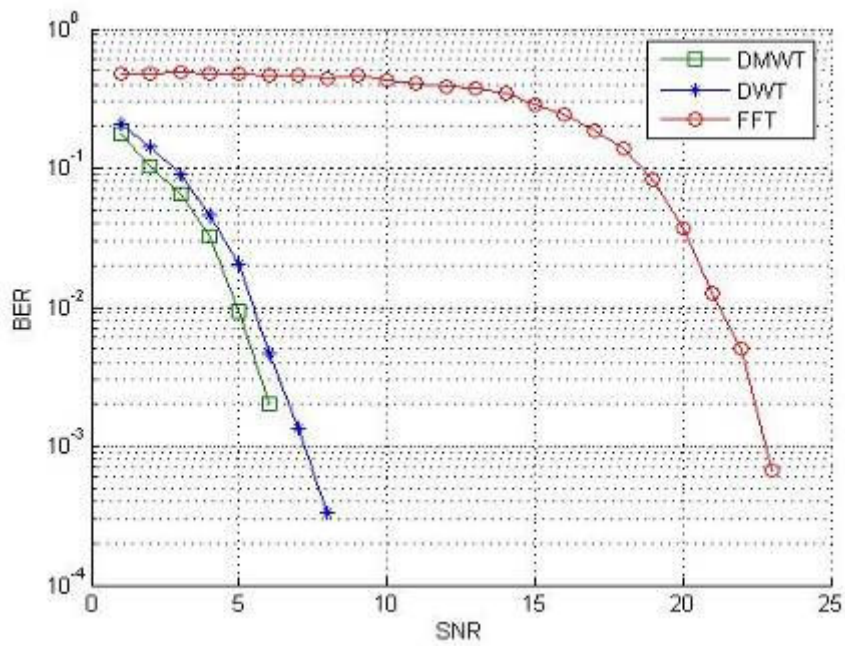


Figure (3.25) Performance of MC-CDMA models in AWGN channel.

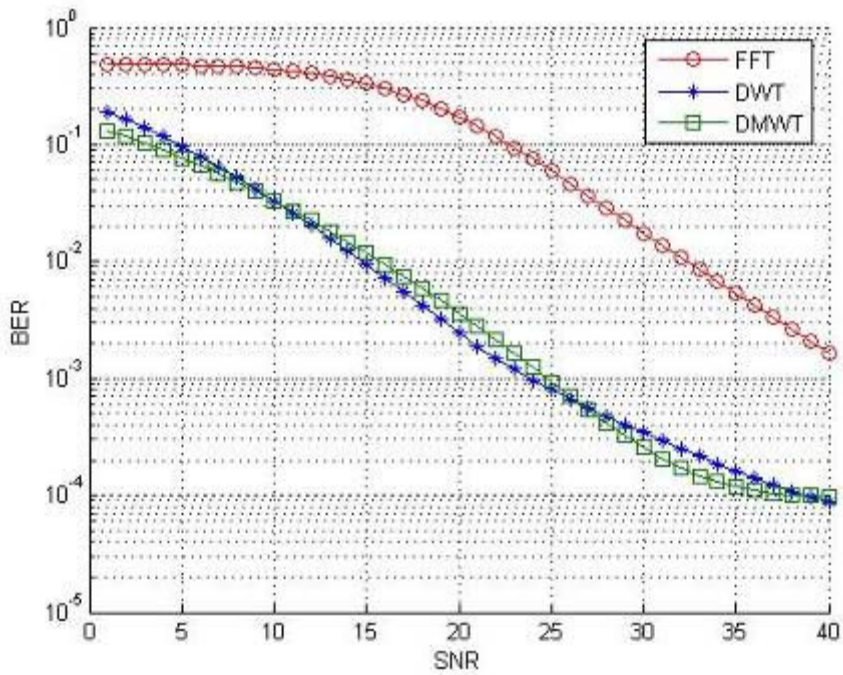


Figure (3.26) Performance of MC-CDMA in Flat Fading Channel at Maximum Doppler Shift =5Hz.

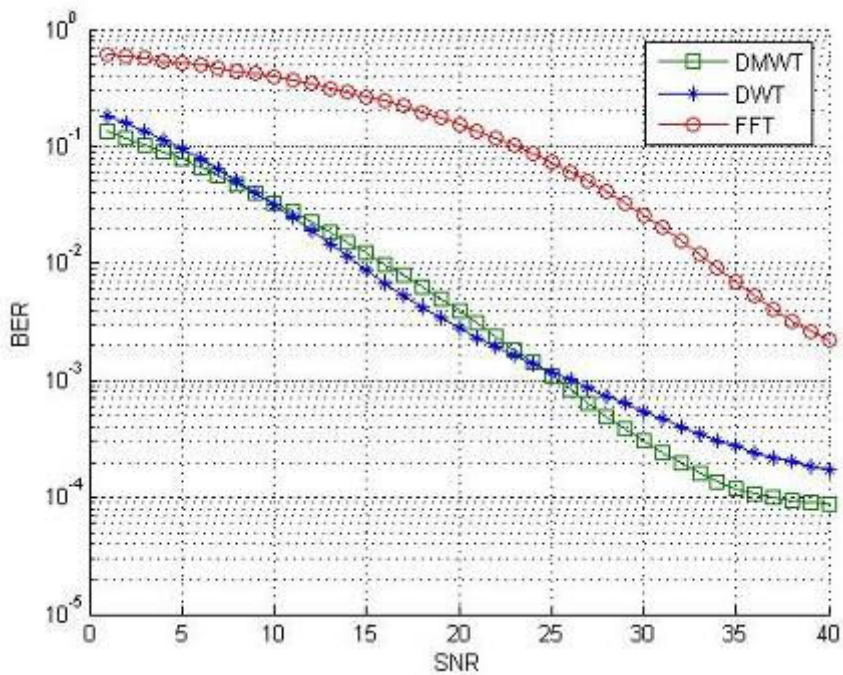


Figure (3.27) Performance of MC-CDMA models in Flat Fading Channel at Maximum Doppler Shift=500Hz.

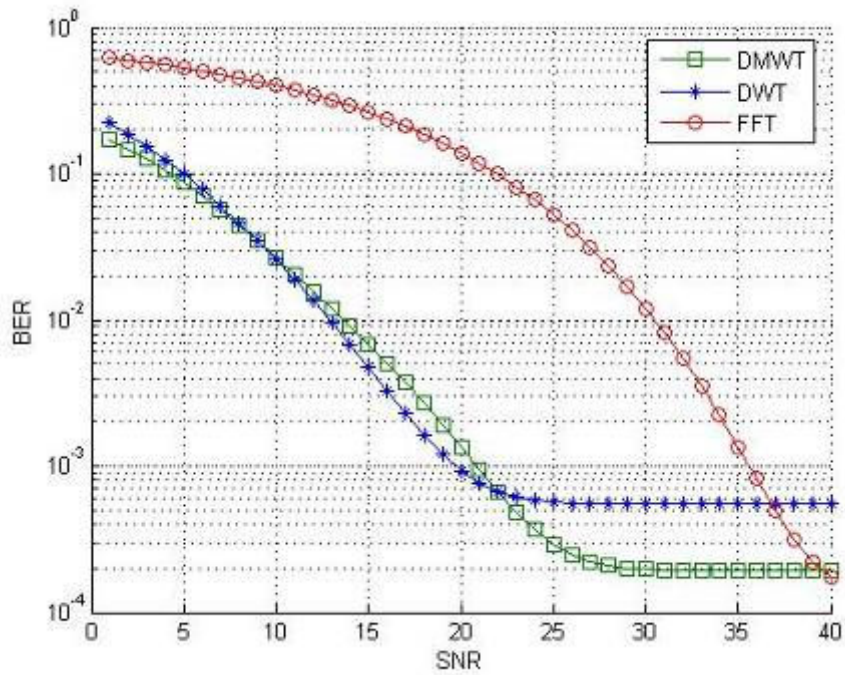


Figure (3.28) Performance of models in Selective Fading Channel at Maximum Doppler Shift=5Hz.

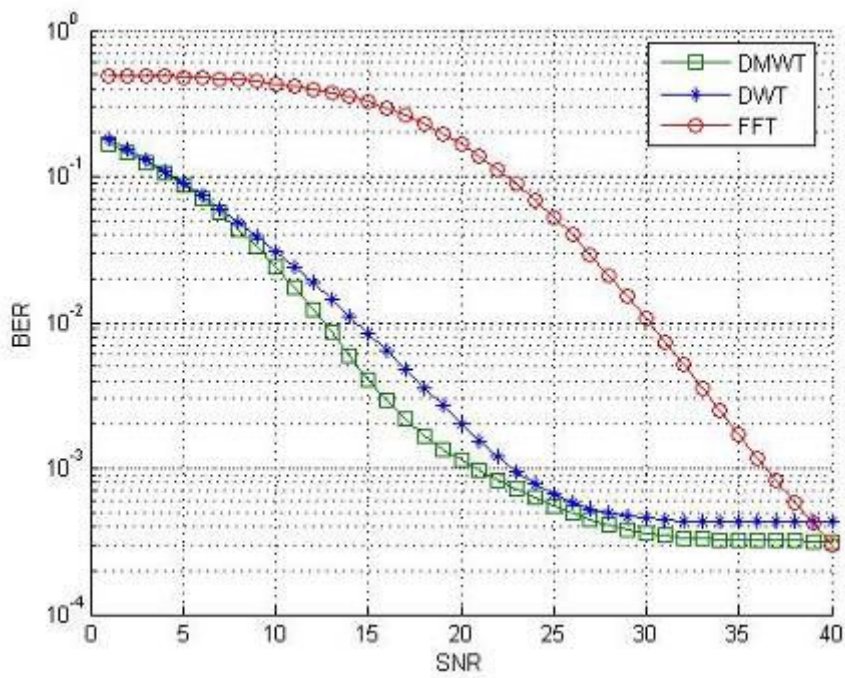


Figure (3.29) Performance of models in Selective Fading Channel at Maximum Doppler Shift=500Hz.

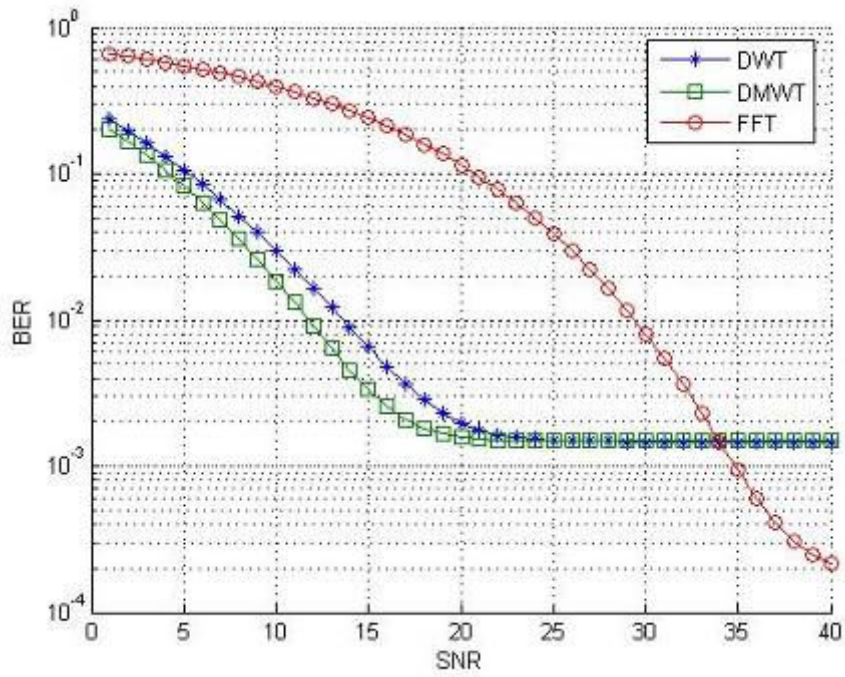


Figure (3.30) Performance of models in Selective Fading Channel at path gain=-1 dB.

### 3.4.9 Conclusions

In this paper, the MC-CDMA based on Multiwavelet structure is proposed and tested. These tests were carried out to verify its successful operation and its possibility of implementation. It can be concluded that this structure achieves much lower bit error rates assuming reasonable choice of the bases function and method of computation. Therefore this structure can be considered as an alternative to the conventional MC-CDMA model. Hence, the new structure was used to improve the performance of the communication system without the use of cyclic prefix, robustness to noise interference.

Comparing the performance of Multiwavelet transform model to the FFT and WT model in AWGN channel, flat fading and selective fading channel, and based on the simulation results some conclusions can be drawn. For the AWGN channel, MC-CDMA based on Multiwavelet transform is performs better; there is almost 16dB gain at  $10^{-2}$  in MC-CDMA when using Multiwavelet structure instead of conventional FFT based structure. On flat fading channel, the scenarios that have been taken in different maximum Doppler shift at 5Hz, and 500Hz. Still the MC-CDMA based Multiwavelet transforms has better performance.

In selective fading channel, the simulation results were presented by isolating individual propagation effects, to discover which channel parameters have the most significant impact on the performance. In Doppler shift, Its shown that MC-CDMA based Multiwavelet transform is still perform better than FFT and WT models, the performance of WT model is degraded with increasing the Doppler shift

## 4 Chapter four

### 4.1 Conclusions

In this thesis, proposed MC-CDMA models based FFT and wavelet transform are suggested and tested under different channel characteristics. These tests were carried out to verify their successful operation, and possibility of implementation

By comparing the performance of the proposed models for MC-CDMA based FFT and wavelet transform in AWGN channel, flat fading and selective fading channel, and based on the simulation results some conclusions can be drawn as follows:

#### 1. The AWGN channel,

It was found that all the proposed models improved their relative performance compared to the traditional systems. At  $BER=10^{-4}$  the gain of the three proposed models gave (18.5, 4.5, and 16.5) dB for model '1, 2, and 3' respectively.

#### 2. Flat fading channel

In this type of channel, have been taken in different maximum Doppler shift at 5Hz and 200Hz the gain of the proposed models based on

##### I. MC-CDMA Based on IN-Place Wavelet (Doppler 5 Hz)

The proposed model achieved at  $BER=10^{-4}$  gain of 24.5dB. The traditional model was failed to work in this type of channel.

##### II. MC-CDMA Based on Multiwavelet Transform (Doppler 5Hz)

The proposed model achieved at  $BER=10^{-3}$  of  $SNR=25$  dB, while the traditional model achieved at  $BER=10^{-3}$  of  $SNR=$  more than 40dB

##### III. MC-CDMA Based on IN-Place Wavelet (Doppler 100Hz)

The proposed model achieved at  $BER=10^{-4}$  of  $SNR=37.5$ dB. The traditional model was failed to work in this type of channel.

##### IV. MC-CDMA Based on Multiwavelet Transform (Doppler 200Hz)

The proposed model achieved at  $BER=10^{-3}$  of  $SNR=25.5$ dB. The traditional model was failed to work in this type of channel.

### 3 Selective fading channel

In selective fading channel was used Doppler shift at 5 Hz, the path delay has been set to 1 sample and the path gain to -8 dB.

#### I. MC-CDMA Based on IN-Place Wavelet ‘model 1’ (Doppler 5, Hz)

**A-** The proposed model gave better performance at the lower values of SNR.

**B-** As the SNR increases for more than 20 dB, the BER will be constant for this model while it is reduces for the conventional model based FFT.

**C-** As the number of constellation mapping increased to 64 points, the BER will increase for both systems.

**D-** The proposed and the conventional models have poor performance in selective fading channel.

#### II. MC-CDMA Based on IN-Place Wavelet and Phase Matrix ‘model 2’ (Doppler 5 Hz)

The proposed MC-CDMA gave SNR=16 dB at BER= $10^{-4}$ , while the traditional model was not approach this value of BER at any simulated SNR range.

#### III. MC-CDMA Based on Multiwavelet ‘model 3’(Doppler 5 Hz, 500 Hz)

Simulation set the Doppler shift at 5Hz, and 500Hz. The path delay has been set to 1 sample and the path gain to -8dB.as follows:

**A-** It was shown that multiwavelet transform model is still performs better than WT and FFT models,

**B-** The performance of WT and FFT models is more degraded with increasing Doppler shift.

## 4.2 Suggestions for Future Work

1. Apply the two dimensional In-Place wavelet transform on the proposed models and compare the results between them.
2. Use the modulation methods such as QAM, PSK, etc, and study the performance of these models with a results comparing between them.
3. Study the performance of DS-CDMA with the proposed algorithms.
4. Study the performance of the proposed models under the existence of multi-user case and compare the results with the traditional models.
5. Performance study is required for MC-DS-CDMA based on phase matrix algorithm.
6. Study the effect of using other spreading codes like Gold codes or maximal length sequences, etc, on the performance of suggested models.
7. Using MIMO-OFDM with the proposed algorithm that requires a minimum memory size for each sweep in the IP-WT, this method can enhance the system performance in selective fading channel.
8. Transmitter diversity with space-time block coding (STBC) is an attractive transmission scheme to improve the performance system; we suggest to implement a space time block coded MC-CDMA based on the new suggested models.

### 3.4.10 Last work

Recently, I am interesting in the subject of Dual-hop transmissions with fixed-gain relays over Generalized  $\alpha$ -Gamma fading channels [78]. The short note on my work and results as follows:

A study on the end-to-end performance of dual-hop wireless communication systems equipped with fixed-gain relays and operating over Generalized-Gamma (GG) fading channels is presented. The analysis is based on the evaluation of the moments of the end-to-end signal-to-noise ratio (SNR). Furthermore; the average bit error probability for coherent and non-coherent modulation schemes as well as the outage probability is also studied using the moment-generating function (MGF) approach. The proposed method for the evaluation of the MGF is based on the Pad'e approximants theory. Extensive numerical and computer simulations examples verify the accuracy of the proposed mathematical analysis.

The conclusion in this paper, the end-to-end performance of dual-hop wireless communication systems with fixed-gain relays operating over GG fading channels was evaluated. A novel closed-form expression for the moments of the output SNR was derived. Moreover, the average error and the outage performance of the considered system were studied using the MGF approach and the Pad'e approximants method. Various numerical and computer simulations results were presented that demonstrated the proposed mathematical analysis. Our results incorporate similar others available in the open technical literature, such as those for Nakagami- $m$  and Weibull fading channels.

## References

- [1] Shinsuke Hara, and Ramjrr Prasad. "Multicarrier. Techniques for 4G Mobile Communications," Artech House, Boston London, (2003)
- [2] Sttot J. H. "Explaining Some of the Magic COFDM," Proceedings of 20<sup>th</sup> International Television Symposium, (1997).
- [3] Chuang J., and Sollenberger N. "Beyond 3G Wideband Wireless Data Access Based on OFDM and Dynamic Packet Assignment," IEEE Communication Magazine, vol. 38, no.7, pp. 78-87, July (2000)
- [4] Kaiser S. "On the Performance of Different Detection Techniques for OFDM-CDMA in Fading Channels," IEEE ICC'95. pp. 2059-2063, June (1995)
- [5] Chang R. W. "Synthesis of Band-Limited Orthogonal Signals for Multichannel Data Transmission," Bell System Technical Journal, vol. 46, pp. 1775-1796, December (1966).
- [6] Hanzo L. et al, "OFDM and MC-CDMA for Broadband Multi-User Communications, WLANs and Broadcasting," John Wiley & Sons, (2003)
- [7] Couasnon T. De. et al, "OFDM for Digital TV Broadcasting," Journal of Signal Processing, vol. 39, pp. 1-32, (1994).
- [8] Weinstein S.B. and Ebert P. M. "Data Transmission by Frequency Division Multiplexing Using the Discrete Fourier Transform," IEEE Transaction on Communication. Technology, vol. com-19, pp. 628 634, October (1971).
- [9] Hirosaki B. "An Analysis of Automatic Equalizers for Orthogonally Multiplexed QAM System," IEEE Transaction on Communications, vol. COM-28, pp. 73-83, January (1980).
- [10] Hirosaki B. "An Orthogonal Multiplexed QAM System Using the Discrete Fourier Transform," IEEE Transactions on Communications, vol. Com29, pp. 983-989, July (1981).

- [11] N. Yee, J. P. Linnartz, and G. Fettweis, "Multicarrier CDMA in Indoor Wireless Radio Networks," In PIMRC 93, pp. 109-113, (1993)
- [12] Chooly A., et al, "Orthogonal Multicarrier Techniques Applied to Discrete Sequence Spread Spectrum CDMA Systems," In Proceedings of IEEE Global Telecommunications Conference 1993 (Houston, TX, USA), pp. 1723-1728, 29 November 2 December (1993).
- [13] Fettweis G. et al, "On Multi-Carrier Code Division Multiple Access (MC-CDMA) Modem Design," In Proceedings of IEEE VTC 94, (Stockholm, Sweden), pp. 1670-1674, IEEE, 8-10 June (1994).
- [14] Fazel K., and Papke L. "On the Performance of Convolutionally Coded CDMA/OFDM for Mobile Communication System," In PIMRC'93, pp. 468-472, (1993).
- [15] Prasad R. and Hara S. "Overview of Multicarrier CDMA," IEEE Communication Magazine, pp. 126-133, December (1997).
- [16] Haar L. "Zur Theorie Der Orthogonalen Funktionen Systeme," Math. Ann., 69: 331-371, (1910).
- [17] Howard L., et al, "Wavelet Analysis," ISBN 0387-98383-x. Springer- Verlag New York, (1998).
- [18] Scott L. Miller. "MMSE Detection of Multicarrier CDMA," IEEE Journal on Selected Areas in Communications, vol. 18, no. 11, November (2000)
- [19] Shinsuke Hara, and Ramjee Prasad. "Design and Performance of Multicarrier CDMA System in Frequency-Selective Rayleigh Fading Channels," IEEE Transaction on Vehicular Technology, vol48, no.5, September (1999)
- [20] Moltier and Castelain D. "A Spreading Sequence Allocation Procedure for MC-CDMA Transmission Systems," Mitsubishi Electric ITE, (2000).
- [21] Eric Phillip Lawrey Be. "Adaptive Techniques for Multiuser OFDM," Ph.D. Thesis Electrical and Computer Engineering, James Cook University, December (2001)
- [22] Ramasamy Venkatasubramanian. "Beamforming for MC-CDMA," Master Thesis, Virginia Polytechnic Institute and State University, January, 31, (2003)
- [23] Hongbing Zhang, "Wavelet Packet Based Multicarrier CDMA Wireless Communication Systems," Ph.D. Thesis, University of Cincinnati, March, (2004).

- [24] Jeffrey G. Andrews, and Teresa H. Y. Meng. "Performance of Multicarrier CDMA with Successive Interference Cancellation in Multipath Fading Channel," IEEE Transactions on Communications, vol. 52, no. 5, May (2004).
- [25] Mustafa S. A. "Design and Implementation of Orthogonal Frequency Division Multiplexing Transceiver on TMS320C6711," Ph.D. Thesis College of Engineering, University of Baghdad/ Iraq, (2004).
- [26] Helard. "Design and Implementation of MC-CDMA Systems for Future Wireless Networks," EURASIP Journal on Applied Signal Processing pp. 1604-1615, October (2004).
- [27] Zang H., et al, "Research of DFT-OFDM and DWT-OFDM on Different Transmission Scenarios," Proceedings of the 2<sup>nd</sup> International Conference on Information Technology for Application (ICITA), (2004).
- [28] Archarya J., et al, "Two Dimensional Spreading for Dispersive Channels," Wireless Information Network Laboratory (WINLAB), Rutgers University, (2005).
- [29] Kasliwal R., et al, "Wavelet OFDM" EE678, Wavelet Application Assignment, (2005).
- [30] Omar Mowaffaq. "A Proposed Radon Based MC-DS-CDMA System," Ph.D. Thesis, College of Engineering, University of Baghdad, January/Iraq (2006).
- [31] Saad N. Abdul-Majeed. "A Model of Multicarrier Code Division Multiple Access Transceiver," Ph.D. Thesis, College of Engineering, University of Baghdad/ Iraq (2006).
- [32] Laith A. Abdul-Rahaim. "Design and Simulation of STBC-(OFDM and CDMA) Transceivers Based on Hybrid Transforms," Ph.D. Thesis, University of Technology/Iraq, January (2007).
- [33] Osama Q. J. Al-Thahab. "A Multi-Carrier Code Division Multiple Access System Using Multiwavelet and Radon Transforms", Ph.D. Thesis, University of Technology/Iraq, January (2007).
- [34] Prasad R. "Universal Wireless Personal Communications," Norwood, MA: Artech House, (1998).
- [35] Van Nee. R., and Prasad R. "OFDM for Wireless Multimedia Communications," Norwood, MA: Artech House, (2000).

- [36] Kaiser S., "Multi-Carrier CDMA Mobile Radio Systems Analysis and Optimization of Detection, Decoding and Channel Estimation," Ph.D. dissertation, VDI-Verlag, Fortschrittberichte VDI, Dusseldorf, (1998).
- [37] Hanzo L., et al, "Single-and Multi-Carrier Quadrature Amplitude Modulation," New York, USA: IEEE Press John Wiley, April (2000).
- [38] Okada M., et al, "A maximum Likelihood Decision Based Nonlinear Distortion Compensator for Multi-Carrier Modulated Signals," IEICE Transactions on Communications, vol. E81B, no.4, pp. 737-744, (1998).
- [39] Dinis R., and Gusmao A. "Performance Evaluation of a Multicarrier Modulation Technique Allowing Strongly Nonlinear Amplification," in Proceedings of ICC 1998, pp. 791-796, IEEE, (1998).
- [40] Pollet T., et al, "BER Sensitivity of OFDM Systems to Carrier Frequency Offset and Wiener Phase Noise," IEEE Transactions on Communications, vol.43, pp. 191-193, February/March/ April (1995).
- [41] Nikookar H., and Parsad R., "On the Sensitivity of Multicarrier Transmission Over Multipath Channels to Phase Noise and Frequency Offset," in Proceedings of IEEE International Symposium on Personal, Indoor, and Mobile Radio Communications (PIMRC96), (Taipei, Taiwan), pp. 68-72, IEEE, 15-18 October (1996).
- [42] Sari H., et al, "Transmission Techniques for Digital TV Broadcasting," IEEE Communication Magazine, pp. 100-109, February (1995).
- [43] Peterson R. L., et al, "Introduction to Spread Spectrum Communication," Prentice Hall International Edition, (1995).
- [44] Persson A. "On Convolutional Codes and Multi-Carrier Techniques for CDMA System," Thesis for the degree of Licentiate, Department of Signals and Systems, School of Electrical Engineering, Chalmers, University of Technology, (2002).
- [45] Zigang Y., et al. "Blind Bayesian Multiuser Receiver for Space Time Coded MC-CDMA System Over Frequency-Selective Fading Channel," IEEE Trans. Veh. Techn, vol. VT-40, pp. 781-785, May (2001).

- [46] Alard M. and Lassalle, R. "Principles of Modulation and Channel Coding for Digital Broadcasting for Mobile Receiver," Tech. Rep., no. 224, pp.47-69, Aug. (1987)
- [47] Zigang Y. et al, "Blind Bayesian Multiuser Receiver for Space Time Coded MC-CDMA System Over Frequency-Selective Fading Channel," IEEE Trans. Veh. Techn., vol. VT-40, pp. 781-785, May (2001).
- [48] Leonard J.Cimini, "Analysis and Simulation of a Digital Mobile Channel Using Orthogonal Frequency Division Multiplexing," IEEE Trans. Commun., vol. 33, no 4, pp. 665-675, July, (1985).
- [49] Russell M., and G.L.Stuber, "Interchannel Interference Analysis of OFDM in a Mobile Environment," in Proc of 45<sup>th</sup> Vehicular Technology Conference, vol.2, pp. 820-824, (1995).
- [50] Rabiner L. R. and Gold B. "Theory and Application of Digital Signal Processing," Englewood Cliffs, N.J, Prentice-Hall, (1975).
- [51] Lonnie C. Ludeman, "Fundamentals of Digital Signal Processing," John Wiley & Sons Ltd. (1987).
- [52] Frigo N. J. "A Model of Intermodulation Distortion in Non-Linear Multicarrier Systems," IEEE Transactions on Communications, vol. 42, no. 2/3/4, pp. 1216-1221, February, March/April (1994).
- [53] Zhang D. "Performance Analysis and Comparison of OFDM Based Packet Transmission System with QAM Modulation," Master Thesis, School of Electrical and Computer Engineering, Chalmers University of Technology, Sweden, April (2004).
- [54] Persson A. "Diversity and Interference Aspects in the Downlink of Code Division Multiple Access Systems," Ph.D dissertation, Department of Signals and Systems, School of Electrical Engineering, Chalmers University of Technology, (2004).
- [55] Negash B. G. and Nikookar H. "Wavelet Based OFDM for Wireless Channels," International Research Center for Telecommunications Transmission and Radar, Faculty of Information Technology and Systems, Delft University of Technology, (2001).
- [56] Robipolikar, "The Wavelet Tutorial," Neural Networks, Short course in Philadelphia, PA 12 and 19 January (2007).

- [57] Nievergelt Yves, "Wavelets Made Easy," Birkhauser, Boston Inc, April (1999).
- [58] Chen Q., et al, "Performance of a Coded Multi-Carrier DS-CDMA System in Multipath Fading Channels," *Wireless Personal Communications*, vol. 2, no. 1-2, pp. 167-187, (1995).
- [59] Kaiser S., "On the Performance of Different Detection Techniques for OFDM-CDMA in Fading Channels," in *IEEE ICC '95*, pp.2059 -2063. June (1995)
- [60] Prasad R. and Hara S., "An Overview of Multicarrier CDMA," in *Proc. IEEE Int. Symp. Spread Spectrum techniques and Applications*, pp. 107-114, September (1996)
- [61] Sourour E. A. and Nakagawa M., "Performance of Orthogonal Multicarrier CDMA in a Multipath Fading Channel," *IEEE Trans. Commun.* vol. 44, pp. 356-366, March (1996).
- [62] Hanzo L., et al, "Single-and Multi Carrier DS-CDMA," John Wiley-IEEE Press, (2003).
- [63] Jack Glas. "The Principle of Spread Spectrum System," Report, August, (1996), Intenet Survey
- [64] Biglieri E., et al, "Fading Channels: Information Theoretic and Communications Aspects," *IEEE Transactions on Information Theory*, vol. 44, no. 6, October (1998).
- [65] L. Gordon Stuber, R. John Barry, W. Steve McLaughlin, Li. Geoffrey Marry Ann Ingram, and G. Thomas Pratt, "Broadband MIMO-OFDM wireless communications" *Proceeding of the IEEE*, vol. 92, no.2, February 2004.
- [66] K. Fazel and Kaiser 'Multi-Carrier and Spectrum Systems' 1<sup>st</sup> edition John Wiley&sons,2002.
- [67] Kit Ming Chee "Hybrid OFDM-CDMA A Comparison of CDMA, MC-CDMA and OFCDM," Dept. of Electrical and Electronic, Adelaide University, SA5005, Australia, 2002
- [68] Venkatasubramanian R., Beamforming for MC-CDMA, M.Sc. thesis submitted to the faculty of Virginia Polytechnic Institute and State University. 2003.
- [69] Lawery E., The Suitability of OFDM as a Modulation Technique for Wireless Telecommunications, with a CDMA comparison, B.Sc. Project submitted to James Cook University Computer Systems Engineering Department.

- [70] V. Strela, P. Heller, G. Strang, P. Topiwala, C. Heil, The application of multiwavelet filter banks to signal and image processing, IEEE Trans. on Image Proc., 1998
- [71] V. Strela, Multiwavelets: Theory and Application, Ph.D. Thesis, MIT, June 1996.
- [72] Strang G., Strela V., Orthogonal Multiwavelets with Vanishing Moments, J. Optical Eng. no. 33, pp.2104-2107, 1994.
- [73] Strang G., Strela V., Short Wavelets and Matrix Dilation Equations, IEEE Transactions on Acoustic, Speech and Signal Processing, no. 43, pp. 108-115, 1995.
- [74] Salih.Salih, Akil Mansour “Performance study of OFDM Based on In- Place Wavelet Transform”. IEEE 10th International Symposium on Volume , Issue , 25-28 Aug. 2008 Page(s): 485 – 489
- [75] G.S.Tombras, Salih.Salih, Akil Mansour “Performance Study of MC-CDMA Based on Multiwavelet Transform”. MASAUM Journal of Basic and Applied Sciences, Vol.1, No.1 August 2009 Page(s): 138-143.
- [76] Akil Mansour, Salih.Salih, G.S.Tombras “Proposed Model for MC-CDMA Based on the In-Place Wavelet Transform and Phase Matrix”. MASAUM Journal of Open Problems in Science and Engineering, Volume 1 Issue 1, October 2009
- [78] Kostas P. Peppas, Akil Mansour and George S. Tombras “Dual-hop transmissions with fixed-gain relays over Generalized-Gamma fading channels” Journal of Telecommunications, volume 1 issue1, February (2010).